eering
rary

MAY 19 1937

UNITED STATES DEPARTMENT OF COMMERCE

Journal of Research

of the

National Bureau of Standards

Vol. 18, No. 5 May 1937

CONTENTS

RP	TITLE AND AUTHOR	Page
990.	Configuration of the pyranoses in relation to their properties and nomenclature. Horace S. Isbell..... [Price 10¢]	505
991.	Rapid electrodeposition of iron from ferrous chloride baths. Charles Kasper..... [Price 5¢]	535
992.	Interference measurements of wave lengths in the ultraviolet spectrum of iron. William F. Meggers and Curtis J. Humphreys.... [Price 10¢]	543
993.	Effect of sizing, weaving, and abrasion on the physical properties of cotton yarn. Walter T. Schreiber, Martin N. V. Geib, and Omar C. Moore..... [Price 5¢]	559
994.	Magnetic method for measuring the thickness of nickel coatings on nonmagnetic base metals. Abner Brenner..... [Price 10¢]	565
995.	The system $PbO-B_2O_3$. R. F. Geller and E. N. Bunting.. [Price 5¢]	585
996.	Preparation of iron oxide as a source of high-purity iron. Harold E. Cleaves and John G. Thompson..... [Price 5¢]	595
997.	Method for approximating the glass content of portland cement clinker. William Lerch and Lorrin T. Brownmiller.. [Price 10¢]	609
998.	State of the sulfur in oxidized wool. Milton Harris and Arthur L. Smith..... [Price 5¢]	623
999.	A contribution to the chemistry of rhenium. G. E. F. Lundell and Howard B. Knowles..... [Price 5¢]	629

The articles listed above may be purchased separately (see cover page II) at the prices listed in the table of contents

A monthly periodical of pure and applied science published by our National Government

Journal of Research

of the

National Bureau of Standards

The January 1937 issue of the Journal of Research of the National Bureau of Standards began the eighteenth semiannual volume of this periodical. Fundamental researches in progress in the Bureau's laboratories are reported in this JOURNAL. If you are interested in new developments in science and technology, you should receive the JOURNAL. If you are not already a subscriber you are invited to send in your subscription.

Technical News Bulletin

This is a monthly publication containing short articles reporting progress of work in the Bureau laboratories, abstracts of papers which appear in the Journal of Research, accounts of scientific and technical meetings in which the Bureau has taken part, a list of all publications by members of the staff, and other items within the Bureau's fields. The BULLETIN is designed primarily to give a general and timely review of the activities of the Bureau in brief form. It is a prompt and reliable source of official information. If you have not already subscribed for the BULLETIN, you are invited to do so.

ANNUAL SUBSCRIPTION	Prices	
	United States, Canada, Cuba, Mexico, Newfoundland, Republic of Panama	Other countries
Journal of Research of the National Bureau of Standards:		
12 monthly issues (2 volumes), paper covers	$2.50	$3.25
Bound volume (½ year, 1 volume), blue buckram . . .	3.00	3.50
Technical News Bulletin, 12 monthly issues	.50	.70

Research Papers, reprinted individual articles appearing in the Journal of Research, are available from the Superintendent of Documents shortly after appearance of monthly issue of the JOURNAL.

Address orders only to
Superintendent of Documents, U. S. Government Printing Office,
Washington, D. C.

UNITED STATES DEPARTMENT OF COMMERCE
DANIEL C. ROPER, Secretary
NATIONAL BUREAU OF STANDARDS
Lyman J. Briggs, Director

✦

Journal of Research

of the

National Bureau of Standards

✦

Volume 18, Number 5
May 1937

UNITED STATES
GOVERNMENT PRINTING OFFICE
WASHINGTON : 1937

For sale by the Superintendent of Documents, Washington, D. C. - - - - - Price 25 cents
$2.50 per year on subscription

The prices of the separate Research Papers appearing in this JOURNAL are given on the front cover page. If 100 or more copies of any separate are ordered, a discount of 25 percent is allowed. Those who desire copies of separate Research Papers should send their orders and remittances without delay to the Superintendent of Documents, U. S. Government Printing Office, Washington, D. C. This will aid him to determine the number of copies to be printed for sale. Research Papers are not printed from electrotypes, and usually no more reprints can be had when the first and only printing is exhausted.

U. S. DEPARTMENT OF COMMERCE NATIONAL BUREAU OF STANDARDS

RESEARCH PAPER RP990

Part of Journal of Research of the National Bureau of Standards, Volume 18, May 1937

CONFIGURATION OF THE PYRANOSES IN RELATION TO THEIR PROPERTIES AND NOMENCLATURE [1]

By Horace S. Isbell

ABSTRACT

Optical rotation, mutarotation, and bromine oxidation measurements are reported for seven heptoses. The results reveal striking similarity in the properties of the sugars classified in the following groups: (1) α-*l*-arabinose, α-*d*-galactose, α-*d*-α-mannoheptose, and α-*l*-β-guloheptose; (2) β-*l*-arabinose $CaCl_2.4H_2O$, β-*d*-galactose, β-*d*-α-mannoheptose; (3) β-*d*-glucose, and β-*l*-β-galaheptose; (4) α-*d*-lyxose, α-*d*-mannose, and α-*l*-α-galaheptose; (5) β-*d*-gulose and β-*d*-α-glucoheptose. The marked parallelism is evidence that the sugars in each group have like conformations for the pyranose ring.

The structural characteristics of the alpha and beta sugars are discussed in relation to their reactions and their nomenclature. The rates of reaction and other properties indicate that there is an important structural difference in the alpha and beta sugars. This difference is in accord with the concept that the pyranose ring is of the strainless multiplanar type rather than monoplanar. The application of Hudson's rule for selecting the alpha and beta names is considered, and it is suggested that an additional criterion be added to this rule in order to obtain a nomenclature for the carbohydrates and their derivatives, based on the most fundamental structural properties in relation to the optical rotations, together with the theory of optical superposition. Comparisons of the optical rotations of the hexose sugars give values for the rotational differences which may be grouped according to the configurations of the neighboring atoms. The rotational differences obtained from substances of similar or related configuration agree; the rotational differences obtained by the comparison of substances of widely different configuration are not in agreement.

CONTENTS

		Page
I.	Correlations of optical rotation and structure	505
II.	Nomenclature of the alpha and beta sugars	510
III.	Mutarotations of the heptoses and the structurally related hexoses	515
IV.	Conformation of the pyranose ring	521
V.	Bromine oxidation measurements	523
VI.	Summary	532
VII.	References	533

I. CORRELATIONS OF OPTICAL ROTATION AND STRUCTURE

The elucidation of the configurational interrelationships of the simple sugars by E. Fischer and others, and the unraveling of the problem of ring structure leave as an outstanding problem the determination of the conformation of the sugar molecule as a whole. Study of the relationship between structure and optical rotation was

[1] A résumé of this paper was given before the Division of Sugar Chemistry of the American Chemical Society in September 1936 at Pittsburgh.

begun by Van't Hoff [1] [2], who advanced the principle of optical superposition. According to this principle, the optical rotation of the molecule is equal to the algebraic sum of the rotations due to the constituent carbon atoms, the rotations of which change from $+a$ to $-a$ when the atomic configuration is replaced by its mirror image.

It has been clearly demonstrated [2, 3] that optical rotation is not uniformly an additive property and that dissimilarity in configuration results in deviations from the Van't Hoff theory of optical superposition. Notwithstanding this fact, the empirical comparison of the optical rotations of related compounds, whose structures are determined by chemical methods, provides a useful means for guiding investigation in the carbohydrate field. The principle of optical superposition has been extended by Hudson [4], who observed that if the formulas for alpha and beta glucose were written as ring structures differing solely in the configuration of carbon 1, by assuming the principle of optical superposition, it is possible to obtain the value for the rotation of carbon 1 by subtracting the observed rotations of the two forms. Thus if the rotation which is due to the end asymmetric carbon be A, and the rotation which is due to the other four asymmetric carbons be B, the molecular rotation of one isomer will be $A+B$, and the molecular rotation of the other will be $-A+B$. The sum of the rotations is $2B$ and their difference $2A$. Like values of $2A$ are obtained for glucose, galactose, and lactose. Hudson recognized that if this equality of rotation should exist throughout the sugar group it would offer a useful means for structural study. A comparison of the pertinent data led to the formulation of two rules. The first states that the rotation of carbon 1 is not affected by structural changes made on the other carbons; the second states that structural changes on carbon 1 do not affect the rotation of the remainder of the asymmetric sugar molecule. Although these rules of isorotation have many exceptions they have materially aided in the determination of the structures of new sugar derivatives, have been used in the classification of the various isomers, and have led to the correction of many mistakes in the literature [5]. Their application gives satisfactory values when the comparisons are made on closely related substances under strictly comparable conditions. For example, lactose, maltose, cellobiose, and gentiobiose have the glucose configuration and give rotational differences in accord with those obtained for glucose. Likewise, 4-glucosido-mannose and 4-galactosido-mannose are merely substitued mannoses and give rotational differences in agreement with those obtained for mannose [6].

In 1929 the writer [7] calculated the optical rotations for the various asymmetric carbons in the hexoses by Van't Hoff's method and pointed out that the preparation of the then unknown hexoses, talose, allose, and altrose would constitute a test for the validity of the principle as applied to these sugars. Subsequently α-*d*-talose (+68.0) [8], β-*d*-talose [3] (+13.3), β-*d*-allose (−0.2) [9] and β-*d*-altrose (−32.6) [10] have been prepared; the optical rotations, noted in the parentheses, are not in satisfactory agreement with the previously calculated values of +60, −30, −60, and −145. It is therefore evident that the principle of optical superposition in the simple form referred to above

[1] Figures in brackets here and elsewhere in the text correspond to the numbered references at the end of this paper.

[2] The preparation and properties of this new sugar will be described in a subsequent paper by W. W. Pigman and the author.

does not give concordant values for this group of configurationally different sugars. The principle, as stated by Van't Hoff, may be valid provided the asymmetric carbon is replaced by its mirror image and no other changes follow. But each atom in the molecule influences the neighboring atoms and consequently a stereomeric change results in a new distribution of atoms, electrons, and electromagnetic fields so that the conditions necessary for the valid application of the principle are not realized. The effect of changes in the configuration of neighboring groups on the optical rotation of an asymmetric carbon was noted by Rosanoff [11]. This concept has been emphasized further by Freudenberg and Kuhn [12], who point out that the configurations of atoms adjacent to a given asymmetric carbon alter its optical rotation markedly, while the configurations of the atoms separated from the given asymmetric carbon have little influence. It is therefore instructive to compare the optical rotations of the sugars, taking into account the configurations of the groups adjacent to the asymmetric centers under consideration.

TABLE 1.—*Optical rotations* [1] *of the hexoses*

Sugar	$[\alpha]^{20}_D$	Optical superposition equation	Molecular rotation
α-*d*-Glucose	+112.2	$+A_{OH}+R_2-R_3+R_4+R_5=$	+20,210
β-*d*-Glucose	+18.7	$-A_{OH}+R_2-R_3+R_4+R_5=$	+3,370
α-*d*-Mannose	+29.3	$+A_{OH}-R_2-R_3+R_4+R_5=$	+5,280
β-*d*-Mannose	−17.0	$-A_{OH}-R_2-R_3+R_4+R_5=$	−3,060
α-*d*-Galactose	+150.7	$+A_{OH}+R_2-R_3-R_4+R_5=$	+27,140
β-*d*-Galactose	+52.8	$-A_{OH}+R_2-R_3-R_4+R_5=$	+9,510
α-*d*-Talose	+68.0	$+A_{OH}-R_2-R_3-R_4+R_5=$	+12,250
β-*d*-Talose	+13.3	$-A_{OH}-R_2-R_3-R_4+R_5=$	+2,400
α-*d*-Gulose $CaCl_2.H_2O$	+37.1	$+A_{OH}+R_2+R_3-R_4+R_5=$	+11,470
β-*d*-Allose	−0.2	$-A_{OH}+R_2+R_3+R_4+R_5=$	−40
β-*d*-Altrose	+28.7	$-A_{OH}-R_2+R_3+R_4+R_5=$	+5,170

[1] With the exception of β-*d*-allose and β-*d*-altrose the optical rotations are taken from measurements by Isbell and Pigman [13]. The rotation of β-*l*-altrose was reported by Austin and Humoller [14] to be −28.7. As the rotation of its antipode, β-*d*-altrose, differs only in direction, the value +28.7 is used. The rotation of β-*d*-allose was obtained by extrapolation of the data reported by Phelps and Bates [9].

TABLE 2.—*Differences in molecular rotations*

Molecular rotations—		Rotational difference		Configuration of adjacent groups [1]
α-*d*-Glucose−β-*d*-Glucose	=	$2A_{OH}$	+16,840	*d*, +
α-*d*-Galactose−β-*d*-Galactose	=	$2A_{OH}$	+17,630	*d*, +
α-*d*-Mannose−β-*d*-Mannose	=	$2A_{OH}$	+8,340	*d*, −
α-*d*-Talose−β-*d*-Talose	=	$2A_{OH}$	+9,850	*d*, −
α-*d*-Glucose−α-*d*-Mannose	=	$2R_2$	+14,930	α, −
α-*d*-Galactose−α-*d*-Talose	=	$2R_2$	+14,890	α, −
β-*d*-Glucose−β-*d*-Mannose	=	$2R_2$	+6,430	β, −
β-*d*-Galactose−β-*d*-Talose	=	$2R_2$	+7,110	β, −
β-*d*-Allose−β-*d*-Altrose	=	$2R_2$	−5,210	β, +
α-*d*-Gulose−α-*d*-Galactose	=	$2R_3$	−15,670	+, −
β-*d*-Allose−β-*d*-Glucose	=	$2R_3$	−3,410	+, +
β-*d*-Altrose−β-*d*-Mannose	=	$2R_3$	+8,230	−, +
α-*d*-Glucose−α-*d*-Galactose	=	$2R_4$	−6,930	−, +
β-*d*-Glucose−β-*d*-Galactose	=	$2R_4$	−6,140	−, +
α-*d*-Mannose−α-*d*-Talose	=	$2R_4$	−6,970	−, +
β-*d*-Mannose−β-*d*-Talose	=	$2R_4$	−5,460	−, +
β-*d*-Mannose−α-*l*-Gulose	=	$2R_5$	+8,410	+, 0
α-*d*-Talose−β-*l*-Allose	=	$2R_5$	+12,210	−, 0
α-*d*-Galactose−β-*l*-Altrose	=	$2R_5$	+32,310	−, 0

[1] The first term of the symbol represents the configuration of the adjacent carbon which lies above the one under consideration, when the formula is written with the reducing group uppermost, while the second term represents the configuration of the carbon which lies below.

The optical rotations of the hexose sugars are given in table 1 with equations representing their optical rotations according to the principle of optical superposition, while the optical rotations of the different asymmetric carbons, calculated algebraically, are given in table 2. In each case the optical rotation of the asymmetric carbon, perhaps better called the rotational difference, is obtained by subtracting the equations representing the optical rotations in such a manner as to eliminate all the variables except one. In order to bring out any possible connections between the various values for the rotational differences and the configurations of the neighboring groups, the structures of the adjacent groups are indicated by symbols. The first term in the symbol represents the configuration of the adjacent carbon which lies above the one under consideration, when the formula is written with the reducing group uppermost, while the second term represents the configuration of the carbon which lies below.

The rotational difference corresponding to the first or reducing carbon has been designated $2A_{OH}$ in accord with the terminology originated by Hudson. Since the more dextrorotatory member of the alpha-beta pair is designated alpha when the oxygen ring lies to the right, it follows that subtracting the rotation of the beta sugar from the alpha must give a positive difference. Therefore, the values of $2A_{OH}$ given in table 2 are necessarily positive. If the alpha and beta names are used merely to distinguish one isomer from another the relationship between the actual configuration and the optical rotation is of little importance in determining which isomer is to be designated alpha and which beta. But when the alpha and beta names are given a structural significance, as in Isbell's nomenclature, the correctness of the assignments depends on a definite relation between the configurations and the sign of the rotational difference. The conductivity measurements of Böeseken [15, 16, 17] and other experimental data show that the hydroxyl of carbon 1 lies to the right in α-*d*-glucose and α-*d*-galactose when the formulas are written in the Fischer conventional manner. Therefore insofar as these compounds are concerned, *the contribution of the first carbon to the optical rotation of the molecule is positive when the hydroxyl of carbon 1 lies to the right.* It is generally assumed and probably true that this relationship between the configuration of the first carbon and the optical rotation applies to all pyranose sugars. Bromine oxidation measurements made with numerous sugars in the course of this investigation have shown that the alpha forms are oxidized more slowly than the beta forms; the consistent agreement of the reactivity with the names allocated from comparison of the optical rotations supports the validity of the relationship which was used for selecting the names. Hence there is a reasonable basis for the assumption that the optical rotations furnish a reliable guide for classifying the alpha and beta sugars. The classification is based on a qualitative relationship between the configuration of the first carbon and the optical rotation. The quantitative aspects of this relationship appear to be affected by other factors, particularly by the configuration of the adjacent groups. The numerical values for $2A_{OH}$ obtained from the alpha and beta modifications of glucose and galactose are 16,840 and 17,640, while the values from the rotations of mannose and talose are 8,340 and 9,850. The two series differ in the configurations of the adjacent groups. Unfortunately, the optical rotations of the other alpha and

beta sugars are not known so that comparisons cannot be made directly. However, a comparison of the optical rotations of the alpha and beta methyl gulosides, glucosides, and galactosides gives values of $2A_{OCH_3}$ of 39,200, 37,460, and 37,900, respectively [18]. The approximate agreement of these indicates that the rotational differences for the first carbon in the gulose series are close to those obtained for the glucose and the galactose series. Virtually no information is available for idose, altrose, and allose. The configuration of the group adjacent to the first carbon in allose resembles that of glucose, while idose and altrose resemble mannose.

The difference in the optical rotations of two sugars which differ merely in the configuration of the second carbon has been called the "epimeric difference" [19]. This difference has been used to correlate substances of like structure and probably has a legitimate application for this purpose. But the problem is complicated because there are four steric arrangements or combinations involving the configurations of the carbons adjacent to the second carbon. These are represented symbolically in the following manner: (1) α, +; (2) α, −; (3) β, +; (4) β, −. Epimeric pairs corresponding to the first group are not known products at present but would be represented by α-*d*-gulose and α-*d*-idose, or by α-*d*-allose and α-*d*-altrose. The second group is represented by α-*d*-glucose and α-*d*-mannose, and by α-*d*-galactose and α-*d*-talose. The epimeric differences obtained from these pairs, 14,930 and 14,890, are in excellent agreement. The third group is represented by β-*d*-allose and β-*d*-altrose. The epimeric difference for these sugars, −5,210, is entirely different from the others. Since these sugars have not been extensively studied it is quite possible that the optical rotations are not correct or that the sugars are improperly classified. In particular, the substance now known as β-*d*-altrose may have the α-*d*-structure. It might be noted, however, that the difference in the molecular rotations of β-*d*-α-glucoheptose and β-*d*-β-glucoheptose (−5,950) is in accord with that obtained for β-*d*-allose and β-*d*-altrose. The fourth group is represented by β-*d*-glucose and β-*d*-mannose, and by β-*d*-galactose and β-*d*-talose. The epimeric differences obtained from these pairs are 6,430 and 7,110. The epimeric differences obtained for various configurations bring out the need for considering the configuration of adjacent groups in making comparisons and emphasize the complex character of the problem.

The rotational difference for the third carbon, obtained from α-*d*-gulose and α-*d*-galactose (−15,670) deviates widely from the values (−3,410 and 8,230) obtained from β-*d*-allose and β-*d*-glucose, and from β-*d*-altrose and β-*d*-mannose. Inasmuch as β-*d*-allose and β-*d*-altrose may not have the β-pyranose structure, the comparisons may not be properly drawn.

The data available for calculating the rotational differences for the fourth carbon in the hexose series is limited to only one combination for the configurations of the adjacent carbon atoms. Four calculations from the optical rotations of eight sugars give values in approximate agreement with each other, namely, −6,930, −6,140, −6,970, and −5,460.

The determination of the optical rotation of the fifth carbon is complicated because any change in its configuration affects the adjacent ring oxygen which in turn determines the alpha and beta

positions of the first carbon. Consequently, the rotational differences (R_5) in table 2 include the rotation of the fifth carbon and any changes which may be induced by the difference in the alpha and beta structures. The data at hand are not sufficient to calculate the two components separately. The comparisons involving the optical rotations of allose and altrose do not appear to be in accord. This may be caused by improper classification, erroneous optical rotations, unknown structural differences, or to the physical characteristics of the phenomena of optical rotation.

The work of Tschugaeff, Kuhn, Lowry, and others [20] shows that each asymmetric carbon in an optically active substance gives rise to one or more partial rotations, which may be correlated with absorption bands of characteristic frequency which have their origin in particular electronic transitions taking place in the molecule. These transitions are not influenced greatly by atoms or groups not closely related to the asymmetric carbon. The neighboring groups, however, influence one another and thereby affect the partial rotations. The optical rotation in the visible spectrum is chiefly governed by the nearest absorption bands. Since the bands are not located at the same wave lengths for all sugars, the optical rotations for light of different wave lengths vary in irregular fashion. For this reason the difference in the rotations of two sugars depends in part on the light used for making comparison, and it is obvious that the optical rotations cannot be rigorously represented by the simple algebraic equations suggested by Van't Hoff.

Nevertheless, the active part that the principles of optical superposition and isorotation have played in the development of carbohydrate chemistry is sufficient justification for continuing their use. It has been amply demonstrated that substances of similar *structure and configuration* give approximately like rotational differences. In order to facilitate comparison, it is desirable to classify the sugars according to the configuration of the five asymmetric carbons which comprise the pyranose ring. The first of these carbons gives rise to the alpha and beta modifications of the separate sugars. The different configurations of carbons 2, 3, 4, and 5 give the eight fundamental pyranoses from which all of the pyranose sugars may be considered to be derived. The optical rotations and other properties of the members in each group parallel one another. Hence the "rotational differences" for the members of each of the fundamental types are fairly constant and characteristic. For example, agreement is found for sugars containing the alpha mannose structure or the beta mannose, or the alpha glucose or the beta glucose, or for other configurationally related substances. But the values from configurationally different substances are frequently inconsistent. The marked resemblance of the various members of the groups represented by these types has been emphasized previously by Hudson and others and is illustrated further by the optical rotations and oxidation measurements reported in this paper.

II. NOMENCLATURE OF THE ALPHA AND BETA SUGARS

In order to bring out more clearly the structural relationships between the various pyranose sugars, the writer has suggested [21] certain changes in the alpha-beta nomenclature. Originally the alpha-beta names were assigned merely to distinguish one isomer

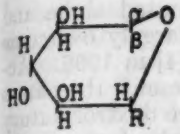

d-Glucose *d*-Xylose *d*-α-Altroheptose *l*-β-Galaheptose

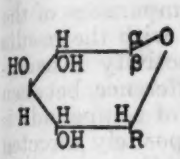

d-Idose *d*-β-Glucoheptose *l*-α-Idoheptose

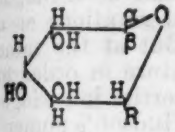

d-Mannose *d*-Lyxose *d*-β-Altroheptose *l*-α-Galaheptose

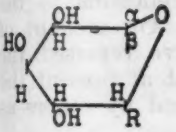

d-Gulose *d*-α-Glucoheptose *l*-β-Idoheptose

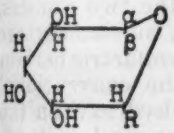

d-Galactose *l*-Arabinose *d*-α-Mannoheptose *l*-β-Guloheptose

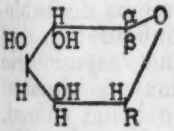

d-Altrose *d*-β-Alloheptose *l*-α-Taloheptose

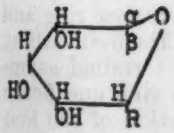

d-Talose *l*-Ribose *d*-β-Mannoheptose *l*-α-Guloheptose

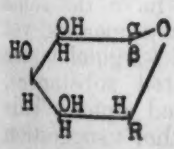

d-Allose *d*-α-Alloheptose *l*-β-Taloheptose

R=CH_2OH R=H R=$\begin{matrix}OH\\|\\C\\|\\H\end{matrix}-CH_2OH$ R=$\begin{matrix}H\\|\\C\\|\\OH\end{matrix}-CH_2OH$

FIGURE 1.—*Structures for the eight pyranose types.*

from another. The first to be prepared was designated alpha and the next beta. This haphazard nomenclature was largely overcome by the introduction of a logical system by Hudson [4] in 1909. According to this system, which is generally used at present, the names are so selected that "in the *d*-series of sugars the more dextrorotatory substance of an alpha-beta pair is designated the alpha form; in the *l*-series the more levorotatory one is so named." Comparisons of the optical rotations of many compounds in conjunction with the results of other investigations, such as the boric acid conductivity measurements of Böeseken, have shown that the large difference between the rotations of the members of an alpha-beta pair of compounds is dependent, at least in large measure, upon the oppositely directed atoms or groups attached to the reducing carbon. On account of this fact and the facility with which comparisons can be made, it seems desirable to retain the comparison of optical rotations as a criterion for naming the alpha and beta sugars. But at the same time it is desirable to modify the present nomenclature in order to classify substances of like structure and similar properties in a single group. It has been recognized for a long time that Hudson's nomenclature results in classifying as beta those derivatives of *l*-arabinose which exhibit chemical and physical properties analogous to the properties of the alpha derivatives of *d*-galactose. On account of these obvious similarities various investigators have reversed the alpha and beta nomenclature for *l*-arabinose so that at present the crystalline sugar is designated by some as alpha and by others as beta.

Hudson's nomenclature depends on two factors, the *d* and *l* configuration of the sugar, and the optical rotation of the two isomers. According to Rosanoff's [22] *d* and *l* classification, substances are designated as *d* when the hydroxyl of the terminal asymmetric carbon lies to the right when the formula is written in the conventional manner with the reducing group uppermost. If the hydroxyl on the terminal asymmetric carbon lies to the left the compound is designated *l*. Thus the antipode of *α*-*d*-glucose is *α*-*l*-glucose. This *d* and *l* classification is satisfactory and no change seems desirable. But there is no fixed relation between the *d* and *l* configuration and the structure of the reducing carbon. The terminal asymmetric carbon which determines the *d* and *l* classification may be situated outside of the pyranose ring remote from the group being named. The configuration of the terminal asymmetric carbon determines the position of the oxygen ring in the aldo-hexoses, but in the heptoses the terminal asymmetric carbon lies outside of the pyranose ring and does not have anything to do with the configuration of the first carbon. Also in the aldo-pentose and keto-hexose series the terminal asymmetric carbon is not involved in forming the oxygen ring and hence it does not have any direct bearing on the configuration of the first carbon. Crystalline *l*-arabinose (+191), *d*-galactose (+151), *d*-*α*-mannoheptose (+120), and *l*-*β*-guloheptose (+120) have the same structure for the pyranose ring and exhibit similar properties, yet according to Hudson's nomenclature *l*-arabinose and *l*-*β*-guloheptose are designated beta, while the structurally related substances, *d*-galactose (+151) and *d*-*α*-mannoheptose, are called alpha. This difficulty may be overcome by application of the author's suggestion [21] to call those isomers in which the hydroxyl of the reducing

carbon (carbon 1 of the aldoses) lies in the same direction as the oxygen of the ring, alpha, and those in which it lies in the opposite direction, beta. This allocation is based on a structural feature and is independent of any specific reaction or property. Classification in accordance with the aforestated concept is presumably obtained by application of the following rule: *The names of the members of the alpha and beta pair of sugars or sugar derivatives are so selected that when the oxygen ring lies to the right, as in d-glucose, the more dextrorotatory member of the alpha-beta pair shall be designated alpha, and the less dextrorotatory member beta; when the oxygen ring lies to the left, as in l-glucose (or in d-galaheptose), the less levorotatory member is called beta.* This results in names for which the subtraction of the rotation of the beta form from that of the alpha gives a positive difference whenever the oxygen ring lies to the right, and a negative difference when the oxygen ring lies to the left.

To provide a convenient means for applying the rule, it is assumed that when the carbon atom, carrying the hydroxyl which originally forms the ring, is asymmetric, the oxygen of the resulting ring lies in the direction of the parent hydroxyl. This direction is ascertained by inspection of the Fischer projectional formulas. Thus the direction of the oxygen ring, as right or left, is defined in a comparative manner in the same way that the Fischer projectional formulas define the positions of the various atoms in optically active substances.

Although the carbon atom united with the ring oxygen in the aldopentoses and keto-hexoses is not asymmetric, it is tied up in the ring, forming a dissymmetric structure which resembles one and only one of the eight fundamental pyranose types. On account of this marked similarity, no difficulty is encountered in selecting appropriate names for the pentoses and other sugars in which the carbon united with the ring oxygen is not asymmetric. The resemblance of crystalline *l*-arabinose to *α-d*-galactose, and of *β-l*-arabinose $CaCl_2.4H_2O$ to *β-d*-galactose, and of *α-d*-xylose to *α-d*-glucose, and of *α-* and *β-d*-lyxose to *α-* and *β-d*-mannose has been pointed out heretofore [13], and it has been shown that the rates of oxidation support the hypothesis that these sugars are genetically related and that in each one the oxygen ring lies to the right. Hence crystalline *l*-arabinose is considered to be related in ring structure to the *d*-hexoses and its classification is made accordingly. This results in a reversal of Hudson's nomenclature for the alpha and beta derivatives of *d-* and *l*-arabinose. Universal adoption of this change would clear up the present confusion in the nomenclature of this sugar. Structures can be assigned to the various keto-hexoses by comparison of their properties with the properties of the keto-heptoses whose structures are fixed by the asymmetry of the carbon atom united with the oxygen ring. The following Fischer projectional formulas reveal that *d*-fructose could be structurally related to *l*-galactose or to *d*-altrose. The keto-heptose analogous to *d*-altrose is *d*-altroheptulose (sedoheptose) [23], and the one analogous to *l*-galactose is *l*-galaheptulose (perselose) [24]. Sedoheptose and *d*-altrose [10] differ markedly from *d*-fructose in that they form anhydro-compounds by merely heating in acid solution. Furthermore, crystalline *d*-fructose is levorotatory and exhibits mutarotation from −133 to −92, while sedoheptose is dextrorotatory and does not exhibit mutarotation. Perselose, on the other hand, resembles *d*-fructose in that it is levorotatory and exhibits mutarotation

from −90 to −80. Therefore the ring in *d*-fructose lies to the left, as in perselose, and the crystalline sugar is called *α*-*d*-fructose. The classification of *d*-sorbose (+42.9) and *d*-tagatose (+1.0) is made in like manner.

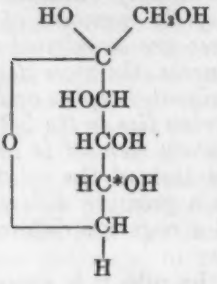

α-*d*-Fructose

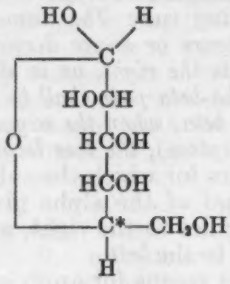

α-*l*-Galactose

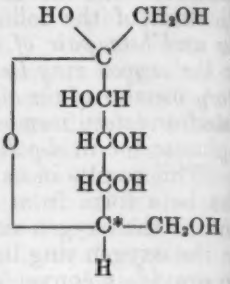

Perselose

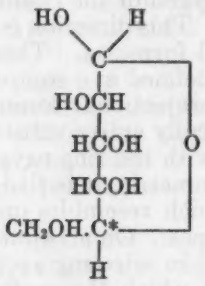

β-*d*-Altrose

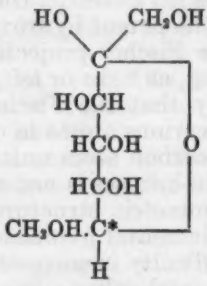

Sedoheptose

Thus *α*-*d*-sorbose (+42.9) resembles *α*-*d*-glucoheptulose (+67.4) and *α*-*d*-tagatose (+1) resembles *α*-*d*-mannoheptulose (+29.37). A number of comparisons can be drawn between the optical rotations of fructose, sorbose, and tagatose, on the one hand, and the structurally related pentoses, hexoses, and heptoses on the other. Such comparisons have been made by Hudson [25] in the course of an investigation having a different concept but which leads to a like correlation of structurally similar sugars. Hudson's work shows that *l*-arabinose, *d*-galactose, and *l*-fructose are related structurally in the same way as *d*-xylose, *d*-glucose, and *d*-sorbose, or *d*-lyxose, *d*-mannose, and *d*-tagatose. As a final result of the above considerations it can be stated that *l*-fructose, *d*-sorbose, and *d*-tagatose are genetically related to the *d*-aldo-hexoses and that it is necessary to change the alpha and beta names for the pyranose derivatives of fructose. The soundness of this classification cannot be tested by bromine oxidation measurements, because the ketoses do not react readily with this reagent. Nevertheless, the optical rotations and other properties furnish a substantial basis for this classification.

The changes in nomenclature which have been suggested will alter the names of those substances in which the configuration of the carbon forming the oxygen ring differs from the configuration of the terminal asymmetric carbon. Thus the names will be reversed for the isomeric sugars and derivatives of arabinose, fructose, and the galaheptoses,

guloheptoses, taloheptoses, and idoheptoses. The changes in the present system of naming the alpha and beta sugars have been advanced in order to eliminate some of the obvious shortcomings of the present system. An attempt has been made to group substances having like pyranose rings, regardless of what may be the configuration of the groups in the appendage. It is recognized that no simple nomenclature will account for all properties because each group in the molecule influences the others and produces characteristic properties.

III. MUTAROTATIONS OF THE HEPTOSES AND THE STRUCTURALLY RELATED HEXOSES

In order to prove that the configuration of the fifth carbon in the aldoses determines the direction of the oxygen ring and that a more satisfactory classification of the alpha and beta sugars is obtained by basing the nomenclature on the configuration of the fifth carbon, rather than on the *d* and *l* configurational series, the writer has synthesized and studied the properties of a number of heptose sugars which are pertinent to this subject. These sugars were prepared from the corresponding hexoses by the cyanhydrin synthesis [26]. The methods used for their preparation are described in the literature and will not be reviewed in this paper. The intermediate products and the crystalline sugars, however, were separated without seed from other sources and with relatively little difficulty.

Characteristic and important variations in the mutarotations of the sugars are indicative of the changes and reactions of the first carbon, and, therefore, it is of interest to compare the mutarotations of the heptoses and hexoses in order to bring out similar characteristics which may be used for the correlation of substances of like structure. It was shown by Smith and Lowry [27] that the optical rotation of a freshly prepared solution of *α-d*-galactose changes rapidly at first, decreasing in a few minutes to a uniform rate; while the optical rotation of a freshly prepared solution of *β-d*-galactose changes slowly at first, increasing in a few minutes to the rate characteristic of the latter part of the mutarotation of the alpha modification. Similar changes are also exhibited by *α-* and *β-l*-arabinose. As two of the heptoses have the galactose structure for the pyranose ring, it is of interest to determine whether they give like mutarotation curves, and if so, to ascertain which of the modifications corresponds to *α-d*-galactose and which to *β-d*-galactose.

The mutarotations of *α-d*-galactose, *α-l*-arabinose, *α-d-α*-mannoheptose, and *α-d-β*-guloheptose are illustrated by the curves of figure 2, while the mutarotations of *β-d*-galactose, *β-l*-arabinose $CaCl_2.4H_2O$, and *β-d-α*-mannoheptose are illustrated in figure 3. The curves for *α-* and *β-d*-galactose and *l*-arabinose are based on the measurements reported recently [13], while those for *α-* and *β-d-α*-mannoheptose and *α-d-β*-guloheptose are based on the data in table 3. As the rotational differences are plotted on a semilogarithmic scale, the deviations from the simple monomolecular course is represented by the divergence of the rotational curve from a straight line. Since the mutarotations of the pentoses take place much more rapidly than the mutarotations of the hexoses and heptoses, the curves are drawn on different time scales, as indicated at the bottom of the figure. The curves show that the optical rotations of the alpha modifications

change more rapidly at first, decreasing in a few minutes to a uniform rate. This is characteristic of the α-*d*-galactose structure. The optical rotations of the beta isomers, however, change slowly at first,

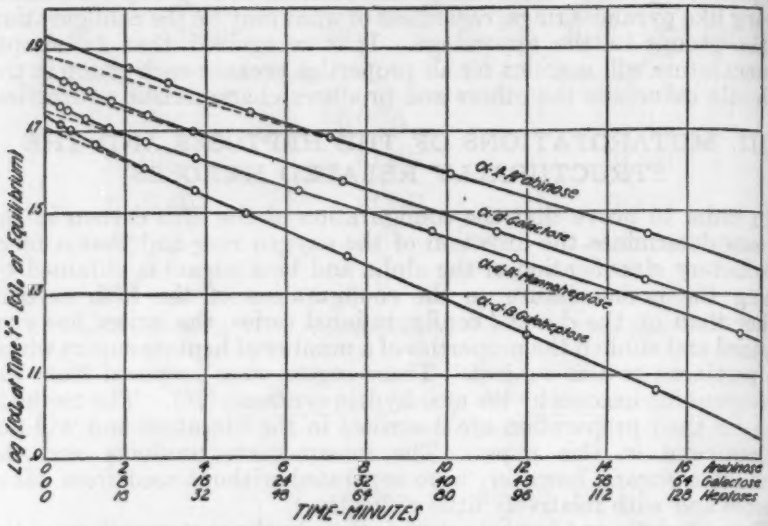

FIGURE 2.—*Mutarotations of sugars related to α-d-galactose.*

increasing in a few minutes to a uniform rate. The striking similarity of the mutarotation curves obtained for the members of the first group, on the one hand, and for the members of the second group on

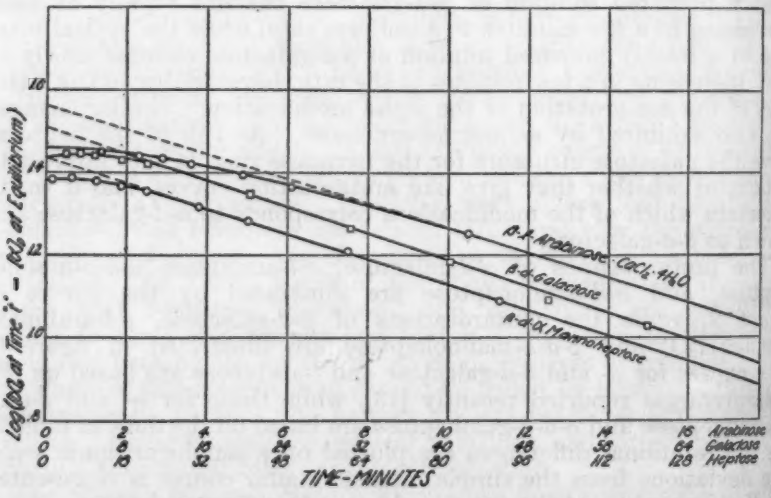

FIGURE 3.—*Mutarotations of sugars related to β-d-galactose.*

the other, supports the nomenclature which designates the members of the first group as alpha, and the members of the second group as beta.

TABLE 3.—*Complex mutarotations of sugars in water* [1]

α-d-a-MANNOHEPTOSE (HYDRATE)

3.5 g per 100 ml at 20° C read in a 4-dm tube.
$°S = 1.37\times10^{-.04881t} + 21.12\times10^{-.003911t} + 26.33.$
$[\alpha]^{20}_D = 3.4\times10^{-.04834t} + 51.9\times10^{-.003911t} + 64.7.$

Time	Observed reading	$(k_1+k)_2\times10^3$	$m_1\times10^3$	Deviation	$m_2\times10^3$
Minutes	°S			°S	
0				(+1.37)	
2.89	+47.90			+0.99	
4.48	+47.42	6.14		+.81	(54.8)
5.88	+47.11	5.42		+.75	40.3
8.20	+46.47	5.61		+.52	52.7
10.31	+46.02	5.34		+.44	47.5
12.81	+45.44	5.30		+.29	53.8
15.36	+44.97	5.08		+.25	47.9
20.02	+44.08	4.94		+.11	(55.7)
25.10	+43.21	4.79		+.03	
30.28	+42.41	4.66			
40.37	+41.02	4.45	3.89		
50.47	+39.72	4.35	3.93		
60.93	+38.57	4.24	3.87		
77.11	+36.92	4.16	3.87		
93.55	+35.46	4.12	3.89		
139.08	+32.30	4.10	3.96		
190.38	+30.06	4.06	3.96		
290.14	+27.85	4.01	3.94		
∞	+26.33				
Average			3.91		48.5

β-d-a-MANNOHEPTOSE (HYDRATE)

4 g per 100 ml at 20° C read in a 4-dm tube.
$°S = 1.4\times10^{-.0481t} - 12.0\times10^{-.003941t} + 30.89.$
$[\alpha]^{20}_D = 2.9\times10^{-.0481t} - 25.1\times10^{-.003941t} + 64.5.$

Time	Observed reading	$(k_1+k_2)\times10^3$	$m_1\times10^3$	Deviation	$m_2\times10^3$
Minutes	°S			°S	
0					
1.20	+20.25			+1.23	
2.25	+20.24	0.00		+1.11	(42.5)
5.18	+20.23	.00		+0.80	46.9
9.96	+20.37	.56		+.47	47.7
15.02	+20.65	1.20		+.27	47.6
20.05	+20.98	1.64		+.14	50.1
24.89	+21.35	2.00		+.09	47.9
30.37	+21.76	2.28		+.04	(51.0)
40.17	+22.48	2.62			
50.26	+23.20	2.87	3.86		
60.00	+23.84	3.04	3.86		
90.17	+25.51	3.33	3.88		
150.09	+27.72	3.53	3.84		
212.51	+29.05	3.61	3.83		
271.0	+29.78	3.64	3.81		
441.5	+30.64	3.70	3.80		
∞	+30.89				
Average			3.84		48.0

[1] The equations and values for m_1 and m_2 are determined by the method described by Isbell and Pigman, J. Research NBS 18, 156 (1937) RP969.

TABLE 3.—*Complex mutarotations of sugars in water*—Continued

α-*d*-β-GULOHEPTOSE

4 g per 100 ml at 20° C read in a 4-dm tube

$°S = -24.06\times10^{-.001331t} - 1.81\times10^{-.0007t} - 30.44$

$[\alpha]_D^{20} = -51.5\times10^{-.001331t} - 3.9\times10^{-.0007t} - 65.1$

Time	Observed reading	$(k_1+k_2)\times10^3$	$m_1\times10^3$	Deviation	$m_2\times10^3$
Minutes	°S			°S	
0				−1.81	
3.13	−54.77			−1.18	
5.09	−53.94	7.68		−.90	60.1
7.84	−52.94	7.21		−.65	55.0
9.95	−52.22	7.05		−.49	56.0
14.92	−50.69	6.76		−.21	63.6
19.89	−49.39	6.48		−.10	64.0
24.89	−48.18	6.40		−(.01)	
29.94	−47.10	6.13			
39.98	−45.22	5.87	5.18		
50.27	−43.45	5.77	5.28		
60.18	−41.93	5.71	5.34		
75.08	−39.94	5.68	5.40		
96.01	−37.84	5.57	5.33		
121.89	−35.87	5.48	5.29		
180.08	−33.06	5.47	5.35		
250.97	−31.45	5.58	5.51		
∞	−30.44				
Average			5.33		59.7

β-*d*-β-GLUCOHEPTOSE

5 g per 100 ml at 20° C read in a 4-dm tube

$°S = +6.5\times10^{-.0004t} - 6.5\times10^{-.0108t} - 0.08$

$[\alpha]_D^{20} = +11.3\times10^{-.0004t} - 11.3\times10^{-.0108t} - 0.13$

Time	Observed reading	$(k_1+k_2)\times10^3$	$m_1\times10^3$	Deviation	$m_2\times10^3$
Minutes	°S			°S	
0				(+6.53)	
1.3	−0.81			+5.57	
3.2	−1.56			+4.53	49.6
5.1	−2.14			+3.67	48.9
7.5	−2.72			+2.77	49.7
10.0	−3.00			+2.15	48.3
15.0	−3.35			+1.21	48.7
18.0	−3.43			+.81	50.3
20.0	−3.41			+.63	50.7
30.0	−3.00				
40.0	−2.48				
50.0	−1.96		10.6		
60.0	−1.56		10.5		
70.0	−1.21		10.8		
80.0	−.92		11.3		
90.0	−.75		11.0		
100.0	−.64		10.6		
120.0	−.40		10.8		
∞	−.08				
Average			10.8		49.5

TABLE 4.—*First-order mutarotations*

α-d-α-GALACTOHEPTOSE (HYDRATE)

4 g per 100 ml at 20° C read in a 4-dm tube.

$°S = -5.19 \times 10^{-.00471t} - 6.48$

$[\alpha]_D^{20} = -11.2 \times 10^{-.00471t} - 14.0$

Time	Observed reading	$(k_1+k_2)\times 10^3$	Time	Observed reading	$(k_1+k_2)\times 10^3$
Minutes	°S		*Minutes*	°S	
1.77	−11.57		60.12	−9.13	4.86
3.55	−11.49	(3.88)	90.17	−8.39	4.82
10.35	−11.14	4.46	121.6	−7.82	4.84
15.07	−10.91	4.53	255.2	−6.86	4.45
19.93	−10.66	4.71	393.0	−6.55	4.76
25.04	−10.42	4.78	∞	−6.48	
30.77	−10.18	4.78			
45.61	−9.61	4.82	Average		4.71

β-d-α-GLUCOHEPTOSE

4 g per 100 ml at 20° C read in a 4-dm tube.

$°S = -3.90 \times 10^{-.00691t} - 9.28$

$[\alpha]_D^{20} = -8.5 \times 10^{-.00691t} - 20.2$

Time	Observed reading	$(k_1+k_2)\times 10^3$	Time	Observed reading	$(k_1+k_2)\times 10^3$
Minutes	°S		*Minutes*	°S	
3.59	−12.93		47.55	−10.88	8.15
5.04	−12.78	(12.57)	60.19	−10.54	8.16
9.85	−12.54	7.84	79.18	−10.12	8.44
15.16	−12.27	7.49	91.03	−9.99	8.13
20.06	−12.02	7.56	121.94	−9.62	8.71
25.23	−11.79	7.51	∞	−9.28	
29.99	−11.55	7.81			
			Average		7.98

β-d-β-GALAHEPTOSE

4 g per 100 ml at 20° C read in a 4-dm tube.

$°S = 16.05 \times 10^{-.00197t} - 24.89$

$[\alpha]_D^{20} = 34.9 \times 10^{-.00197t} - 54.1.$

Time	Observed reading	$(k_1+k_2)\times 10^3$	Time	Observed reading	$(k_1+k_2)\times 10^3$
Minutes	°S		*Minutes*	°S	
4.54	−9.15		90.24	−14.24	1.98
8.08	−9.39	1.88	120.02	−15.54	1.96
11.29	−9.65	2.08	179.96	−17.85	1.99
14.80	−9.91	2.09	264.79	−20.10	1.99
19.93	−10.17	1.89	329.25	−21.24	1.95
30.40	−10.87	1.94	415.00	−22.37	1.94
39.94	−11.45	1.94	∞	−24.89	
61.36	−12.71	1.96			
			Average		1.97

TABLE 5.—*Optical rotations of related sugars*

Sugar	Initial $[\alpha]_D^{20}$	Equilibrium $[\alpha]_D^{20}$	$[\alpha]_D^{20}$ at t minutes after dissolving crystals	Molecular rotation $[M]$
α-*l*-Arabinose	+190.6	+104.5	$+8.8\times10^{-.138t}+77.3\times10^{-.030t}+104.5$	+28,610
α-*d*-Galactose	+150.7	+80.2	$+5.6\times10^{-.0760t}+64.9\times10^{-.00803t}+80.2$	+27,150
α-*d*-α-Mannoheptose (hydrate)	+120.0	+64.7	$+3.4\times10^{-.0455t}+51.9\times10^{-.00291t}+64.7$	+27,380
α-*l*-β-Guloheptose[a]	+120.5	+65.1	$+3.9\times10^{-.0697t}+51.5\times10^{-.00233t}+65.1$	+25,320
β-*l*-Arabinose [b]	+75.5	+104.5	$+7.6\times10^{-.1764t}-36.6\times10^{-.030t}+104.5$	+11,560
β-*d*-Galactose	+52.8	+80.2	$+4.9\times10^{-.0883t}-32.3\times10^{-.00813t}+80.2$	+9,510
β-*d*-α-Mannoheptose (hydrate)	+42.3	+64.5	$+2.9\times10^{-.045t}-25.1\times10^{-.003564t}+64.5$	+9,650
β-*l*-Glucose [a]	−18.7	−52.7	$+34.0\times10^{-.00588t}-52.7$	−3,370
β-*d*-β-Galaheptose	−19.2	−54.1	$+34.9\times10^{-.00197t}-54.1$	−4,030
α-*l*-Lyxose [a]	−5.6	+13.8	$-19.4\times10^{-.0858t}+13.8$	−860
α*l*-Mannose [a]	−29.3	−14.2	$-15.1\times10^{-.0173t}-14.2$	−5,280
α-*d*-α-Galaheptose (hydrate)	−25.2	−14.0	$-11.2\times10^{-.00471t}-14.0$	−5,750
β-*d*-Gulose	(c)	−26.4		
β-*d*-α-Glucoheptose	−28.7	−20.2	$-8.5\times10^{-.0090t}-20.2$	−4,240
β-*d*-Idose	(c)	(c)		
β-*d*-β-Glucoheptose	−0.1	−0.1	$+11.3\times10^{-.0504t}-11.3\times10^{-.0168t}-0.1$	−40

[a] Data from results obtained with the optical antipode.
[b] Data from the calcium chloride compound.
[c] Unknown.

As may be observed from the data given in table 4, the mutarotation of α-*d*-α-galaheptose follows, within the experimental error, the unimolecular course and gives a constant value of 0.0047 for k_1+k_2. This is not in accord with the observations of Hann, Merrill, and Hudson [28] who report a drift in the velocity constant from 0.032 to 0.016. The mutarotation of β-*d*-β-galaheptose is in essential agreement with that reported recently by Hann and Hudson [46] except that it is slightly slower. The mutarotation of β-*d*-α-glucoheptose was also found to take place at a slower rate ($k_1+k_2=0.008$) than that (0.0122) reported by Hudson and Yanovsky [29]. The mutarotations of the sugars having the glucose, mannose, and gulose structures follow the unimolecular formula, while the mutarotations of the heptoses having the galactose and idose structures do not follow the unimolecular course and require for expression equations containing two exponential terms. The striking similarity of substances with like configurations for the carbons comprising the pyranose ring clearly indicates that the members of such groups have like structures. The complex mutarotations may arise from the formation of the free aldehyde or furanose modifications in the equilibrium solution or from the interconversion of two or more strainless ring isomers.

IV. CONFORMATION OF THE PYRANOSE RING

It was pointed out by Haworth [30] that various geometric forms are possible for the pyranose ring. Thus if the carbon and oxygen atoms comprising the ring were coplanar the valence angles would be larger than 109°, required to give a strainless ring; if the ring is strainless the valence angles for the carbon atoms will be about 109° and the carbon and the oxygen atoms cannot lie in a single plane. As measurements of dipole moments for simple substances containing the pyranose ring reveal that the oxygen valence bonds form an angle considerably less than 109°, it seems probable that the pyranose ring is bent or puckered [31, 32]. Although ten or more strainless ring structures are possible [33] they can be reduced to three types, as represented in fig. 4: (I) a *trans* structure in which four atoms lie in one plane, and the two remaining atoms lie on opposite sides of this plane; (II) a *cis* or boat-shaped structure in which 2 atoms lie on the same side of the plane formed by the four remaining atoms; (III) and (IV) structures in which the carbon atoms are coplanar and the ring-oxygen is not in the same plane. The monoplanar strained model is represented by (V).

The X-ray investigations of Cox [32] and others indicate that the carbon atoms forming the ring in many sugars are coplanar, while the ring-oxygen lies outside the plane of the carbon atoms. Two structures of this character are possible for each hexose; in one of these the sixth carbon lies approximately in the plane of the carbon ring, as in (III); in the other it lies opposite the ring-oxygen, directed towards the first carbon as in (IV). At this time there is not a satisfactory chemical method for deciding which models correspond to the free sugars. Several sugar derivatives exist which for stereomeric reasons are limited to certain models. Thus trimethyl 1,4-anhydroglucopyranose [34] requires the conformation of a boat-shaped ring in which carbons 1 and 4 lie in the trough. The model which will serve for this compound, however, will not serve for 2,3-4,6-diacetone α-methyl mannopyranoside [35], because in order to form a 1,4-

anhydro derivative the hydroxyl on carbon 4 (which is the same for mannose and glucose) must be directed towards carbon 1 which is in opposition to carbon 6. It is thus apparent that the conformation of the pyranose ring is not the same for all sugar derivatives. It is possible that the various modifications exist in dynamic equilibrium. Consequently the particular modification which results after condensation with a second group is not necessarily the same modification

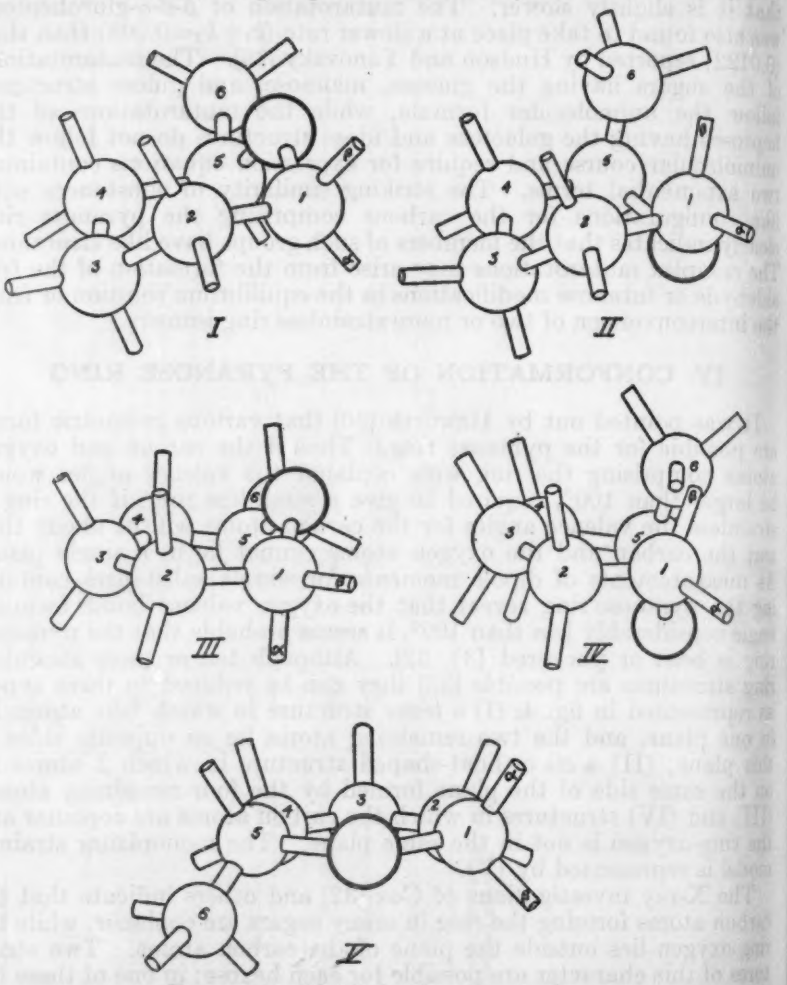

FIGURE 4.—*Models for the pyranose ring.*

as that of the original sugar. It seems probable, however, that structurally related substances such as *α-l*-arabinose, *α-d*-galactose, *α-d*-fucose, *α-l*-fructose, *α-d-α*-mannoheptose, etc., have similar ring conformations. It can be observed from models (III) and (IV), illustrated in figure 4, that the ring-oxygen might be directed to either side of the plane of the carbon atoms. But since no more than two isomers of any one ring type are known, it seems probable that each free sugar occurs in only one ring conformation. The separate sugars, however, may have different conformations.

If the sugars had the coplanar ring, the alpha and beta positions would be symmetrically located with respect to the plane of the carbon-oxygen ring, and there would be no fundamental difference between the alpha and beta sugars. But if the oxygen and carbon atoms forming the ring did not lie in one plane, the alpha and beta positions would not be symmetrically located with respect to the carbon-oxygen skeleton, and would be influenced to different degrees by the oxygen of the ring. Presumably this unequal influence would result in differences in the reactivity of the alpha and beta modifications. The positions of the hydrogen and hydroxyl groups of carbons 2, 3, and 4 might also affect the reaction rates of the alpha and beta sugars, either directly or by causing alterations in the conformation of the pyranose ring to give various strainless ring isomers. Thus a comparison of the reaction rates of the alpha and beta pyranoses should provide information about the conformation of the pyranose ring.

V. BROMINE OXIDATION MEASUREMENTS

As shown by Isbell and Hudson [36, 37], the aldose sugars are oxidized by bromine water in slightly acid solution to give delta lactones in nearly quantitative yield. Presumably the ring modifications of the sugar are oxidized directly according to the following equation:

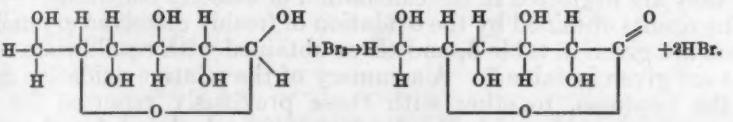

Since this reaction is nearly quantitative and is characteristic of the glycosidic group, it is particularly suitable for investigating the relationships between the stereomeric configurations and the reaction rates. In order to do this, the author developed a set of experimental conditions under which it is possible to follow the oxidation of the separate isomers [38, 39]. The oxidation is conducted at 0° C in the presence of barium carbonate and carbon dioxide. These reagents act as a buffer and maintain a slightly acid reaction, so that the interconversion of the various isomeric modifications of the sugar is slow and the oxidation reaction is rapid. The crystalline sugar is added to the buffered aqueous bromine solution, and the rate of reaction is determined by analysis. The alpha and beta sugars are oxidized at widely different rates, thus providing a convenient means for determining the proportions of these sugars in mixtures. Kinetic studies with equilibrium solutions provide information on the composition of the equilibrium mixture and enable the determination of reaction rates for isomers which are not known in the crystalline state. Heretofore oxidation measurements have been published on the pentoses and on the hexoses with the exception of allose, altrose, and idose. In this paper work on six heptoses is reported.

The procedure previously used was modified slightly to permit the use of smaller quantities of the sugars. The crystalline sugar (0.210 g) and 1.2 g of barium carbonate are placed in a 100-ml long-neck flask and cooled to 0° C in an ice bath. Twenty milliliters of a cold solution, containing 60 g of barium bromide [$Ba(Br)_2.2H_2O$], 20 ml of bromine, and 4 ml of *N* hydrobromic acid per liter, is added and the mixture is shaken continuously. After definite time intervals,

the oxidation is stopped by mixing the solution with 5 ml of linseed oil dissolved in 10 ml of benzene. The oil is separated by centrifuging, and the quantity of reducing sugar in the aqueous solution is determined by use of alkaline copper sulphate in the usual manner.

The oxidation of the equilibrium mixture is conducted in like manner except that a solution of the sugar in 10 ml of water is mixed with 1.2 g of barium carbonate and 10 ml of an oxidizing solution, containing 120 g of barium bromide, 40 ml of bromine, and 8 ml of *N* hydrobromic acid per liter. This gives the same concentrations of the reactants as is used for the crystalline sugars. The total bromine in the oxidizing solution is determined by thiosulphate titration, and the concentration of the oxidant (free bromine) and the velocity constants are calculated as described in previous papers [13, 39].

In each case the concentration of sugar at zero time should have been 10.5 mg per milliliter, but the concentrations obtained by extrapolation of the results from the analyses to zero time are usually slightly larger than this figure. The difference, which appears to be somewhat larger than the experimental error, cannot be explained at present. It is possible that the bromine reacts during the first few minutes in such manner as to increase temporarily the reducing power of the solution.[4] The increase is small and by making all calculations on the analytical data the errors are largely compensated, and therefore they are neglected in the calculation of velocity constants.

The results obtained by the oxidation of freshly dissolved crystalline sugars are given in table 6, and those obtained with equilibrium solutions are given in table 7. A summary of the relative oxidation rates for the heptoses, together with those previously reported for the hexoses, is given in table 8. Each rate is calculated for the total reaction and is based on the rate for the oxidation of α-*d*-glucose as 1. The relative reaction rates marked by asterisks are obtained by the oxidation of the equilibrium mixtures; the others are from the measurements on the freshly dissolved crystalline sugars.

The results are in accord with the author's earlier observations [21] that isomers in which the hydroxyl groups of carbon 1 are *trans* to the ring-oxygen are oxidized more rapidly than those in which the hydroxyl and ring-oxygen atoms lie in the same direction. This difference in reactivity is in harmony with the postulation that the two positions are not symmetrically located with respect to the ring-oxygen and that the substances containing the hydroxyl in the *cis* and *trans* positions differ fundamentally in structure. This concept is in agreement with a strainless ring structure in which the ring-oxygen is not symmetrically located with respect to the alpha and beta positions. In view of the large number of strainless ring isomers which might be postulated, the determination of the location of the various atoms in space appears to represent an extremely long and complicated problem. By considering the pentoses, heptoses, and higher sugars as substituted hexoses, the problem may be reduced to the determination of the structures of the alpha and beta modifications of the eight hexose types.

[4] If a sugar solution, buffered with sodium acetate and acetic acid, is treated first with bromine and then with linseed oil to remove the excess bromine, a colorless solution is obtained which on standing several hours regenerates a small quantity of free bromine. Thus it would appear that an addition product, hypobromite, peroxide, or other substance capable of yielding free bromine in the presence of a bromide is formed in small quantity during the oxidation or by the linseed oil treatment. This substance may be a byproduct or an intermediate in the reaction. Such substances may account for the small discrepancy in the analytical data. In any case the byproduct does not accumulate in solution because the sugars appear to be converted to the corresponding monobasic acids or lactones in yields which exceed 95 percent.

TABLE 6.—*Bromine oxidations of freshly dissolved crystalline sugars at* 0° C

Time after beginning oxidation	Unoxidized sugar	Averages for oxidation period			Velocity constants $ak=\frac{1}{t}\log\frac{A}{A-X}$	
		Bromide ($\overline{Br}$)	Bromine (Br_2)	Free bromine (a)	$ak\times10^3$	$k\times10^3$
α-d-a-MANNOHEPTOSE (HYDRATE)						
Minutes	mg/ml	*Moles/liter*	*Moles/liter*	*Moles/liter*		
10	9.30	0.364	0.366	0.087		
20	8.64	.367	.364	.085	0.00320	37.6
30	7.91	.370	.363	.084	.00362	43.1
Average						40.4
β-d-a-MANNOHEPTOSE (HYDRATE)						
0.8	9.39	.366	.363	.085		
5.0	3.01	.403	.346	.070	117.6	1680
10.0	0.62	.416	.335	.064	128.3	2005
Average						1843
α-d-β-GULOHEPTOSE						
10.0	9.28	.366	.365	.086		
30.0	8.23	.372	.262	.083	2.61	31.4
60.0	6.48	.382	.357	.079	2.92	37.0
Average						34.2
β-d-β-GALAHEPTOSE						
0.6	9.61	.364	.366	.086		
5.0	3.06	.403	.347	.070	113.0	1614
10.0	0.85	.423	.337	.063	112.0	1778
Average						1696
α-d-a-GALAHEPTOSE (HYDRATE)						
10.0	10.38	.361	.367	.088		
30.0	7.76	.374	.361	.082	6.31	77.0
60.0	5.68	.385	.356	.078	5.24	67.2
Average						72.1
β-d-a-GLUCOHEPTOSE						
0.3	10.62	.360	.368	.088		
5.0	7.65	.374	.361	.082	30.3	370
10.0	5.49	.387	.355	.077	29.5	383
20.0	2.81	.404	.346	.070	29.3	419
30.0	1.58	.415	.341	.066	27.8	421
60.0	0.47	.428	.334	.061	22.7	372
Average						393
β-d-β-GLUCOHEPTOSE						
0.7	10.74	.360	.368	.088		
5.0	7.75	.374	.361	.082	33.0	402
10.0	5.58	.386	.355	.077	30.6	397
20.0	3.47	.400	.348	.071	25.4	358
60.0	1.09	.421	.338	.064	16.8	263
Average						355

TABLE 7.—*Bromine oxidations at 0° C of aqueous sugar solutions in equilibrium at the beginning of the oxidation*

Time	Unoxidized sugar			Averages for the oxidation period			Velocity constants			
							More reactive fraction		Less reactive fraction	
	Total	More reactive fraction	Less reactive fraction	Bromide (Br^-)	Bromine (Br_2)	Free bromine (a)	$ak_B \times 10^3$	$k_B \times 10^3$	$ak_A \times 10^3$	$k_A \times 10^3$
d-α-MANNOHEPTOSE (HYDRATE)										
Minutes	mg/ml	mg/ml	mg/ml	*Moles/liter*	*Moles/liter*	*Moles/liter*				
0	10.47	7.04	3.43							
0.5	9.43	6.02	3.40	0.365	0.375	0.090				
5.0	4.76	1.48	3.34	.372	.372	.087	135.4	1,556		
20.0	2.88		2.88	.392	.358	.076				
60.0	2.12		2.12	.420	.347	.067			3.33	49.7
Average								1,556		49.7
d-β-GULOHEPTOSE										
0	10.92	6.88	4.04							
0.5	9.85	5.83	4.02	.363	.376	.090				
5.0	5.22	1.31	3.91	.383	.365	.081	144.1	1,779		
20.0	3.55		3.55	.409	.354	.071				
60.0	2.75		2.75	.422	.347	.066			2.77	42.0
120.0	2.08		2.08	.430	.343	.064			2.32	36.2
Average								1,779		39.1
d-β-GALAHEPTOSE										
0	11.27	7.08	4.19							
0.5	9.94	5.77	4.18	.363	.376	.090				
5.0	5.21	1.11	4.10	.386	.365	.080	158.9	1,987		
20.0	3.85		3.85	.409	.354	.071				
60.0	3.31		3.31	.420	.348	.067			1.64	24.5
120.0	2.59		2.59	.426	.345	.065			1.72	26.5
Average								1,987		25.5
d-α-GALAHEPTOSE (HYDRATE)										
0	10.91	2.25	8.66							
0.5	10.46	1.86	8.60	.361	.377	.091				
5.0	8.56	0.43	8.13	.369	.373	.087	141.3	1,624		
8.0	7.93	.10	7.83	.374	.371	.086	169.3	1,969		
20.0	6.75		6.75	.380	.367	.083				
30.0	5.91		5.91	.389	.363	.079			5.77	73.0
60.0	4.58		4.58	.399	.357	.074			4.21	56.9
Average								1,797		65.0
d-α-GLUCOHEPTOSE										
0	11.12	9.81	1.31							
0.6	10.56	9.26	1.30	.360	.378	.091				
5.0	7.47	6.21	1.27	.375	.372	.086	39.6	460		
20.2	3.06	1.92	1.15	.395	.362	.077	35.0	455		
60.0	0.88		0.88	.428	.345	.065				
120.0	0.61		0.61	.441	.338	.060			2.65	44.2
Average								458		44.2
d-β-GLUCOHEPTOSE										
0	10.74	8.39	2.35							
0.5	10.41	8.12	2.35	.360	.378	.091				
5.0	8.10	5.85	2.30	.369	.373	.087	31.8	366		
20.0	4.18	2.07	2.14	.393	.361	.077	30.6	397		
60.0	1.78		1.78	.426	.350	.067				
120.0	1.37		1.37	.432	.342	.063			1.90	30.2
Average								382		30.2

TABLE 8.—*Rates of oxidation of the alpha and beta sugars in aqueous solutions at 0° C containing 0.05 mole of sugar, and approximately 0.08 mole of free bromine per liter and buffered with barium carbonate and carbon dioxide*

Sugar	Relative reaction rates $\frac{k_{sugar}}{k_{\alpha\text{-}d\text{-}glucose}}$		k_β/k_α	Less reactive fraction in equilibrium solution
	Alpha form (*cis*)	Beta form (*trans*)		
HEPTOSES				
				Percent
d-β-Galaheptose	*0.8	53	66	37
d-α-Galaheptose	2.3	*56	25	79
d-α-Mannoheptose	1.3	58	46	33
d-β-Guloheptose	1.1	*56	52	37
d-α-Glucoheptose	*1.4	12	9	12
d-β-Glucoheptose	*.9	11	12	22
HEXOSES				
Glucose	1.0	39	39	37
Mannose	1.6	24	15	69
Galactose	1.3	50	38	31
Gulose	2.2	13	6	18
Talose	2.4	*26	11	56

* Rate derived from the measurement with the sugar present in the equilibrium solution.

The striking parallelism between the heptose sugars and the structurally related hexoses is illustrated clearly by their behavior on bromine oxidation and by the equilibrium which is established when they are dissolved in water. Freshly dissolved β-*d*-β-galaheptose [40, 46] is oxidized by bromine rapidly at a rate comparable to the oxidation of the structurally related β-*l*-glucose. The oxidation of the equilibrium solution of the heptose shows the presence of about 37 percent of slowly oxidizable modification, supposedly α-*d*-β-galaheptose. The proportion of this constituent parallels the proportion of the slowly oxidizable substance in equilibrium solutions of glucose [39]. Furthermore, the optical rotation of β-*d*-β-galaheptose is close to that of β-*l*-glucose and the optical rotation of the sugar in equilibrium is near to that of *l*-glucose. Obviously the equilibrium states for the two sugars are similar.

The oxidation of α-*d*-α-galaheptose with bromine water takes place slowly and resembles the oxidation of the alpha sugars in general. Consequently the bromine oxidation measurements support its classification as alpha. The similarity of this sugar to α-*l*-mannose was noted by Hann, Merrill, and Hudson [28] with respect to other properties but they called it β-*d*-α-galaheptose in accordance with Hudson's nomenclature.

As may be seen by inspection of the curves given in figures 5 and 6, the oxidation of the equilibrium solution of *d*-α-galaheptose differs from that of *d*-β-galaheptose in that it contains only a small proportion of the rapidly oxidizable sugar. This characteristic was also found [13] for equilibrium solutions of *d*-mannose, *d*-lyxose, and *l*-rhamnose. It is thus apparent that the equilibrium state for *d*-α-galaheptose is analogous to that of mannose.

The heretofore described modification of *d*-α-mannoheptose (+85) [41] appears to be a mixture of the alpha and beta isomers, perhaps forming a double compound of the type described by Hockett and

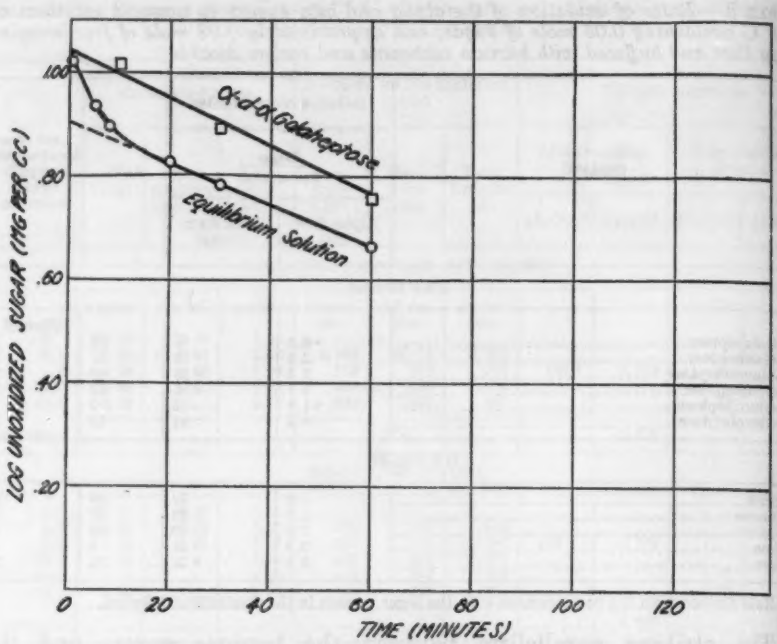

FIGURE 5.—*Bromine oxidation of d-α-galaheptose.*

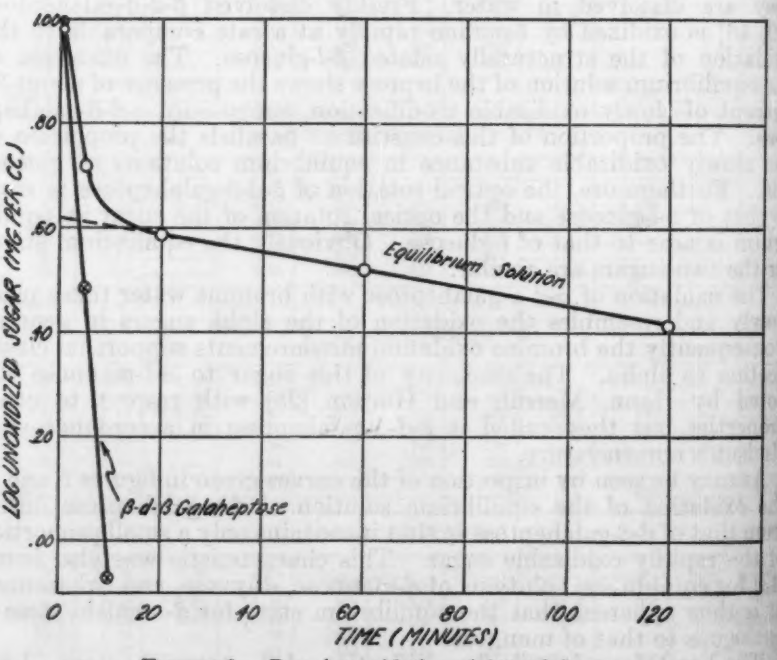

FIGURE 6.—*Bromine oxidation of d-β-galaheptose.*

Hudson [42]. As may be observed from figure 7 the oxidation of this substance proceeds rapidly until approximately half of the original sugar is oxidized and then more slowly as the less reactive component continues to be oxidized. The author has now prepared *α-d-α*-mannoheptose in what appears to be a pure state. As illustrated in figure 7, it is oxidized at a uniform rate and gives $[\alpha]^{20}_D = +120$. Crystalline *β-d-α*-mannoheptose monohydrate was also prepared. This sugar, which is structurally related to *β-d*-galactose, is oxidized rapidly as shown in figure 7. The equilibrium solution of *d-α*-mannoheptose contains 33 percent of slowly oxidizable material. This proportion compares favorably to the percentages of 31, 32, and 37 found for the

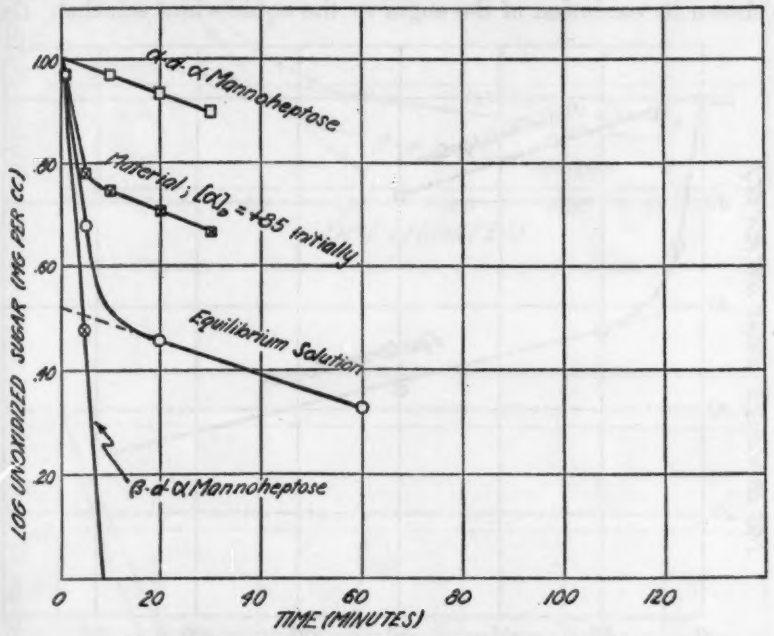

FIGURE 7.—*Bromine oxidation of d-α-mannoheptose.*

structurally related sugars, *d*-galactose, *l*-arabinose, and *d-β*-guloheptose. Furthermore, it will be recalled that the complex mutarotations of *α-* and *β-d-α*-mannoheptose resemble the complex mutarotations of *α-* and *β-d*-galactose.

The crystalline guloheptose which was originally prepared by La Forge [43] and called *α*-guloheptose has been designated *α-d-β*-guloheptose.[5] It is structurally related to *α-l*-galactose and exhibits

[5] The two epimeric heptoses formed from glucose by the cyanhydrin synthesis were designated *α*-glucoheptose and *β*-glucoheptose by Fischer. The designation alpha and beta in this case signifies which one of the parent acids was separated first, and does not have anything to do with the two modifications of the reducing group in the sugars. Attempts have been made to clarify this double use of alpha and beta but no uniform system has been adopted. Elsner (Tollens-Elsner, Kurzes Handbuch der Kohlenhydrate, page 390) discusses the subject and proposes the use of the letters "a" and "b" instead of alpha and beta for distinguishing between the epimeric sugars. The Greek letters are employed in Chemical Abstracts, and consequently they will be used in this paper for naming the epimeric heptoses as well as for naming the two pyranose modifications. The position preceding the *d* or *l* symbol is used exclusively for characterizing the configuration of the reducing group, while the position following the *d* or *l* is used for indicating the configuration of the second carbon. Originally the heptonic acid most easily separated was designated alpha. It seems advisable to rationalize this nomenclature by giving alpha and beta a structural rather than a historic significance. Thus the two epimeric substances formed by extending the carbon chain might be designated "alpha" and "beta" according to whether the hydroxyl of the new asymmetric carbon is of the same or different configuration from that of the terminal asymmetric carbon (the one which determines the *d* or *l* classification). Then the guloheptose prepared by La Forge and called *α*-guloheptose would be designated *α-d-β*-guloheptose and its enantiomorphic isomer would be *α-l-β*-guloheptose.

analogous properties. The oxidation of the crystalline sugar is represented by the upper curve of figure 8. The oxidation of the sugar in the equilibrium solution resembles the oxidation of galactose and gives clear evidence for the existence of a large proportion of the rapidly oxidizable modification, supposedly β-*d*-β-guloheptose.

The oxidation of *d*-α-glucoheptose resembles that of the structurally related hexose, *d*-gulose, in that there is relatively small difference in the rate of oxidation of the freshly dissolved crystalline sugar and of the sugar in the equilibrium solution. The crystalline sugar, which is classified as beta, is structurally related to β-*d*-gulose. It is oxidized about nine times as rapidly as the alpha modification whose presence is shown by oxidation of the sugar in the equilibrium solution. Only

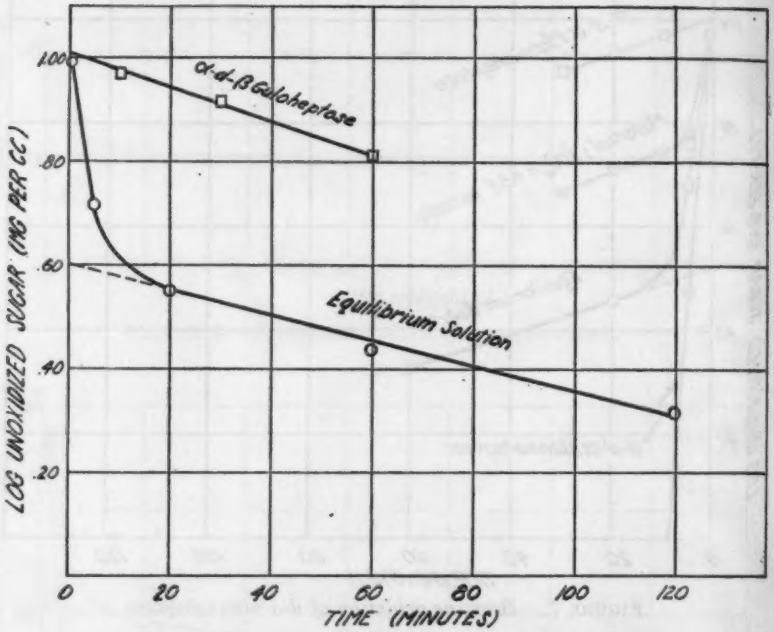

FIGURE 8.—*Bromine oxidation of d-β-guloheptose.*

12 percent of the alpha modification is present, which accounts for the relatively small difference in the behavior of the freshly dissolved crystalline sugar and that of the sugar in the equilibrium solution.

The reactions and properties of β-*d*-β-glucoheptose are of unusual importance because it is the first crystalline sugar to be obtained which has the structure of *d*-idose. It represents an unexplored field of carbohydrate chemistry, namely, the idopyranoses. The crystalline modification (tentatively designated beta) is oxidized more slowly than any beta sugar heretofore investigated, but it is also oxidized more rapidly than any alpha sugar. The oxidation of the equilibrium solution reveals that it contains about 22 percent of a slowly oxidized modification and that the equilibrium lies in the direction of the form which is known in the crystalline state and which is designated beta. The hydroxyl of carbon 1 of this substance, supposedly lies on the same side of the ring as the hydroxyl of carbon 2. If this be true, this

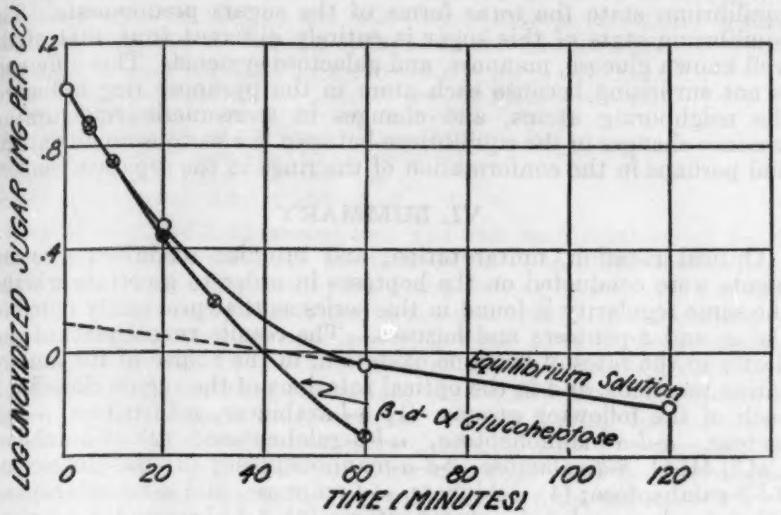

FIGURE 9.—*Bromine oxidation of d-α-glucoheptose.*

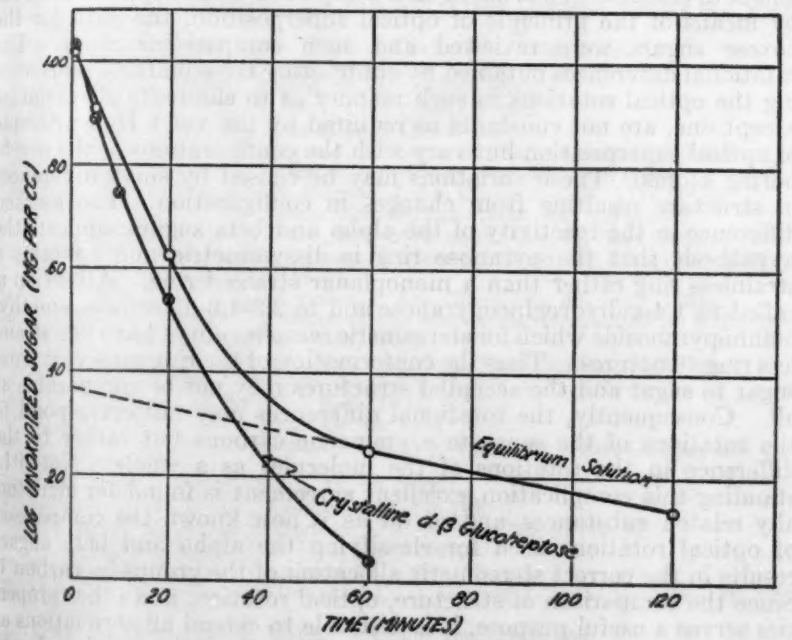

FIGURE 10.—*Bromine oxidation of d-β-glucoheptose.*

sugar provides an exception to the generalization [44] that in the equilibrium state the *trans* forms of the sugars predominate. The equilibrium state of this sugar is entirely different from that of the well known glucose, mannose, and galactose systems. This difference is not surprising because each atom in the pyranose ring influences the neighboring atoms, and changes in stereomeric configuration produce changes in the equilibrium between the various modifications, and perhaps in the conformation of the rings in the separate isomers.

VI. SUMMARY

Optical rotation, mutarotation, and bromine oxidation measurements were conducted on the heptoses in order to ascertain whether the same regularity is found in this series as that previously noted for the α- and β-pentoses and hexoses. The results reveal marked similarity in the rates of bromine oxidation, in the course of the mutarotation reactions, and in the optical rotations of the sugars classified in each of the following groups: (1) α-*l*-arabinose, α-*l*-fructose, α-*d*-galactose, α-*d*-α-mannoheptose, α-*l*-β-guloheptose; (2) β-*l*-arabinose $CaCl_2.4H_2O$, β-*d*-galactose, β-*d*-α-mannoheptose; (3) β-*d*-glucose and β-*l*-β-galaheptose; (4) α-*d*-lyxose, α-*d*-mannose, and α-*l*-α-galaheptose; (5) β-*d*-gulose and β-*d*-α-glucoheptose; (6) β-*d*-idose and β-*d*-β-glucoheptose. In every case the beta aldose is oxidized by bromine water more rapidly than the alpha, and the equilibrium solution contains two or more substances which differ in reaction rates. Since the alpha and beta classification is based on a comparison of the optical rotations by means of the principle of optical superposition, the data for the hexose sugars were reviewed and such comparisons made. The rotational differences obtained by subtracting the equations representing the optical rotations in such manner as to eliminate all variables except one, are not constants as required by the van't Hoff principle of optical superposition but vary with the configurations of the neighboring atoms. These variations may be caused by small differences in structure resulting from changes in configuration. The marked difference in the reactivity of the alpha and beta sugars supports the hypothesis that the pyranose ring is dissymmetric and contains a strainless ring rather than a monoplanar strained ring. Attention is called to 1,4-anhydroglucopyranose and to 2,3-4,6-diacetone α-methyl mannopyranoside which for stereomeric reasons cannot have like strainless ring structures. Thus the conformation of the ring may vary from sugar to sugar and the accepted structures may not be comparable at all. Consequently, the rotational differences may not correspond to the rotations of the separate asymmetric carbons but rather to the difference in the rotations of the molecules as a whole. Notwithstanding this complication, excellent agreement is found for structurally related substances, and so far as is now known the comparison of optical rotations used for classifying the alpha and beta sugars results in the correct stereomeric allocation of the groups on carbon 1. Since the comparison of structure, optical rotation, and other properties serves a useful purpose, it is desirable to extend all correlations as far as the experimental work justifies. The rules of isorotation should be modified to take into account the configuration of the neighboring atoms, perhaps by restricting the comparisons to substances of analogous configuration and basing the classification on the eight fundamental pyranose types.

The specific rotations $[\alpha]_D^{20}$ of the heptoses prepared in this investigation are represented by the following equations in which t is time measured in minutes after the sugar is dissolved in water.

α-*d*-α-Mannoheptose hydrate $= +3.4\times10^{-.0488t} + 51.9\times10^{-.00391t} + 64.7$.
β-*d*-α-Mannoheptose hydrate $= +2.9\times10^{-.0480t} - 25.1\times10^{-.00384t} + 64.5$.
α-*d*-β-Guloheptose $= -3.9\times10^{-.0597t} - 51.5\times10^{-.00533t} - 65.1$.
β-*d*-β-Glucoheptose $= +11.3\times10^{-.050t} - 11.3\times10^{-.0108t} - 0.1$.
α-*d*-α-Galaheptose hydrate $= -11.2\times10^{-.00471t} - 14.0$.
β-*d*-β-Galaheptose $= +34.9\times10^{-.00197t} - 54.1$.
β-*d*-α-Glucoheptose $= -8.5\times10^{-.0080t} - 20.2$.

Pure α- and β-*d*-α-mannoheptose and the mutarotation of β-*d*-β-guloheptose are reported for the first time. The mutarotation constants for α-*d*-α-galaheptose hydrate and β-*d*-α-glucoheptose are substantially lower than those found in the literature. A comparison of the mutarotations of the heptoses with those of structurally similar hexoses reveals that the configuration of the five carbon atoms comprising the pyranose ring determines the equilibrium proportions of the various stereomeric modifications. Sugars having the α-*d*-galactose structure exhibit mutarotations similar to that of α-*d*-galactose, while those having the β-*d*-galactose structure are like that sugar. Correlations of this character apply throughout the series.

VII. REFERENCES

[1] Van't Hoff, The Arrangement of Atoms in Space (translated by Eiloart), page 160 (Longmans, Green and Co., London, 1898).
[2] K. Freudenberg, Stereochemie, page 423 (Franz Deuticke, Leipzig and Wien, 1933).
[3] W. N. Haworth and E. L. Hirst, J. Chem. Soc. **1930,** 2615.
[4] C. S. Hudson, J. Am. Chem. Soc. **31,** 66 (1909).
[5] C. S. Hudson, BS Sci. Papers **21,** 241 (1926) S533.
[6] H. S. Isbell, BS J. Research **5,** 1179 (1930) RP253.
[7] H. S. Isbell, BS J. Research **3,** 1041 (1929) RP128.
[8] H. S. Isbell and W. W. Pigman, J. Research NBS **16,** 553 (1936) RP892.
[9] F. P. Phelps and F. J. Bates, J. Am. Chem. Soc. **56,** 1250 (1934).
[10] N. K. Richtmyer and C. S. Hudson, J. Am Chem. Soc. **57,** 1716 (1935).
[11] M. A. Rosanoff, J. Am. Chem. Soc. **28,** 525 (1906); **29,** 536 (1907).
[12] K. Freudenberg and R. Kuhn, Ber. deut. chem. Ges. **64,** 703 (1931).
[13] H. S. Isbell and W. W. Pigman, J. Research NBS **18,** 141 (1937) RP969; J. Org. Chem. **1,** no. 6 (1937).
[14] W. C. Austin and F. L. Humoller, J. Am. Chem. Soc. **56,** 1153 (1934).
[15] J. Böeseken, The Configuration of the Saccharides (translated by S. Coffey), page 57 (A. W. Sijhoff, Leyden, 1923).
[16] J. Böeseken and H. Couvert, Rec. trav. chim. Pays-Bas **40,** 354 (1921).
[17] B. Verschurer, Rec. trav. chim. Pays-Bas **47,** 123, 423 (1928).
[18] H. S. Isbell, BS J. Research **8,** 3 (1932) RP396.
[19] C. S. Hudson, J. Am. Chem. Soc. **48,** 1434 (1926).
[20] T. M. Lowry, Optical Rotatory Power, p. 429. (Longmans, Green and Co., London, 1935).
[21] H. S. Isbell, J. Chem. Educ. **12,** 96 (1935).
[22] M. A. Rosanoff, J. Am. Chem. Soc. **28,** 114 (1906).
[23] F. B. La Forge and C. S. Hudson, J. Biol. Chem. **30,** 61 (1917).
[24] G. Bertrand Bul. soc. chim. [4] **5,** 629 (1909).
[25] C. S. Hudson, J. Am. Chem. Soc. **52,** 1693 (1930).
[26] C. S. Hudson, Olive Hartley, and C. B. Purves, J. Am. Chem. Soc. **56,** 1248 (1934).
[27] G. F. Smith and T. M. Lowry, J. Chem. Soc. **1928,** 666.
[28] R. M. Hann, Alice T. Merrill, and C. S. Hudson, J. Am. Chem. Soc. **57,** 2100 (1935).
[29] C. S. Hudson and E. Yanovsky, J. Am. Chem. Soc. **39,** 1037 (1917).
[30] W. N. Haworth, The Constitution of Sugars, p. 90 (Edward Arnold & Co., London, 1929).

[31] H. Hibbert and J. S. Allen, J. Am. Chem. Soc. **54**, 4115 (1932); **56**, 1308 (1934).
[32] E. G. Cox, J. Chem. Soc. **1931**, 2313; **1932**, 138, 1844; **1935**, 1495.
[33] O. L. Sponsler and W. H. Dore, Annual Review of Biochemistry, page 66 (1936).
[34] F. Micheel and K. Hess, Ber. deut. chem. Ges. **60**, 1898 (1927).
[35] R. G. Ault, W. N. Haworth, and E. L. Hirst, J. Chem. Soc. **1935**, 1012.
[36] H. S. Isbell and C. S. Hudson, BS J. Research **8**, 327 (1932) RP418.
[37] H. S. Isbell, BS J. Research **8**, 615 (1932) RP441.
[38] H. S. Isbell, J. Am. Chem. Soc. **54**, 1692 (1932).
[39] H. S. Isbell and W. W. Pigman, BS J. Research **10**, 337 (1933) RP 534.
[40] E. Fischer, Liebigs Ann. Chem. **288**, 154 (1895).
[41] E. Fischer and F. Passmore, Ber. deut. chem. Ges. **23**, 2226 (1890).
[42] R. C. Hockett and C. S. Hudson, J. Am. Chem. Soc. **53**, 4455 (1931).
[43] F. B. La Forge, J. Biol. Chem. **41**, 251 (1920).
[44] W. N. Haworth and E. L. Hirst, J. Chem. Soc. **1928**, 1226.
[45] H. S. Isbell, J. Am. Chem. Soc. **56**, 2789 (1934).
[46] R. M. Hann and C. S. Hudson, J. Am. Chem. Soc. **59**, 550 (1937).

WASHINGTON, March 23, 1937.

U. S. DEPARTMENT OF COMMERCE NATIONAL BUREAU OF STANDARDS

RESEARCH PAPER RP991

Part of Journal of Research of the National Bureau of Standards, Volume 18, May 1937

RAPID ELECTRODEPOSITION OF IRON FROM FERROUS CHLORIDE BATHS

By Charles Kasper

ABSTRACT

Ductile iron can be deposited from ferrous chloride solutions at current densities up to 30 amp/dm² (280 amp/ft²), which is several times the customary rate of iron deposition. The temperature and acidity of the baths must be controlled within narrow limits.

	Page
I. Introduction	535
II. Review of literature	536
III. Scope of investigation	536
IV. Exploratory experiments	536
1. Conditions employed	536
2. Results	537
V. Quantitative tests	538
1. Conditions employed	538
2. Results	539
VI. Conclusions	541

I. INTRODUCTION

Many of the plates used for printing currency and securities at the U. S. Bureau of Engraving and Printing consist principally of electrodeposited iron. Under the conditions [1] there used it requires a total of about 96 hours to deposit the desired thickness of nickel (0.4 mm or 0.015 in.) and of iron (5 mm or 0.20 in.). Ordinarily, this period is not objectionable, but when new designs are to be issued, it takes a considerable period to produce a sufficient number of plates (at least four) to start the printing operations. For such purposes it would be desirable to greatly increase the speed of deposition, preferably to at least four times the present rate. Methods for the rapid deposition of nickel and iron were therefore investigated.

The results [2] obtained with nickel showed that relatively smooth soft, ductile deposits can be produced from concentrated solutions of nickel sulphate (4 *N*), at a low pH (pH=1), a high temperature (100° C), and current densities up to 30 amp/dm² (280 amp/ft²), which is about 15 times the current density regularly employed for this process. Corresponding deposits from chloride solutions are harder and more brittle.

The present paper describes the experiments on iron deposition. As the very rapid deposition of both nickel and iron requires special equipment and more critical control, these processes are not in regular use at the Bureau of Engraving and Printing, but they can be applied if necessary.

[1] C. T. Thomas and W. Blum. *The production of electrolytic iron printing plates.* Trans. Am. Electrochem. Soc. 57, 59 (1930).

[2] W. Blum and C. Kasper. *The structure and physical properties of nickel deposited at high current densities.* Trans. Faraday Soc. 31, 1203 (1935).

II. REVIEW OF LITERATURE

The earlier publications on iron deposition were reviewed by W. E. Hughes,[3] and more recent applications were discussed by Thomas and Blum.[4] A very complete discussion and bibliography of iron deposition, with special reference to the preparation of pure iron, will be found in a recent monograph.[5] As most of these studies involved deposition at relatively low current densities, they have no direct relation to the present problem.

III. SCOPE OF INVESTIGATION

The purpose of this investigation was to define the conditions for depositing smooth, soft, ductile iron at current densities of at least 10 amp/dm^2 (93 amp/ft^2) and preferably higher, in contrast to the present practice of about 6 amp/dm^2 (56 amp/ft^2). This was accomplished by first conducting a large number of exploratory experiments, the deposits from which were tested manually by bending. The conditions found to yield suitable properties were then employed for the preparation of larger specimens, of which the indentation hardness, tensile strength, and ductility were measured. The quantitative tests were limited to deposits that did not crack during deposition or during removal from the underlying steel.

The principal factors investigated were the composition, concentration and pH of the baths, the temperature and current density, and the type of diaphragm. The experiments were confined to chloride baths, because they have better conductivities than do sulphate baths, and because preliminary tests showed that (unlike nickel) ductile iron can be rapidly deposited from chloride solutions.

IV. EXPLORATORY EXPERIMENTS

1. CONDITIONS EMPLOYED

It was found necessary to conduct even the exploratory experiments on a relatively large scale. Iron deposition is one process in which it is difficult to reproduce on a very small scale the results obtained in larger vessels. For example, it is not possible to duplicate in 1-liter jars the type of deposits regularly produced at the Bureau of Engraving and Printing. This difference may be caused partly by the greater ease of oxidation of ferrous solutions in the small vessels, and partly by the difference in circulation when diaphragms are used in small and in large vessels.

Most of the experiments were made in a rectangular cast-iron tank holding about 10 liters, which was lined with acid-proof enamel. The enameled tank was placed in a larger metal tank containing water, which in turn was heated by current passing through resistance wires surrounding the outer tank. The water level in the latter was maintained with a siphon. When necessary, for example at very high current densities, cold water was introduced into the water bath. It was thereby possible to control the temperature in the iron bath within close limits from 60 to 108° C (140 to 226° F) for any desired period. As the boiling point of the solution was approached the temperature could be kept more nearly constant.

[3] Trans. Am. Electrochem. Soc. 40, 185 (1920).
[4] See reference 1.
[5] H. E. Cleaves and J. G. Thompson. The Metal—Iron. Alloys of Iron Research Monograph Series. (McGraw-Hill Book Co., New York, 1935).

The anodes were of Armco iron, surrounded by asbestos diaphragms in order to prevent particles from passing into suspension and causing rough deposits.

Diaphragms of light weight, loose cloth of either blue or white asbestos are successfully used in the regular iron baths at current densities up to 6 amp/dm² (56 amp/ft²). This cloth was, however, not suitable for use with more acid solutions and higher temperatures and current densities. After numerous trials it was found that the best material for the latter conditions is dense cloth made of blue African asbestos (crocidolite). Satisfactory imported cloth of this material had 36 threads per inch in direction *A*, and 12 threads in direction *B*, with 2-ply yarns in each direction, a 4-harness weave, 2/2 twill, and a weight of 65 oz/yd². When necessary, this was sewed with thread made of similar asbestos.

The cathodes were flat steel plates that had been nickel-plated adherently, rubbed with graphite, and plated with a thin (0.0025 mm or 0.001 in.) separable layer of nickel. The deposits for the preliminary tests were about 0.25 mm (0.01 in.) thick.

Special care was required to maintain any specified conditions, especially during the beginning of a run, when the temperature and acidity tend to change rapidly. The technique finally adopted was to heat the bath externally to about 90° C, introduce a "dummy" cathode of the same size as the regular cathode into the solution, which was made slightly more acid than was desired in the final run, and pass the specified current until the desired temperature and acidity were attained. (If necessary, adjustments of the heating current were made during this "breaking in" process.) The current was then increased for a few minutes to raise the temperature slightly. By the time the dummy cathode was removed and the regular cathode inserted, the conditions were those desired, which could then be maintained during the run.

The acidity was maintained constant by suitable additions of hydrochloric acid at intervals of about 20 minutes. In the preliminary experiments water to replace that lost by evaporation was added between the runs.

The ferrous chloride and other chemicals were of commercial grades that were found to be nearly pure. The small amount of ferric chloride always present in the ferrous salt was reduced by adding hydrochloric acid and introducing strips of pure iron. This also removed copper, lead, and most other heavy metals that might be present. To avoid introduction of copper into the bath the copper bus bars were heavily nickel-plated.

2. RESULTS

A large number of exploratory experiments led to the following conclusions regarding the favorable conditions for producing ductile iron at high current densities:

1. The solution should be clear green in color, i. e., nearly free from ferric salts. Ferric salts reduce the cathode efficiency and tend to cause brittle deposits.

2. A high concentration of ferrous chloride is desirable, at least 4 *N* and preferably 5 *N*. With lower concentrations more brittle deposits are obtained.

3. The acidity (rather than the pH) should be controlled within fairly close limits. Insufficient free acid leads to brittle deposits, while excess acidity lowers the cathode efficiency.

4. Ductile metal can be produced at high efficiencies. The maximum observed was about 85 percent. Considerable gas is evolved, and adequate ventilation is required to protect the operators.

5. Calcium chloride has no appreciable effect on the deposits.

6. Addition of potassium chloride leads to brittle deposits.

7. The temperature is the most important single factor, as variations of 5° C (9° F) may produce a marked change in the properties. In general, under given conditions, a decrease in temperature decreases the ductility. For example, in a 4 *N* ferrous chloride solution with 0.1 *N* free HCl, a temperature of at least 100° C. (212° F) is required for ductile deposits at 20 amp/dm^2 (186 amp/ft^2), and a temperature of 105° C (221° F) at 30 amp/dm^2 (280 amp/ft^2).

V. QUANTITATIVE TESTS

1. CONDITIONS EMPLOYED

For reliable tensile and hardness tests, smooth deposits at least 20 cm (8 in.) long and with a uniform thickness of at least 0.75 mm (0.03 in.) are required. These were made in the enameled tanks previously described, but with additional precautions.

To obtain uniform current distribution, shields were employed. Each shield consisted of a glass plate in which was cut a rectangular opening that was slightly smaller than the cathode. When this shield was placed parallel to and a short distance from the cathode it prevented an excessive current density on the edges of the cathode. High local current densities are objectionable, not only because they yield a nonuniform thickness of deposit, but also because any "trees" that grow on the edges are likely to become detached and to give rise to small metal particles that cause roughness over the rest of the surface.

Similarly, it was necessary to support the asbestos diaphragms around the anodes in order to keep them parallel to the electrodes and thus yield uniform current distribution. Strips of cypress wood were used for this purpose. The wood was slightly attacked and some organic matter may have entered the solution. If so, it might be expected to yield brittle deposits. Actually, however, no such effects of the cypress could be detected in qualitative tests. The quantitative results are comparable, even though their absolute values may have been slightly affected.

To produce deposits of the prescribed thickness required from 3 to 8 hours of deposition. To maintain uniform conditions over such periods automatic control was applied. The acid was added through a calibrated capillary, and the rate of flow was controlled by adjusting the height of the reservoir bottle. To prevent stoppage of the capillary, the acid was filtered through a sealed-in alundum thimble. Water was added continuously by means of a sealed flask with a constant-level device and a capillary tube. It was necessary to maintain the current constant by manual adjustment, owing to slight fluctuations in the generator voltage.

By taking the above precautions, it was found possible in most cases to produce deposits suitable for testing. However, some of the deposits had a few rough spots, and others had some pits. The tendency for the latter could be reduced by approaching the specified temperature from above. Only those specimens that were practically free from either projections or pits could be used in tensile tests, but the hardness measurements could be made on almost all of the specimens, at points free from surface defects. Moreover, as each of the recorded values for hardness usually represents the average of 10 or more measurements, the values are more significant than the tensile strength.

2. RESULTS

In general, the quantitative tests confirmed the qualitative observations recorded in the discussion of the exploratory experiments. The principal conclusions are illustrated in tables 1, 2, and 3. Each value for tensile strength and elongation represents the average of two or more measurements from selected specimens. The agreement of duplicate runs on tensile tests was very good, but the elongation values were more erratic, except in the case of exceptionally perfect and ductile specimens. The Brinell number was determined with a 15-kg load, 1/16-inch (1.55-mm) ball, and a period of 30 seconds. Unless otherwise noted, the baths contained simply ferrous chloride approximately 5 *N*, that is, 497 g/liter or 66 oz/gal of $FeCl_2.4H_2O$; and hydrochloric acid in the concentration designated under "acidity." (0.1 *N* HCl is equivalent to 3.6 g/liter or 0.5 oz/gal of HCl; or to 10 ml/liter or 0.13 fl oz/gal of concentrated hydrochloric acid, sp gr 1.18). When boric acid was added (for example, 0.5 *M*, equal to 30 g/liter or 4 oz/gal of H_3BO_3), the acidity was still expressed in terms of the hydrochloric acid.

TABLE 1.—*Effect of temperature on physical properties*

(5 *N* $FeCl_2$)

At 10 amp/dm² (93 amp/ft²) and 0.06 *N* acidity

Experiment	Temperature		Tensile strength		Elongation	Brinell number
	°C	°F	kg/cm²	lb/in.²	%	
B5	97	207	5,110	73,000	5	167
A7, A8	100	212	4,270	61,000	18	135
B8	102	216				127
At 20 amp/dm² (186 amp/ft²) and 0.10 *N* acidity						
A6	95	203	7,910	113,000	4	210
A5	100	212	5,740	82,000	13	182
A10	106	222	5,040	72,000	16	150

The results in table 1 show clearly that relatively small changes in temperature have large effects upon the properties of the deposits. In general, a rise in temperature produces softer and more ductile deposits.

TABLE 2.—*Effect of acidity on physical properties*

(5 N $FeCl_2$)

At 100° C (212° F) and 20 amp/dm² (186 amp/ft²).

Experiment	Acidity *N*	Tensile strength		Elongation	Brinell number
		kg/cm²	lb/in.²	%	
A4	0.04	7,630	109,000	0	228
A5	.10	5,740	82,000	13	182
A3	.13	4,760	68,000	10	169

From table 2 it may be seen that an increase in acidity lowers the hardness and tensile strength and increases the ductility. Practically, it is difficult to make satisfactory deposits under given conditions over a wide range of acidity. If the latter is very low, the deposits crack during deposition, and if it is too high, the efficiency falls off very rapidly, but no embrittlement of the deposits is observed. In general, similar, if not identical, properties are obtained by varying the acidity in the same direction and proportion as the current density. This is illustrated in table 3.

TABLE 3.—*Effect of current density and acidity at 102°* C (*216°* F)

(5 *N* $FeCl_2$)

Experiment	Acidity *N*	Current density		Tensile strength		Elongation	Brinell number
		amp/dm²	amp/ft²	kg/cm²	lb/in.²	%	
A7, A8	0.06	10	93	4270	61,000	18	135
A6	.10	20	186	5740	82,000	13	182
A14	.15	30	280	5110	73,000	5	156

For these reasons it is difficult to make satisfactory deposits at a fixed temperature and acidity over a wide range of current density. In general, it was found that an increase in current density produced harder and less ductile deposits.

The quantitative results did not show any marked effects of either boric acid (0.5 *M*, i.e., 30 g/liter or 4 oz/gal of H_3BO_3) or of calcium chloride (1.5 *N*, i.e., 165 g/liter or 22 oz/gal of $CaCl_2$). In several experiments, the deposits with boric acid were about 10 Brinell numbers softer than those without boric acid, but there were no consistent effects on the tensile strength or elongation. No definite effects were found with the calcium chloride.

All the deposits produced under the conditions prescribed had relatively fine structures, and there were no such pronounced differences as were observed with hard and soft nickel deposits. In general, greater hardness and tensile strength were accompanied by a finer structure. This relation is illustrated by photomicrographs of typical cross sections in figure 1.

The fact that the hardest deposits were produced at low acidities or high current densities is consistent with the hypothesis supported by Macnaughtan and his associates,[6] that hardness of nickel or iron deposits is caused by, or associated with, the inclusion of oxides or

[6] D. J. Macnaughtan, G. E. Gardam, and R. A. F. Hammond, Trans. Faraday Soc. 29, 729 (1933).

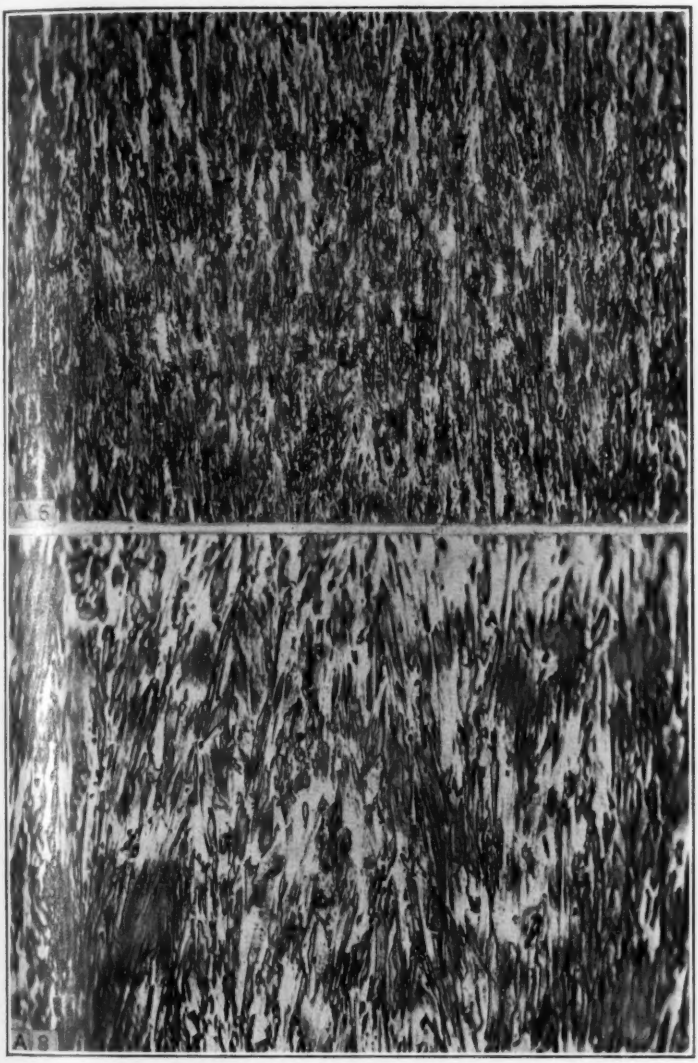

FIGURE 1.—*Structure of typical iron deposits* (× *500*).

No.	°C	amp/dm²	kg/cm²	Elongation (%)	Brinell no.
A6	95	20	7,910	4	210
A8	100	10	4,270	18	135

UNIV. OF MICH.

basic materials. This hypothesis was confirmed by analysis of two typical deposits by fusion in a vacuum. One of the hardest specimens (*A6*) showed an oxygen content of 0.015 percent, and one of the softest (*A8*) a content of only 0.005 percent.

VI. CONCLUSIONS

1. Relatively soft, ductile iron can be deposited from a bath containing 5 *N* $FeCl_2$ and 0.10 *N* HCl, at a temperature of 106° C (222° F) and a current density of 20 amp/dm² (186 amp/ft²).
2. Under any given conditions, softer deposits are produced by increasing (*a*) the acidity or (*b*) the temperature or by decreasing (*c*) the current density.
3. Additions of boric acid or of calcium chloride to the baths have little effect on the properties of the deposits.
4. The harder deposits are finer grained and contain more oxygen than the softer deposits.
5. The rapid production of dense, ductile iron deposits, free from roughness or pits, requires very careful control of all factors, especially the acidity and temperature, and the use of effective diaphragms, preferably made of blue asbestos cloth.

The author acknowledges the assistance received in this investigation from T. F. Slattery and C. T. Thomas of the U. S. Bureau of Engraving and Printing, and W. Blum, J. G. Thompson, W. H. Swanger, and C. S. Aitchison of the National Bureau of Standards.

WASHINGTON, February 20, 1937.

U. S. Department of Commerce National Bureau of Standards

RESEARCH PAPER RP992

Part of Journal of Research of the National Bureau of Standards, Volume 18, May 1937

INTERFERENCE MEASUREMENTS OF WAVE LENGTHS IN THE ULTRAVIOLET SPECTRUM OF IRON

By William F. Meggers and Curtis J. Humphreys

ABSTRACT

The wave lengths of 252 ultraviolet lines (3498 to 2101 A) characteristic of the international iron arc were measured relative to cadmium, krypton or neon standards. These measurements were made with Fabry-Perot étalon interferometers and stigmatic spectrographs. Invar étalons of 2, 3, 5, 7.5, or 10 mm length, and aluminized quartz plates were used. The spectrographs consisted of a concave grating, a Littrow quartz, or a Cornu quartz instrument. With the first, simultaneous exposures were obtained of red neon lines in the first-order spectrum, and of ultraviolet iron lines in the overlapping second-order spectrum. The use of quartz spectrographs required alternate exposures of primary and secondary sources. The final values in many cases are given to eight figures since calculations of probable error and tests of relative value by means of the combination principle indicated average errors smaller than 0.0005 A.

CONTENTS

		Page
I.	Introduction	543
II.	Experiments	544
III.	Measurements	546
IV.	Corrections	547
V.	Results	548
VI.	References	557

I. INTRODUCTION

Nearly half a century ago Kayser and Runge [1][1] proposed the arc spectrum of iron as a source of wave-length standards for spectroscopic measurements. Since that time very considerable effort has been exerted to select suitable standards, refine their values, and to extend measurements throughout a long range of spectrum [2]. Although steady progress has been made toward the establishment of a trustworthy, homogeneous system of standards, the task is still unfinished.

The greatest advance followed the invention and use of interferometers, a primary standard being thus determined by comparing the red radiation from cadmium with the meter, and secondary standards from the arc spectrum of iron being measured relative to this primary standard. Since 1919 this program has been sponsored by the International Astronomical Union, which, in 1928, adopted 244 values (3370.787 to 6677.993 A) of iron lines as international secondary standards, and recommended that the system be extended both to longer and to shorter waves [3]. Interference measurements of the shorter waves of iron have since been published by Burns and Walters

[1] Numbers in brackets refer to literature citations at the end of this paper.

[4] and by C. V. Jackson [5], but according to rule no line may be considered for adoption as an international secondary standard until three independent and concordant determinations exist. In the present paper another series of measurements in the ultraviolet spectrum of iron (3500 to 2100 A) is reported. Other measurements by Buisson and Fabry [6], by Burns [7], and by Pressentin [8] will not be considered here since they cover only a part of this range with relatively few observations, and have been adequately discussed by Jackson [5].

II. EXPERIMENTS

The results reported in this paper were derived from interference spectrograms of cadmium, neon, krypton, and iron spectra obtained by employing combinations of Fabry-Perot interferometers and stigmatic spectrographs.

The primary sources consisted of cadmium lamps of the type specified by the International Committee on Weights and Measures [9] or of Geissler tubes containing pure neon or krypton. On account of frequent fracture of the cadmium lamps owing to unfortunate choice of glass whose expansion differed from that of the sealed-in wires, the majority of spectrograms were exposed either to neon or to krypton sources.

The secondary source was the iron arc specified by the International Astronomical Union for the production of secondary and tertiary standards [10]. It consisted of an iron arc operated at 220 volts with 5 amperes at a length of 15 mm, an iron rod 7 mm in diameter serving as the upper pole (cathode), and a bead of iron oxide on a massive iron rod as the lower pole (anode). The upper rod was surrounded by a 2-inch brass cylinder bored with vertical holes to act as a heat radiator. An image of threefold magnification was projected on the interferometer with an aluminized mirror of 1-m focal length, and a diaphragm selected light from the central 1.5-mm zone of the 15-mm-arc flame.

Crystal quartz plates coated with evaporated aluminum were used in the étalon type of Fabry-Perot interferometer. The two plates produce respectively right-handed and left-handed polarization, both plates being cut with faces perpendicular to the optic axes and polished accurately plane. A small angle between surfaces of each plate prevented intersurface reflections. Étalons of three invar rods separated the aluminized surfaces either 2, 3, 5, 7.5, or 10 mm.

An excellent quartz-fluorite achromatic lens (made by Carl Zeiss) of 25-cm focal length was employed for imaging interference patterns on the spectrograph slits.

Three different spectrographs were used in making the observations. The first was an Anderson ruled grating of 650-cm radius mounted to perform stigmatically [11]. A compromise between horizontal and vertical focus was adopted for 15 cm on either side of the axis or grating normal, and observations were made simultaneously in the first two orders of grating spectra. Since the dispersion is 10 A/mm in the first order, it was possible to record on a 10-inch plate 4700 to 7200 A in this order and simultaneously 2350 to 3600 A in the second order. By filtering the iron light through a piece of Corex A glass the ultraviolet spectrum was photographed in the second order, and simultaneously in the first order the neon spectrum was superposed

when neon light was reflected from the rear surface of the Corex A filter or from a plane quartz mirror. The transmission of the Corex A filter set a limit on the iron spectrum near 2600 A. It was found that the dispersion was sufficient to prevent confusion of overlapping orders if the slit was not too wide, so that many exposures were made with both orders of iron spectra present as well as the neon spectrum. Line identification was facilitated by the difference in scale of interference patterns in first- and second-order grating spectra. From these grating spectrograms, measurements of iron lines down to 2388 A were secured. This series of iron and neon comparisons is the most reliable because of strict simultaneity of exposure under identical optical conditions and no disturbance of the apparatus.

In order to observe the shorter ultraviolet these grating spectrograms were supplemented by alternate exposures to krypton and iron with a Littrow type quartz spectrograph (Hilger *E1*). Since it is impossible with an instrument of this type to observe the visible (4400 A) and the ultraviolet (below 2500 A) with a single adjustment, we tried the procedure which Jackson used [5]. The krypton (or cadmium) spectrum was photographed with the spectrograph set for visible light, and then the spectrograph was changed (prism rotated, lens refocused, and the plate tilted) to record the ultraviolet iron spectrum, followed by a return to the first setting for a second krypton (or cadmium) exposure. In this way, the iron lines (2700 to 2100 A) were compared with krypton standards (4273 to 4502 A) or with the cadmium standard (6438 A). By selecting for measurement only those spectrograms which showed no serious differences between the first and last exposures self-consistent results were obtained, but when these were compiled, it was distressing to find them systematically 0.0025 A higher than for the same lines measured relative to neon with the grating spectrograph.

Then the ultraviolet (2813 to 2100 A) of iron was compared again with krypton standards (4273 to 4502 A) by exposing them alternately in a Cornu prism spectrograph (Hilger *E2*) which covers the entire range with a 10-inch plate. In this case, it was necessary only to rack the plate down for successive exposures without otherwise changing the spectrograph adjustments. The results of these measurements were in good agreement with those of the grating spectrograms, and it was concluded that those obtained with the *E1* spectrograph were 0.0025 A too large. Seeking the explanation for this discrepancy we investigated the effect of spectrograph focus on the fractional order of interference and found variations of this order of magnitude. It appears that systematic errors may be introduced unless exactly the same type of focus is used in spectrograph settings for different spectral regions. The values of *E1* spectrograms were finally reduced by 0.0025 A and averaged with the other two series.

Finally, another series of observations was made with the *E1* spectrograph after careful investigation of its horizontal and vertical focus for different spectral regions and choosing the same compromise in each. In this last series the interval 2400 to 2100 A was remeasured relative to krypton standards (4273 to 4502 A) with 2-, 3-, and 5-mm étalons, the dispersion of phase at reflection being determined again from 2- and 5-mm values. After applying the proper corrections for standard air density and dispersion of phase, these results were averaged with the others.

For the grating spectrograms we employed Eastman *144F* plates. The same, or Eastman *33*, emulsions were used in making the prism spectrograms, except in the shortest ultraviolet (2400 to 2100 A) where observations were made with Schumann plates having greater sensitivity and contrast.

On account of the considerable range of intensity of iron lines suitable as standards, the best interference measurements require a variety of exposures, short ones for strong lines, long ones for weak lines, and intermediate ones for the remainder. The exposures with the grating spectrograph ranged from 5 minutes to an hour. With the prism spectrographs they ranged from 5 seconds to 30 minutes for iron and averaged about 5 minutes for cadmium or krypton. When making long exposures to the iron arc a quartz cell containing water was usually placed near the interferometer to absorb most of the heat radiation.

Accurate alignment of the light sources, condensers, interferometer, ring telescope, and spectrographs was effected in each case by placing an incandescent lamp at the center of the plate holder and centering each piece of apparatus in the light beam emerging from the slit in reverse order. Mirrors and lenses were so placed that each light source was first focused on the interferometer and again on the grating or prism of the spectrograph.

The interferometer plates were adjusted parallel by observing Haidinger's fringes when diffusely illuminated by light from a mercury lamp or a neon lamp. After adjustment they were allowed to stand for some hours and tested. If no further adjustment was required they were oriented so that the center of the interference patterns fell on the center of the spectrograph slit. This was accomplished in each case by observing, with magnification at the focus, the images of a wide slit and then reducing the slit width to $\frac{1}{10}$ or $\frac{1}{20}$ mm for exposures. If the fringes are not accurately centered on the slit systematic errors will appear in their measurement.

Typical interference spectrograms are reproduced in figures 1 and 2.

III. MEASUREMENTS

These interference spectrograms were measured with a micrometer originally designed by Dr. Keivin Burns and constructed in the Bureau's instrument shop about 24 years ago. All interference measurements of wave lengths reported by our spectroscopic laboratory have been made with it, but its description has been neglected. It has a screw of $\frac{1}{2}$ mm pitch, a revolution counter [2] and head with 100 divisions, which moves a microscope (and reticule) across the interference pattern. Figure 3 illustrates this interference measuring device.

In measuring the grating spectrograms the diameters of three neon rings and five iron rings were determined. The same is true of cadmium and iron rings on prism spectrograms, but the number of krypton and iron rings measured was usually three and four respectively. This procedure resulted in measuring about the same over-all size of interference patterns for both primary and secondary standards, which was thought advisable to minimize errors due to possible distortion in the image forming systems. Such distortion would be

[2] The adaptation of a commercial counter was suggested by Mr. O. G. Lange, chief of the Bureau's instrument shop.

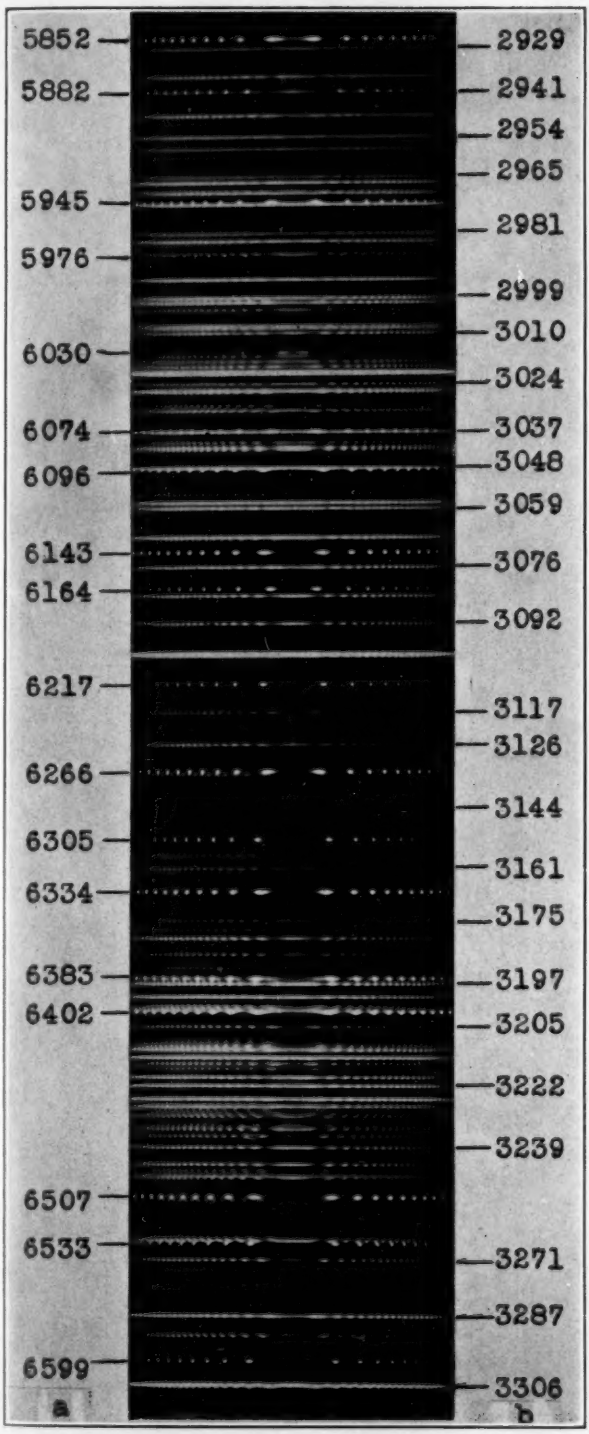

FIGURE 1.—*Fabry-Perot interference patterns of neon and iron (5-mm étalon) photographed simultaneously, (a) neon spectrum in gratings first order, and (b) iron in second.*

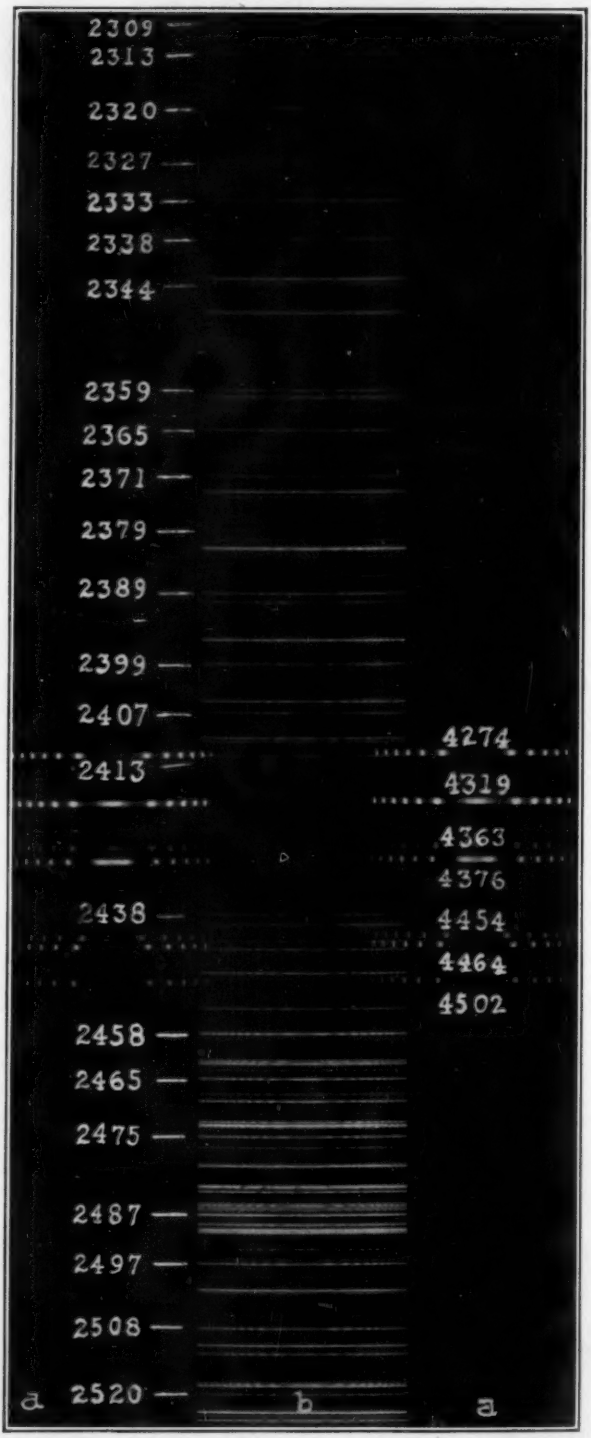

FIGURE 2.—*Fabry-Perot interference patterns of (a) krypton, and (b) iron (5 mm étalon) photographed alternately with different settings of quartz Littrow spectograph.*

revealed by slightly different fractional orders of interference from successive ring diameters, but no differences of this kind could be detected. The measured ring diameters were squared with the aid of Gauss's table of squares, and the average difference of squares for each line was plotted against wave length. A straight line was drawn to fit these points and for each wave length the value indicated by this line was divided into the successive squares of measured ring diameters to obtain the fractional order of interference at the center of the pattern. Although the interpolated value rarely differed from the observed by more than 1 percent, this procedure causes all the measurements on each plate to contribute to the accuracy of determining the fractional-order denominator for each wave length. For making the divisions a 20-inch slide rule was found most convenient and rapid.

The interference path or double étalon distance was found either from cadmium, krypton, or neon lines, the correct order number in every case being readily deduced by the method illustrated for neon by Meggers [12]. When cadmium was used, the value 6438.4696 A for its red radiation served as the primary standard. When neon was employed, a group of six lines (6304.7892, 6334.4279, 6382.9914, 6506.5279, 6532.8824, 6598.9529 A), with the center of gravity at 6437 A, was regarded as identical with the primary standard [13]. Substituting krypton for the primary standard, the separation of interferometer plates was determined from six to eight blue lines (4273.9700, 4318.5525, 4319.5797, 4362.6423, 4376.1220, 4453.9179, 4463.6902, 4502.3547 A), whose values have been accurately measured relative to cadmium or neon and have been adopted as standards by the International Astronomical Union [14]. Within the error of observation, our comparisons of iron wave lengths with these three different primary standards all yielded the same final values.

Since the general theory and method of comparing wave lengths with the Fabry-Perot interferometer have been given many times in other papers [15] no further details are required here.

IV. CORRECTIONS

Interference comparisons of wave lengths require corrections for deviations of atmospheric density from standard conditions (dry air at 15° C and 760 mm), and for the dispersion of phase change at reflection from the interferometer surfaces. Both corrections are important when the primary and secondary standards are in different spectral regions, and are especially large for the ultraviolet, where the dispersion curve of air rises steeply and the reflecting properties of surfaces usually change most rapidly with wave length.

The first correction was derived from observations of the mean air temperature and barometric pressure for each exposure. The air temperature near the interferometer was usually between 23 and 24° C, and the barometer was generally a little under normal so that these corrections were always negative, amounting to −0.0032 A for 2100 A relative to 4400 A in extreme cases. When ultraviolet lines are measured relative to blue krypton lines instead of red cadmium or neon the corrections are reduced by the difference of their values at 4400 and 6400 A. In all cases our corrections for standard air density were taken from the tables prepared for this purpose by Meggers and Peters [16]. Separate tables of corrections for temperature deviations and

for pressure deviations from normal were calculated relative to 6000 A by Jackson [17], who was apparently unaware that the combined result is obtainable relative to any fixed point from the tables referred to above.

After correcting to standard atmospheric conditions the apparent wave lengths calculated from interference measurements require an adjustment for the dependence of phase change at reflection upon wave length. This phase correction is readily obtained from the wave-length comparisons, if these are made with a variety of étalons [12]. In the present instance consistent and reliable results were given by a comparison of the data from 7.5- and 2-mm étalons, or from 5- and 2-mm étalons.

For our aluminized quartz plates this phase correction was always negative in the ultraviolet, −0.0008 A at 3500 A, but increased rapidly beyond 2900 A, and amounted to −0.0040 A at 2500 A for the 5-mm étalon. The largest correction of this type amounted to −0.0205 A for 2100 A measured with 2-mm étalons. The phase correction was extrapolated beyond 2153 A because no measurements were made there with étalons greater than 3 mm. Only when these corrections are properly determined and applied will the final values for homogeneous lines be the same from all étalons.

V. RESULTS

Although the primary standard is defined to eight significant figures (6438.4696 A) and some eight-place values of secondary standards from noble gas spectra (neon, krypton) have been adopted [13, 14], the published values of iron lines have heretofore been restricted to seven-place values for the reason that iron lines excited in a high-temperature arc are intrinsically less sharp and more difficult to measure.[3] The Doppler width of iron lines is 5 to 10 times that of the primary line, or of certain neon and krypton lines, and moreover the wave lengths of some iron lines have been found to vary from arc center to pole [18, 19]. This pole effect is eliminated by taking light from a narrow central zone of a long arc flame and the sharpness $\lambda/\Delta\lambda$ of the average iron line is closely described by its limiting order of interference, $N=100{,}000$ approximately. This means that the total width of a line at 3000 A is about 0.03 A, and to evaluate the wave length to ± 0.0003 A requires that the center of gravity be determined within 1/100 of the width. Fortunately, no trouble on account of hyperfine structure need be feared because according to DeGier and Zeeman [20] the isotopic constitution of iron consists of 90.2 percent mass number 56; 6.5 percent mass number 54; 0.5 percent mass number 58; and 2.8 percent mass number 57. It may be assumed that observed spectral lines are due to mass 56 and any lines due to isotopes 54, 57, and 58 will be too faint to affect wave-length measurements of those from isotope 56. The principal factor limiting the precision of wave-length measurement of iron lines (aside from pole effect and line width) is the overlapping of interference patterns of very close lines of comparable intensity. We presume that this explains a number of cases in which consistent results were obtained with individual étalons, but the final mean values from different étalons disagreed by many times the probable error of each.

[3] Burns and Walters [4] and Jackson [5] have published eight-place wave numbers taken from eight-place wave lengths before reducing to seven, but no analysis was presented to justify this procedure.

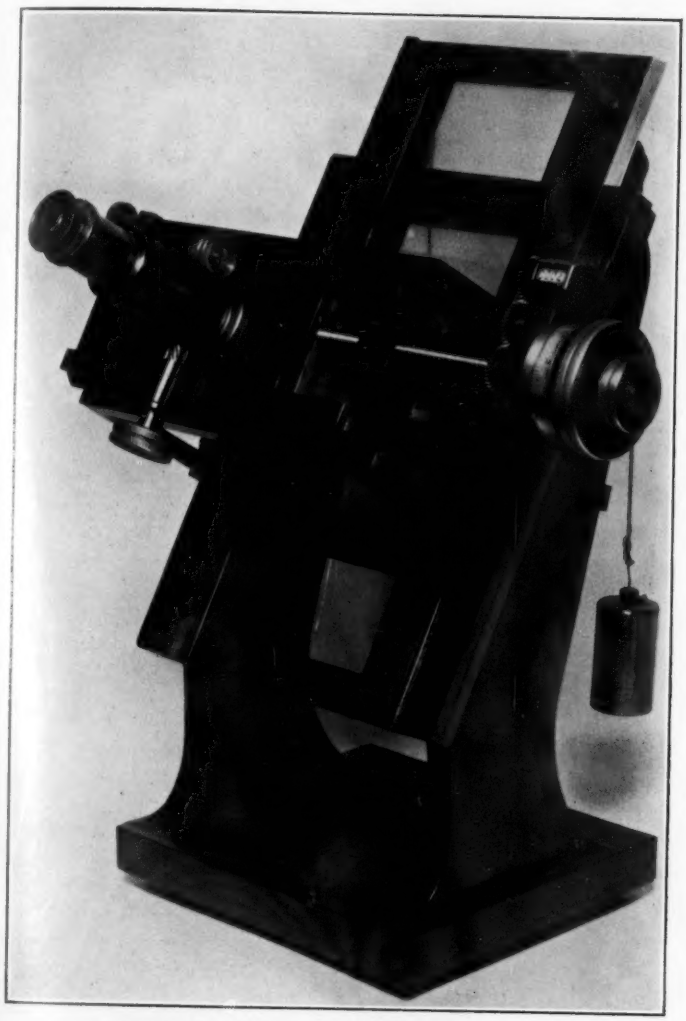

FIGURE 3.—*Interference measuring machine.*

UNIV. OF MICH.

TABLE 1.—*Individual values for various étalons* [1]

Wave length	Étalon			
	2 mm	5 mm	7.5 mm	10 mm
A				
3497.8418	8423	8404	8419	8411
	8414	8406	8420	8423
	8428	8421	8420	----
	8408	8433	8421	----
	8412	----	----	----
3370.7845	7841	7837	7858	7858
	7829	7838	7846	7847
	7845	7835	7847	----
	7840	7835	7839	----
	7862	7852	7831	----
	----	7853	7849	----
	----	7848	7837	----
	----	7858	----	----
3217.3796	3787	3800	3800	3798
	3789	3793	3798	3792
	3815	3795	3786	----
	3785	3790	3795	----
	3829	3798	3794	----
	----	3781	3800	----
	----	3787	3793	----
	----	3796	----	----
2851.7970	7981	7973	7984	7973
	7975	7962	7978	7974
	7968	7973	7966	----
	7961	7958	7963	----
	7946	7967	7975	----
	----	7964	7972	----
	----	7958	----	----
	----	7970	----	----

[1] The whole number is shown only in the first column.

The concordance of fractional-order determinations from four or five successive rings for each line induced us to carry the wave-length calculations and corrections to the fourth-place decimal of an angstrom. When the corrected results were assembled and averaged the fourth-decimal place was retained with the intention of rounding to three places for publication. Since most of the lines were observed on 10 to 20 or more spectrograms and each value was based upon four or five measured ring diameters, each final value rests on from 80 to 200 bisections of ring segments. Where so many observations exist, it would seem that the least squares calculation of probable error might have physical significance. In taking the final means, the individual values from each étalon were given equal weight, and then the various étalon mean values were averaged by weighting according to the number of observations with each. For the majority of lines the calculated probable error of the mean was less than 0.0005 A both for étalon means (table 1) and for final means (table 2). Now the term analyses of iron spectra permit a crucial test of the precision of wave-length measurements by means of the

combination principle. Most of the lines we have measured have been classified and among them are 20 pairs of eight-figure values where wave-number differences measure the level separations of low atomic-energy states. These are listed in table 3.

TABLE 2.—*Mean values from various étalons* *

Wave length	2 to 3 mm	Obs.	5 mm	Obs.	7.5 mm	Obs.	10 mm	Obs.
A								
3497.8418	8417	5	8415	4	8420	4	8417	2
3401.5196	5197	4	5193	8	5198	6	5200	2
3355.2285	2281	2	2283	6	2287	3	2293	2
3286.7538	7533	5	7542	7	7538	6	7544	2
3217.3796	3801	5	3793	8	3795	7	3795	2
3175.4465	4469	5	4460	8	4464	7	4469	2
3091.5777	5768	5	5777	8	5781	6	5782	2
3015.9129	9132	5	9128	8	9129	6	9134	2
2959.9924	9928	5	9921	8	9921	6	9930	2
2912.1581	1572	5	1587	8	1577	5	1586	2
2851.7970	7966	5	7966	8	7974	6	7974	2
2804.5200	5193	5	5202	10	5203	7	5205	2
2755.7366	7357	5	7360	7	7376	4	7364	2
2706.5812	5804	4	5816	5	5808	1	5820	1
2643.9972	9966	3	9965	6	9976	4	9986	1
2413.3087	3088	10	3084	6	3090	2	----------	-----
2327.3940	3940	15	3941	8	3935	2	----------	-----

* The whole number is shown only in the first column.

TABLE 3.—*Energy-level differences*

Term symbols	Wave numbers	Differences	Term symbols	Wave numbers	Differences
			a^7D_6–$a^7D_5^1$	31027.036–30815.486	211.550
a^5D_0–$a^5D_1^1$	28844.618–28754.676	89.942		31072.250–30860.694	211.556
	33804.031–33714.093	89.938		31482.556–31271.012	211.544
	43523.036–43433.091	89.945			
			a^5D_1–$a^5D_0^1$	38246.715–38132.274	114.441
a^5D_1–$a^5D_1^1$	29028.750–28844.618	184.132		41538.728–41424.284	114.443
	33988.163–33804.031	184.132		42758.377–42643.934	114.443
	43479.629–43295.502	184.127			
	43707.159–43523.036	184.123	a^5D_2–$a^5D_1^1$	41667.176–41472.250	194.926
				42953.306–42758.377	194.929
a^5F_1–$a^5F_1^1$	35983.665–35535.177	448.488			
	37315.443–36866.941	448.502	a^5D_3–$a^5D_2^1$	38474.191–38191.328	282.863
	41001.740–40553.249	448.491		42273.457–41990.584	282.873

The average deviation from the mean is 0.0034 wave number, which corresponds to an average probable error of less than 0.0004 A in the relative values of these wave lengths. We feel that these experiences justify the retention of the fourth decimal place when the probable error of the final mean is less than 0.0005 A. Our final values are exhibited in table 4, together with values quoted from Burns and Walters [4] and from Jackson [5] for purposes of comparison. The values measured by Burns and Walters apply to the iron arc at reduced pressure, and are not strictly comparable with the others unless corrected for pressure displacement. Comparison of 219 B and W

lines and 108 J lines with our values shows the following differences in Angstrom units:

	NBS—B and W	NBS—J
Systematic difference	+0.0008	±0.0000
Accidental difference	±0.0014	±0.0011

The systematic difference is of the expected order and sign for the displacement due to atmospheric pressure, but the accidental differences are two or three times our average probable error. If correction is made for the former, the averaging of three independent and concordant observations will yield satisfactory seven-place secondary standards of wave length throughout a considerable range of ultraviolet.

Our observations were purposely extended above 3370 A to test the agreement of the present series with the values adopted by the IAU [10]. For 13 lines (3370.7 to 3497.8 A) there is an accidental difference of 0.0010 A, and a systematic difference (NBS—IAU)= −0.0009 A. This discrepancy would appear to be larger than the probable error of either set, but we are unable to account for it. It illustrates again the extreme difficulty of accurately determining the relative values of wave lengths widely separated in the spectrum. Assuming that this difference is not due to errors of focus for the primary and secondary lines and that the corrections for standard air density and dispersion of phase have been correctly made in each case, the only uncertainty (neglecting error of measurement) is a secondary correction due to water vapor in the air since interference measurements are always made in moist air. But the corrections for standard air density are taken from data applying to dry air. Considering the data on refraction and dispersion of steam by C. and M. Cuthbertson [21], it is obvious that the correction for absolute humidity of average air must be a differential one of negligible magnitude for ordinary interference comparisons.

It may be recalled that the scale of secondary standards adopted by the IAU in 1928 was somewhat lower than the values of 1922. This revision [22] ranged from −0.001 A for 3370 to 4000 A to −0.009 A for 6663 to 6750 A. It appears probable from our measurements that the ultraviolet values may still be 1 part in 4 million too large.

Our final results are displayed in the first column of table 4, the second column of which indicates the number of spectrograms on which each line was measured. The fractional values and number of observations reported by Burns and Walters [4] and by Jackson [5] are quoted in columns 3 and 4, respectively. In column 3 the letter c means computed value. Spectral-term combinations as given by Burns and Walters [4], by Catalán [23], and by Russell [24] are entered in column 5. Here odd multiplicities designate lines due to neutral atoms and even multiplicities designate those characteristic of singly ionized atoms. Vacuum wave numbers calculated from the data in column 1 with the aid of Kayser's Tabelle der Schwingungszahlen appear in the last column.

TABLE 4.—*Interference measurements of wave length in the ultraviolet spectrum of iron*

λ_{air}A NBS	Number of observations N	Burns and Walters		Jackson		Term combination	Wave number in vacuum
		λ	N	λ	N		
3497. 8418	15	841	7	843	3	a^5D_1–a^5P_2	28580. 909
3490. 5746	5	574	4	575	3	a^5D_3–a^5P_2	28640. 411
3485. 3415	20	339	8	342	4	a^5P_2–a^5P_1	28683. 413
3476. 7035	14	702	6	703	1	a^5D_0–a^5P_1	28754. 676
3465. 8622	9	860	5	863	3	a^5D_1–a^5P_1	28844. 618
3445. 1506	20	148	11	150	2	a^5P_2–19R$_2$	29018. 021
3443. 8774	13	878	6	878	3	a^5D_2–a^5P_1	29028. 750
3427. 1207	16	119	9	121	5	a^5P_2–18R$_2$	29170. 679
3413. 1335	20	131	11			a^5P_2–d^5D_3	29290. 219
3407. 4608	18	460	9			a^5P_3–c^3F_4	29338. 979
3401. 5196	20	518	8	522	4	a^5F_1–b^5P_2	29390. 221
3399. 3343	21	333	10	337	4	a^5P_2–d^3D_2	29409. 115
3396. 9772	19	974	5			a^5F_2–b^5P_2	29429. 520
3383. 9808	22	979	8			a^5P_3–c^3F_3	29542. 543
3380. 1111	18	110	8			(Fe I)	29576. 364
3370. 7845	22	784	8	786	4	(Fe I)	29658. 195
3355. 2285	13	228	7	229	4	(Fe I)	29795. 697
3347. 9262	11	926	3	928	4	a^3P_2–4R$_2$	29860. 682
3340. 5659	13	565	3	566	4	a^3P_2–2R$_2$	29926. 473
3337. 6655	10	666	2	667	4	(Fe I)	29952. 476
3328. 8669	19	867	5	866	4	(Fe I)	30031. 644
3323. 7374	19	735	6	737	4	(Fe I)	30077. 990
3314. 7421	21	741	7	741	4	(Fe I)	30159. 610
3306. 356	3	352	8			a^5P_1–e^5P_2	30236. 10
3305. 971	3	970	9			a^5P_2–e^5P_2	30239. 62
3298. 1328	19	132	9	131	6	a^5P_1–4R$_2$	30311. 488
3286. 7538	20	753	10	754	6	a^5P_2–e^5P_2	30416. 425
3284. 5892	9	588	5	587	5	a^5P_2–e^5P_2	30436. 469
3280. 2613	19	260	8	261	5	(Fe I)	30476. 624
3271. 0014	21	0. 999	10	001	7	a^5P_2–e^5P_1	30562. 898
3257. 5937	19	593	7	592	5	a^5P_2–4R$_2$	30688. 685
3254. 3628	20	363	8	362	5	(Fe I)	30719. 153
3244. 1887	21	187	10	190	7	a^7D_4–34W$_3$	30815. 486
3239. 4362	21	434		437	7	a^7D_4–33W$_4$	30860. 694
3236. 2226	22	223	10	222	7	a^5D_3–a^3F_4	30891. 337
3225. 7883	17	788	10	790	7	a^7D_5–53W$_6$	30991. 256
3222. 0682	19	067	10	069	7	a^7D_5–34W$_3$	31027. 036
3217. 3796	22	377	9	381	7	a^7D_5–33W$_4$	31072. 250
3215. 9398	18	939	9	940	7	a^7D_5–20W$_2$	31086. 159
3205. 3992	20	399	9	400	7	a^7D_4–43W$_1$	31188. 380
3200. 4741	9	471	10	474	7	a^7D_5–17W	31236. 375
3196. 9288	8	927	11	930	8	a^7D_4–25W$_3$	31271. 012
3191. 6583	9	659	9	660	7	a^5D_4–a^3D_3	31322. 649
3184. 8948	22	894	8	896	7	a^5D_3–a^3F_3	31389. 164
3178. 0137	16	013	6	016	7	a^7D_5–27W$_4$	31457. 126
3175. 4465	22	445	8	447	7	a^7D_5–25W$_3$	31482. 556
3160. 6582	22	659	6	657	2	a^7D_5–16W$_4$	31629. 854
3157. 0388	17	038	4	042	2	a^7D_4–13W$_4$	31666. 113
3143. 9896	12					(Fe I)	31797. 540
3134. 1113	21	108	7	111	7	a^5F_3–c^5D_4	31897. 757

TABLE 4.—*Interference measurements of wave length in the ultraviolet spectrum of iron*—Continued

λ_{air} A NBS	Number of observations N	Burns and Walters		Jackson		Term combination	Wave number in vacuum
		λ	N	λ	N		
3125. 653	14	652	3	658	7	$a^7D_5^5$–10W_4	31984. 07
3116. 6329	22	632	8	633	7	a^5F_1–$c^5D_2^3$	32076. 636
3091. 5777	21	577	11	579	12	a^5F_1–$c^5D_3^3$	32336. 585
3083. 7419	21	741	12	743	12	a^5F_2–$c^5D_1^3$	32418. 751
3075. 7204	20	721	9	722	9	a^5F_3–$c^5D_2^3$	32503. 296
3067. 2433	14	244	9	245	10	a^5F_4–$c^5D_3^3$	32593. 122
3059. 0874	16	090	2	085	2	a^5D_3–$b^5D_2^3$	32680. 015
3057. 4452	12	447	6	447	9	a^5F_5–$c^5D_4^3$	32697. 567
3055. 2631	22	264	8			a^3F_3–$c^3D_2^3$	32720. 920
3047. 6059	12	607	2	605	2	a^5D_2–$b^5D_3^3$	32803. 128
3040. 4281	22	427	11			a^5F_4–$c^5F_5^3$	32880. 566
3037. 3891	9	394	2	387	3	a^5D_1–$b^5D_2^3$	32913. 462
3030. 1491	22	148	10			(Fe I)	32992. 100
3024. 0330	21	033	10			a^5D_1–$a^3P_2^3$	33058. 823
3015. 9129	16					(Fe I)	33147. 826
3009. 5698	20	570	11			a^5F_4–$c^5F_4^3$	33217. 689
3003. 0311	22	031	9			a^5F_3–$c^5F_3^3$	33290. 012
2999. 5123	10	514	9	513	7	a^5F_5–$c^5F_5^3$	33329. 065
2990. 3923	9	391	9			(Fe I)	33430. 705
2987. 2919	21	292	12	291	9	a^5F_4–$c^5F_3^3$	33465. 401
2981. 4448	13	445	8	446	8	a^5D_3–$a^3P_2^3$	33531. 028
2965. 2551	11	255		255	10	a^5D_0–$b^5F_1^3$	33714. 093
2959. 9924	21	991	14			(Fe I)	33774. 031
2957. 3654	11	366	17	365	9	a^5D_1–$b^5F_1^3$	33804. 031
2953. 9400	18	939	9	940	8	a^5D_2–$b^5F_2^3$	33843. 229
2941. 3430	14	344	19	343	2	a^5D_2–$b^5F_1^3$	33988. 163
2929. 0081	17	008	16	008	10	a^5D_3–$b^5F_3^3$	34131. 291
2920. 6906	14	689	19			a^5F_2–$c^5F_2^3$	34228. 484
2912. 1581	20	159	21	158	11	a^5D_4–$b^5F_4^3$	34328. 767
2899. 4156	13	414	21			(Fe I)	34479. 631
2895. 0352	13	034	19			a^3F_3–$c^3F_4^3$	34531. 798
2894. 5050	15	504	19			(Fe I)	34538. 122
2877. 3005	12	301	19			a^3F_4–18R$_4^3$	34744. 631
2874. 1722	21	172	19			a^5D_4–$a^5G_5^3$	34782. 445
2869. 3075	20	308	18	307	8	a^5D_3–$a^5G_4^3$	34841. 412
2863. 864	10	864	15			a^5D_2–$a^5G_3^3$	34907. 63
2851. 7970	21	797	22	797	11	a^5F_1–$b^5G_2^3$	35055. 334
2845. 5945	15	595	18			a^5F_2–$c^5P_2^3$	35131. 740
2838. 1193	22	119	21	120	7	a^5F_2–$b^5G_3^3$	35224. 266
2832. 4350	21	437	21	436	10	a^5F_3–$b^5G_4^3$	35294. 951
2823. 2753	22	274	21	276	3	a^5F_3–$b^5G_3^3$	35409. 455
2813. 2861	17	287	19	288	9	a^5F_4–$b^5G_5^3$	35535. 177
2806. 9840	16	985	22	985	8	a^5F_4–80B	35614. 955
2804. 5200	25	521	21	521	5	a^5F_4–$b^5G_4^3$	35646. 244
2797. 7751	11	775	20			a^5F_5–83B	35732. 175
2781. 8347	6	836	18			a^5F_2–$d^5D_3^3$	35936. 917
2778. 2205	25	221	18	220	10	a^5F_5–$b^5G_6^3$	35983. 665
2767. 5208	19	522	15	525	9	a^5F_5–$d^5D_4^3$	36122. 776
2763. 1078	7	108	19			a^5F_3–52R$_3^3$	36180. 464
2755. 7366	19	738	19			a^4D_4–$a^4F_5^3$	36277. 237

TABLE 4.—*Interference measurements of wave length in the ultraviolet spectrum of iron*—Continued

λ_{air} A NBS	Number of observations N	Burns and Walters		Jackson		Term combination	Wave number in vacuum
		λ	N	λ	N		
2749. 325	12	322	11			a^4D_3–$a^4F_4^5$	36361. 83
2746. 9823	13	983	18			a^4D_3–$a^4D_3^3$	36392. 842
2746. 4833	14	482	18			a^4D_3–$a^4F_3^4$	36399. 454
2739. 5467	25	546	19			a^4D_4–$a^4D_4^4$	36491. 611
2735. 473	15	475	19	476	5	a^5F_4–$d^5D_3^3$	36545. 95
2727. 540	4	538	19			a^4D_3–$a^4D_2^2$	36652. 24
2723. 5770	6	576	11	577	2	a^5D_2–$b^5P_1^1$	36705. 568
2718. 4352	12	435	15			a^5F_2–47R$_1^1$	36774. 989
2714. 413	6	411	16			a^4D_4–$a^4D_3^3$	36829. 48
2711. 6548	9	654	17			a^5F_4–50R$_2^3$	36866. 941
2706. 5812	11	582	19			a^5F_3–51R$_2^3$	36936. 043
2699. 1060	16	104	17	108	8	a^5F_4–49R$_1^1$	37038. 333
2689. 2117	26	212	14	212	7	a^5F_4–48R$_2^3$	37174. 597
2679. 0608	26	061	20	063	9	a^5F_5–50R$_2^3$	37315. 443
2673. 2127	6	213	6			a^5F_1–$c^5D_1^1$	37397. 072
2662. 0563	14	056	14			a^5F_3–$c^5D_2^3$	37553. 789
2651. 7059	7	706	12			a^5F_3–$b^3G_4^4$	37700. 363
2647. 5576	10	557	13			a^5D_3–$b^3D_3^3$	37759. 431
2643. 9972	22	999	15	4. 005	7	a^5F_1–$c^5G_2^3$	37810. 273
2635. 8082	15	808	15	807	8	a^5F_2–$c^5G_3^4$	37927. 736
2628. 2923	27	292	11	292	3	a^6D_1–$a^6D_2^3$	38036. 188
2625. 6663	24	666	18	668	5	a^6D_4–$a^6D_3^4$	38074. 227
2621. 6690	8	667	21			a^6D_1–$a^6D_1^2$	38132. 274
2617. 6160	16	615	17			a^6D_3–$a^6D_3^3$	38191. 328
2613. 8240	13	823	23	822	2	a^6D_2–$a^6D_1^2$	38246. 715
2611. 8725	14	873	19	872	3	a^6D_4–$a^6D_4^4$	38275. 290
2598. 3689	8	368	20	369	9	a^6D_4–$a^6D_3^3$	38474. 191
2585. 8753	9	877	19	876	10	a^6D_5–$a^6D_4^4$	38660. 066
2584. 5349	7	538	19	535	8	a^5F_5–$c^5G_4^5$	38680. 115
2576. 1033	6					(Fe I)	38806. 705
2575. 7442	7	744	23			(Fe I)	38812. 116
2562. 5348	11	533	17	534	8	a^4D_4–$a^4P_3^3$	39012. 172
2551. 0936	11	090	23			(Fe I)	39187. 122
2542. 1007	11	101	17	102	2	(Fe I)	39325. 739
2530. 6938	10	691	14	692	1	(Fe I)	39502. 984
2519. 6279	11	627	19			(Fe I)	39676. 464
2507. 8987	11	898	20	900	7	(Fe I)	39862. 013
2496. 5324	11	534	20	533	8	(Fe I)	40043. 485
2487. 0643	8	064	17			(Fe I)	41195. 915
2474. 8131	11	813	16	814	8	(Fe I)	40394. 883
2468. 8782	11	878	20	879	7	(Fe I)	40491. 982
2465. 1479	11	148	22	148	8	a^5F_4–142B	40553. 249
2457. 5956	10	595	18	595	8	(Fe I)	40677. 862
2453. 4746	11	472	20			(Fe I)	40746. 181
2447. 7086	10	707	17	708	5	a^5D_4–$c^5F_5^5$	40842. 159
2443. 8707	8	870	18			a^5F_5–26R$_1^1$	40906. 292
2442. 5674	9	567	19			(Fe I)	40928. 117
2438. 1811	11	179	15			a^5F_5–142B	41001. 740
2431. 025	4	023	12			(Fe I)	41122. 43
2413. 3087	18	308	18	309	10	a^6D_1–$a^6F_2^3$	41424. 284
2411. 0663	17	064	22	066	7	a^6D_1–$a^6F_1^1$	41462. 808
2410. 5172	11	518	13	517	8	a^6D_2–$a^6F_3^3$	41472. 250
2406. 6593	20	659	18	657	3	a^6D_3–$a^6F_4^5$	41538. 728
2404. 430	3	429	19			a^6D_2–$a^6F_1^1$	41577. 24
2399. 2396	12	239	19	238	5	a^6D_3–$a^6F_3^4$	41667. 176

TABLE 4.—*Interference measurements of wave length in the ultraviolet spectrum of iron*—Continued

λ_{air} A NBS	Number of observations N	Burns and Walters λ	Burns and Walters N	Jackson λ	Jackson N	Term combination	Wave number in vacuum
2389. 9713	15	970	19			a^5D_2–$c^5P_3^3$	41828. 746
2388. 6270	18	627	16	625	2	a^5D_4–$a^5F_4^4$	41852. 284
2384. 386	3	385	17			a^4F_2–$a^4D_3^3$	41926. 72
2380. 7591	17	759	18	757	3	a^5D_3–$a^5P_2^2$	41990. 584
2379. 2756	20	275	17	273	3	a^4F_4–$a^4D_4^4$	42016. 766
2375. 193	2	191	19			a^4F_2–$a^4D_1^1$	42088. 98
2374. 517	2	516	17			a^5D_0–$c^5P_1^1$	42100. 96
2371. 4285	18	427	19			a^5D_2–$c^5P_2^3$	42155. 787
2370. 497	2	495	12			a^4F_2–$a^4F_2^2$	42172. 35
2368. 595	20	594	19			a^4F_3–$a^4D_3^3$	42206. 21
2366. 592	3	590	10			a^4F_3–$a^4F_3^3$	42241. 93
2364. 8269	21	826	20	825	4	a^5D_4–$a^5P_3^4$	42273. 457
2362. 019	4	019	15			a^4F_4–$a^4F_4^4$	42323. 71
2360. 294	2	292	19			a^4F_4–$a^4D_3^3$	42354. 64
2359. 997	2	997	18			a^4F_5–$a^4F_4^4$	42359. 96
2359. 1039	23	104		102	3	a^5D_3–$a^5P_3^3$	42376. 000
2354. 8888	17	888	14			a^4F_3–$a^4F_3^3$	42451. 843
2344. 2802	19	279	24			a^5D_1–$a^5P_2^2$	42643. 934
2338. 0052	25	005	21	002	2	a^5D_2–$a^5P_2^2$	42758. 377
2332. 7972	22	796	22	795	3	a^5D_4–$a^5P_3^3$	42853. 827
2331. 3067	25	305	19	305	3	a^4F_5–$a^4F_4^4$	42881. 222
2327. 3940	25	394	22	392	3	a^5D_3–$a^5P_3^3$	42953. 306
2320. 3561	15	355	19			a^5D_3–$d^5D_4^4$	43083. 575
2313. 1022	16	102	22			a^5D_2–$d^5D_3^3$	43218. 672
2308. 9971	16	996	21			a^5D_1–$d^5D_2^2$	43295. 502
2303. 579	6	577	19			a^5D_1–45R$_2^3$	43397. 32
2303. 4225	6	422	17			(Fe 1)	43400. 274
2301. 6818	18	681	16			a^5D_0–$d^5D_1^1$	43433. 091
2300. 1397	18	139	18			a^5D_2–52R$_2^3$	43462. 210
2299. 2180	16	218	17			a^5D_2–$d^5D_2^2$	43479. 629
b2297. 785	5	787	13			a^5D_3–$d^5D_3^3$	43506. 74
2296. 9247	14	926	10			a^5D_1–$d^5D_1^1$	43523. 036
2294. 4059	16	406	10			a^5D_1–$d^5D_0^1$	43570. 812
2293. 8454	8	847	3			(Fe 1)	43581. 457
2292. 5227	16	523	20			a^5D_3–53R$_2^3$	43606. 601
2291. 122	5	117	11			(Fe 1)	43633. 26
2287. 632	5	628	9			(Fe 1)	43699. 82
2287. 2477	9	248	20			a^5D_2–$d^5D_1^1$	43707. 159
2284. 087	10	083	20			a^5D_3–$d^5D_2^2$	43767. 63
2283. 653	2	652	9			a^5D_1–51R$_2^3$	43775. 95
b2279. 922	7	927	7			a^5D_2–48R$_2^3$	43847. 58
2277. 098	9	094	7			(Fe 1)	43901. 96
2276. 0247	9	023	10			a^5D_4–$d^5D_3^3$	43922. 654
2274. 0885	12	087	8			a^5D_2–51R$_2^3$	43960. 047
2272. 0670	8	065	12			a^5D_3–49R$_1^2$	43999. 157
2271. 781	6	778	9			(Fe 1)	44004. 69
2270. 8601	14	858	5			a^5D_4–53R$_2^3$	44022. 538
d2265. 053	12	047	8			a^5D_3–48R$_2^3$	44135. 39
2264. 3894	15	390	8			(Fe 1)	44148. 324
2260. 079	12	078	6			a^5D_3–$a^4F_3^3$	44232. 51
2259. 511	7	511	12			(Fe 1)	44243. 63
2255. 861	5	859	6			(Fe 1)	44315. 21
2253. 1251	18	122	4			a^5D_4–$a^4F_4^4$	44369. 017
2249. 177	8	173	4			a^5D_3–$a^4D_3^3$	44446. 89
2248. 858$_2^1$	8	855	5			(Fe 1)	44453. 20

TABLE 4.—*Interference measurements of wave length in the ultraviolet spectrum of iron*—Continued

λ_{air} A NBS	Number of observations N	Burns and Walters		Jackson		Term combination	Wave number in vacuum
		λ	N	λ	N		
2245.651	12	646	3			a^5D_2–$c^5D_3^\circ$	44516.67
2240.627	9					(Fe I)	44616.48
2231.211	13	211	5			a^5D_2–$c^5D_2^\circ$	44804.75
2228.1704	13	164	3			a^5D_3–$c^5D_3^\circ$	44865.880
2211.234	5	232	c			a^5D_2–$c^5G_3^\circ$	45209.48
2210.686	7	684	c			a^5D_4–$c^5D_3^\circ$	45220.69
2207.068	5	063	c			a^5D_4–$b^5G_3^\circ$	45294.81
2201.117	5	113	c			a^5D_3–$c^5G_3^\circ$	45417.26
2200.7227	8	721	6			a^5D_1–$d^5P_2^\circ$	45425.393
2196.040	5	037	6			a^5D_1–$d^5P_1^\circ$	45522.24
2191.202	10	201	2			a^5D_0–20 R_1°	45622.74
2187.192	4	188	6			a^5D_2–$d^5P_1^\circ$	45706.38
2186.890	7	888	5			a^5D_1–20R_1°	45712.69
2183.979	9					(Fe I)	45773.61
2180.866	6	863	c			a^5D_1–$b^3P_2^\circ$	45838.94
2176.837	11	835	c			a^5D_0–$b^3P_1^\circ$	45923.77
2173.212	12	208	3			a^5D_1–16R_2°	46000.37
2172.581	10	579	c			a^5D_1–$b^3P_1^\circ$	46013.72
2165.861	4	859	3			(Fe I)	46156.48
2164.547	8	543	c			a^5D_2–16R_2°	46184.49
2163.860	7	856	c			a^5D_0–10R_1°	46199.15
2163.368	5	363	1			(Fe I)	46209.66
2161.577	11	574	c			a^5D_1–$d^3D_2^\circ$	46247.94
2157.792	9	793	4			a^5D_3–19R_2°	46329.06
[d]2154.458	3					(Fe I)	46400.74
2153.004	11	001	c			a^5D_2–$d^3D_2^\circ$	46432.07
2151.099	5	095	c			a^5D_3–$c^3F_4^\circ$	46473.19
2150.182	4	179	c			a^5D_2–$c^3F_3^\circ$	46493.01
2147.787	2					(Fe I)	46544.84
2145.188	9	185	c			a^5D_3–$d^3D_3^\circ$	46601.23
2141.715	7	713	c			a^5D_3–$c^3F_3^\circ$	46676.79
2139.695	9	693	c			a^5D_4–18R_3°	46720.85
2138.589	7	587	c			a^5D_4–19R_3°	46745.01
2135.957	5					(Fe I)	46802.60
2132.015	9	011	c			a^5D_4–$c^3F_3^\circ$	46889.13
2130.962	7					(Fe I)	46912.29
2115.168	5	164	c			a^5D_3–$e^5P_3^\circ$	47262.54
[d]2112.966	2	963	c			a^5D_0–$e^5P_1^\circ$	47311.79
2110.233	6					(Fe I)	47373.06
2108.955	5	954	c			a^5D_1–$e^5P_1^\circ$	47401.76
2102.349	3	349	c			a^5D_2–$e^5P_3^\circ$	47550.69
2100.795	4	792	c			a^5D_2–$e^5P_1^\circ$	47585.86

NOTES TO TABLE 4

[a] Mean value from 5- and 7.5-mm étalons. 3160.060 from 2 mm and 0.049 from 10 mm. Possibly 3 lines, a^5G_4–163B, a^5F_2–$c^5D_2^\circ$, and $a^3D_2^\circ$–10W_4.

[b] Probably double.

[c] Spark line a^5D_4–$a^4F_4^\circ$ at 43847.76.

[d] Measured only with 2-mm étalons.

VI. REFERENCES

[1] H. Kayser and C. Runge, Abhandl. Berlin Akad. (1888 and 1890).
[2] H. Kayser and H. Konen, Handbuch der Spectroscopie **7**, 405–497 (S. Hirzel, Leipzig, 1934).
[3] Trans. Int. Astron. Union **3**, 77–102 (1928).
[4] K. Burns and F. M. Walters, Jr., Pub. Allegheny Obs. **6**, 159–211 (1929); **8**, 39–64 (1931).
(Although these observations were made with the vacuum iron arc, most of the values may be converted to atmospheric iron arc by calculation from spectral terms corrected for a pressure of one atmosphere (H. D. Babcock, Astrophys. J. **67**, 240; 1928).
[5] C. V. Jackson, Proc. Roy. Soc. (London) [A] **130**, 395–410 (1931); [A] **133**, 553–564 (1931).
[6] H. Buisson and Ch. Fabry, Astrophys. J. **28**, 169 (1908).
[7] K. Burns, BS Sci. Pap. **12**, 179–197 (1915) S251.
[8] H. Pressentin, Z. Physik **60**, 125–136 (1930).
[9] Proces-Verbaux, Comité Int. Poids et Mesures 91 (1935).
[10] Trans. Int. Astron. Union **2**, 36 (1925).
[11] W. F. Meggers and K. Burns, BS Sci. Pap. **18**, 191–196 (1922) S 441.
[12] W. F. Meggers, BS Sci. Pap. **12**, 198 (1915) S251.
[13] Trans. Int. Astron. Union **5**, 86 (1935).
[14] Trans. Int. Astron. Union **5**, 87 (1935).
[15] C. J. Humphreys, BS J. Research **5**, 1044 (1930) RP245.
[16] W. F. Meggers and C. G. Peters, BS Sci. Pap. **14**, 724 (1918) S327.
[17] C. V. Jackson, Proc. Roy. Soc. (London) [A] **133**, 555–556 (1931).
[18] F. Goos, Astrophys. J. **38**, 141 (1913).
[19] L. Lang, Z. wiss. Phot. **15**, 223–292 (1915).
[20] J. DeGier and P. Zeeman, Proc. Roy. Acad. Sci. (Amsterdam) **38**, 959–960 (1935).
[21] C. and M. Cuthbertson, Phil. Trans. [A] **213**, 16 (1913).
[22] Trans. Int. Astron. Union **4**, 60 (1932).
[23] M. A. Catalán, Anal. Soc. Esp. Fis. Quim. **28**, 1239 (1930).
[24] H. N. Russell, Astrophys. J. **64**, 194 (1926).

WASHINGTON, January 27, 1937.

U. S. DEPARTMENT OF COMMERCE NATIONAL BUREAU OF STANDARDS

RESEARCH PAPER RP993

Part of Journal of Research of the National Bureau of Standards, Volume 18, May 1937

EFFECT OF SIZING, WEAVING, AND ABRASION ON THE PHYSICAL PROPERTIES OF COTTON YARN [1]

By Walter T. Schreiber, Martin N. V. Geib, and Omar C. Moore

ABSTRACT

A method was developed for determining the effects of the amount and quality of sizing on the physical properties of cotton warp yarns and on their performance during weaving and abrasion tests. The strength, elongation under a 35-gram load and at rupture, and the permanent set under a load of 35 gram were measured on yarns before and after sizing them with white-potato starch; after weaving and removal from the cloth; and before and after abrasion in a laboratory apparatus simulating the effects of a loom. The experimental results show that the sized yarns have greater strength, less elongation, lower permanent set, and are more uniform in their physical properties, and possess better weaving qualities than unsized yarns. A simple mill method for the testing and control of sized yarns, based on these results, is suggested.

CONTENTS

	Page
I. Introduction	559
II. Experimental work	560
1. Preliminary experiments	560
2. Effect of weaving on the physical properties of cotton warp strands	560
3. Effect of abrasion on the yarns	562
(a) Abrading machine	562
(b) Specimens of yarns	562
(c) Results of tests	562
III. Effect of sizing on the performance of yarns	563
IV. Suggested mill control	563

I. INTRODUCTION

Sizing cotton warp yarns with starch is an important process used as standard practice in the textile industry. There appears to be little published information on the effect of the sizing on the physical properties of the yarn and on the performance of the yarn in the weaving operation. A quantitative knowledge of these effects is necessary if one wishes to study the possibility of using other sizing materials, as, for example, starch manufactured from sweet potatoes, which is of interest in connection with the industrial utilization of farm products.[2 3 4] Accordingly, the National Bureau of Standards, in cooperation with the Alabama Polytechnic Institute, has investigated the effect of sizing cotton yarn with the white-potato starch commonly used for this purpose.

[1] This study was carried out in the laboratories of and in cooperation with the Alabama Polytechnic Institute, Auburn, Ala.

[2] Balch and Paine. *Production of starch from sweet potatoes. Ind. Eng. Chem.* **23,** 1205 (1931).

[3] Weber, Shaw, and O'Leary. Quality of Sweet-Potato Starch for Beater Sizing of Paper. Misc. Pub. BS 150 (June 1935).

[4] Schreiber, Geib, and Moore. *Consistency of potato starch size.* BS J. Research **11,** 765 (1933), RP623.

II. EXPERIMENTAL WORK

1. PRELIMINARY EXPERIMENTS

Four spools of 20s cotton warp yarns were prepared containing different percentages of white-potato starch. Sixty ends from each spool were laid side by side and tied into the center of a warp beam. Before entering the loom, the yarns passed through the lingoes of a small jacquard harness frame to make sure that each yarn was under the same tension when weaving began. The number of yarns in 60 ends which broke in weaving 5 yards is shown in table 1.

TABLE 1.—*Number of yarns in 60 ends which broke in weaving 5 yards of fabric*

Amount of starch in yarns	Number of broken yarns	
	First run	Second run
Percent		
7.85	0	1
6.75	0	0
4.93	1	0
0	5	6

By means of a pair of clamps and a Jolly balance, an attempt was made to measure the tautness of each yarn before and after weaving. The results were not conclusive.

There were great differences in the elongation and other properties of different samples from the same skein of unsized yarn, and there was some indication that the differences were increased by weaving. On the other hand, the weaving appeared to have little effect on the sized yarn, whose properties were more uniform.

2. EFFECT OF WEAVING ON THE PHYSICAL PROPERTIES OF COTTON WARP STRANDS

An experimental yarn sheet of 20s cotton warp yarns was sized so that it contained 9.75 percent of white-potato starch. This yarn was threaded through a dobby loom as a part of the warp. The loom had been set up to make a fabric having 45 ends and 23 picks per inch. The lingoe arrangement previously described was used to bring all the warp yarns under the same initial tension before the weaving was begun. After weaving, the fabric was split along the warp and the warp yarns unravelled for test.

All of the physical tests were made on 50 specimens of yarn conditioned at 65-percent relative humidity and 70° F.

The breaking strength and elongation at rupture were measured with a single-strand tester, the jaws being 18 inches apart at the beginning of the test. The speed of the pulling jaw was 12 inches per minute.

The elongation and permanent set caused by a load of 35 g were measured with the apparatus shown in figure 1. A loop is made at one end of the specimen, 6, to which is attached a pointer, 2, weighing 8 g. The specimen passes over the pulley, 4, and is fastened to the base by the clamp, 5, in such a position that the free length is 36 inches under the tension of 8 g produced by the weight of the

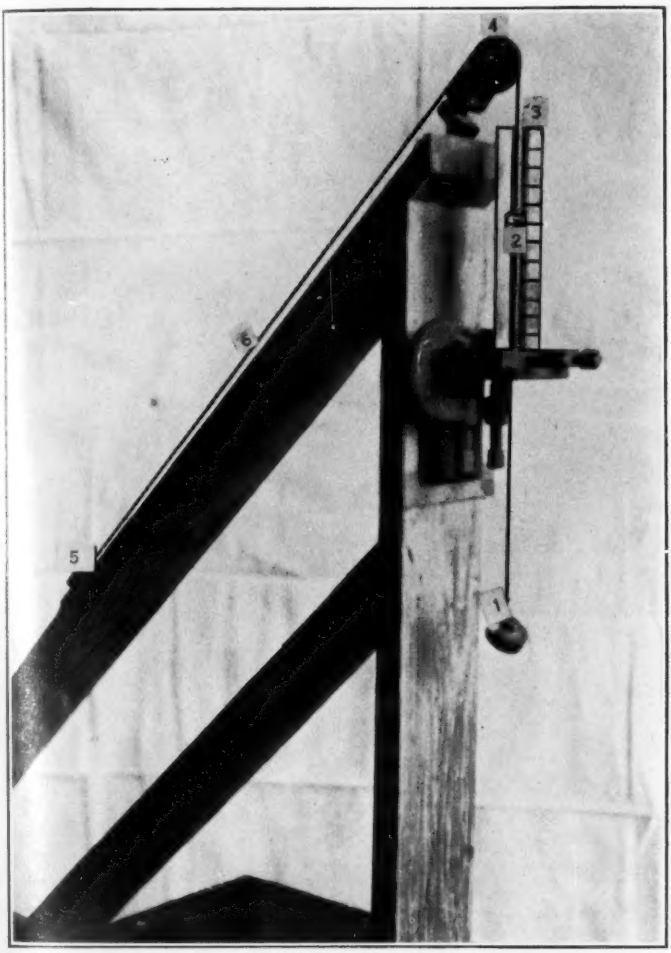

FIGURE 1.—*Apparatus for measuring elongation and set of yarns.*

1, Weight; 2, pointer; 3, scale; 4, pulley; 5, clamp for holding specimen; and 6, specimen of yarn.

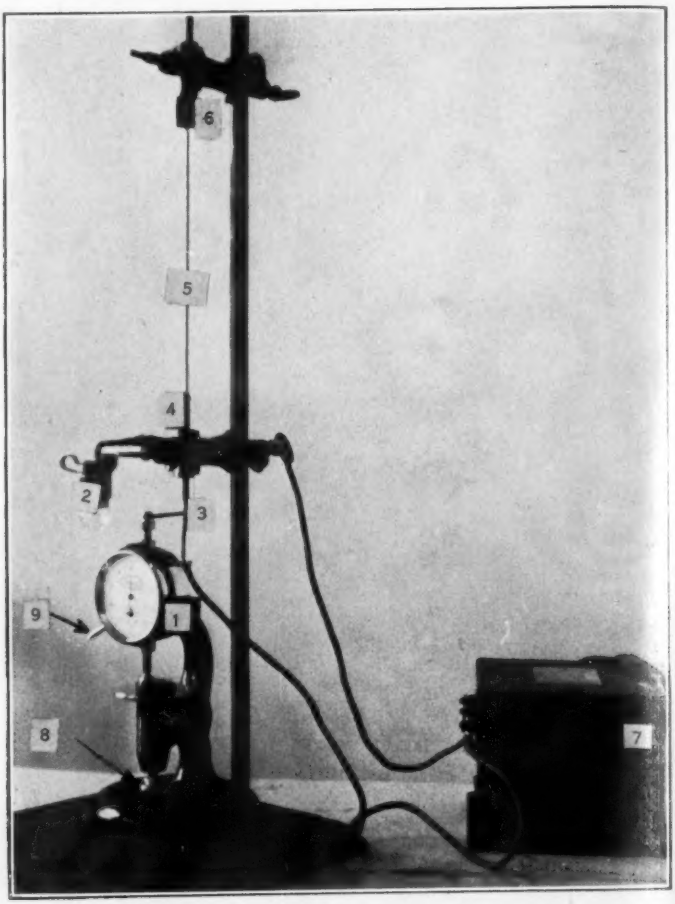

FIGURE 2.—*Apparatus for measuring length of yarns.*

1 Dial micrometer; 2, incandescent electric light to indicate contact between 3 and 4; 3, contact on upper end of plunger of dial micrometer; 4, contact affixed to specimen; 5, yarn specimen; 6, upper hook, in actual use 36 inches above contact 4; 7, transformer; 8, screw for zero adjustment of dial micrometer; and 9, micrometer dial lever.

pointer. The pointer moves over the scale, 3. Readings are made (a) under the load of the pointer only (8 g); (b) 30 seconds after the addition of a weight, 1, of 27 g; and (c) 30 seconds after the removal of the 27-g weight. The difference between readings (a) and (b) is called the "elongation at 35-g load" and the difference between readings (a) and (c) the "set at 35-g load."

The change in length caused by weaving was measured by the apparatus shown in figure 2. A dial micrometer, 1, with a working range of 0.5 inch is held in a clamp stand with the lower end of its plunger resting on the zero adjustment screw, 8, and the upper end carrying a metal contact, 3. The specimen carries a brass strip, 4, which serves as a second contact. When the contact, 3, just touches the contact, 4, an electric circuit is completed through the transformer, 7, as indicated by the incandescent electric light, 2. The apparatus is prepared for measurement as follows: A piece of wire exactly 36 inches long is suspended from the hook, 6, and the brass contact strip, 4, weighing 8 g, is attached to its lower end. A suitable thickness gage is placed under the plunger to make the micrometer dial read 0.250 inch, and sufficient shims are inserted under the micrometer base to make contacts 3 and 4 barely touch and complete the electric current through the electric light 2. The 0.250-inch thickness gage is then removed. The wire is then taken out and the warp yarn with the end loops is inserted in place of the wire. By moving the dial lever, 9, to bring 3 and 4 into contact, the difference between the over-all length of the yarn and 36 inches can be read directly from the dial, provided this difference does not exceed 0.250 inch. In preparing the specimen for this test care must be taken to prevent untwisting the yarn during handling and measuring.

Each of 50 specimens was provided with end loops, measured, and tied into a warp sheet in such a way that about 11 inches of the specimen was included in the fabric, without permitting the loop on either end to get into the loom. After the weaving the fabric was unravelled, and the specimen removed and retested. The data from these experiments are shown in table 2, only averages of the 50 specimens and average deviations being given.

Table 2 results show that the sized yarn had greater strength, lower elongation at rupture and at a 35-g load, and lower set at 35-g load, than the unsized yarn. Weaving caused a decrease in strength, but it had little effect on set or elongation for both sized and unsized yarn. It produced a considerable increase in length of the unsized yarn, whereas the length of the sized yarn was not affected.

TABLE 2.—*Effect of weaving on properties of yarns*

Sizing	Weaving	At rupture				At 35-g load				Length increase due to weaving	
		Breaking strength		Elongation		Elongation		Set			
		Average	AD [1]	Average	AD	Average	AD	Average	AD	Average	AD
		oz.		%		%		%		%	
Sized [2]	Before	17.0	1.3	4.3	0.4	0.42	0.02	0.14	0.01		
Do	After	15.8	1.7	3.9	.4	.33	.02	.08	.02	0.05	0.02
Unsized	Before	13.3	1.5	6.0	.7	.90	.06	.25	.04		
Do	After	9.5	1.4	6.1	.6	.98	.07	.36	.05	.78	.21

[1] AD is average deviation.
[2] Sized yarns contained 9.75 percent of white-potato starch.

3. EFFECT OF ABRASION ON THE YARNS

(a) ABRADING MACHINE

Since the actual weaving of experimental yarns is a laborious process, and tying them into the warp and ravelling them out of the fabric may cause unintentional changes in the yarns, an effort was made to develop a laboratory device which would simulate the action of the loom. Although it is not known whether the principal effect of the loom is to stretch the yarn by repeated tensile forces or actually to remove part of the yarn by abrasion, the simulating device shown in figure 3 is designated for convenience an "abrading machine."

(b) SPECIMENS OF YARNS

The specimens for this machine were identical with those used for the length-measurement apparatus, i. e., yarns with loops at each end and 36 inches in over-all length. A 20-g weight, 1, is hung on the loop at one end of each specimen. The specimens run through heddle eyes, 3, over a smooth-glass guide bar, 4, to a bar, 5, which is caused to travel in a cylindrical path by the driving mechanism, 6. The result of the motion of the bar, 5, is to pull the yarn back and forth through the heddle eye with a stroke or travel of 11½ inches.

(c) RESULTS OF TESTS

Of 100 similar specimens, 50 were tested for breaking strength and elongation at rupture (thus destroying these specimens) and 50 were measured for length and elongation and set at 35-g as previously described. These latter specimens were then placed in the abrading machine for a definite number of strokes, and the physical properties redetermined. The results shown in table 3 indicate that the abrading machine produces the same qualitative effect as the loom, i. e., a decrease in strength but little change in elongation or set for both sized and unsized yarn, and considerable increase in length for unsized yarn, but little increase in length for sized yarn.

TABLE 3.—*Effect of abrading machine on properties*[1] *of yarns*

Sizing	Abrasion	At rupture				At 35-g load				Length increase	
		Breaking strength		Elongation		Elongation		Set			
		Average	AD[2]	Average	AD	Average	AD	Average	AD	Average	AD
		oz		%		%		%		%	
Sized	None	17.0	1.3	4.3	0.4	0.42	0.02	0.14	0.01		
Sized[3]	6 strokes	15.2	1.5	3.8	.4	.37	.02	.09	.02	0.02	0.01
Sized	16 strokes	15.7	1.5	4.0	.4	.45	.03	.14	.02	.09	.03
Unsized	None	13.3	1.5	6.0	.7	.90	.06	.25	.04		
Unsized	6 strokes	10.2	1.0	6.0	.4	.94	.05	.34	.03	.40	.08
Unsized	16 strokes	11.6	1.1	6.6	.3	1.04	.07	.43	.05	.63	.14

[1] Data based on 50 determinations.
[2] AD is average deviation.
[3] Sized yarns contained 9.75 percent of white-potato starch.

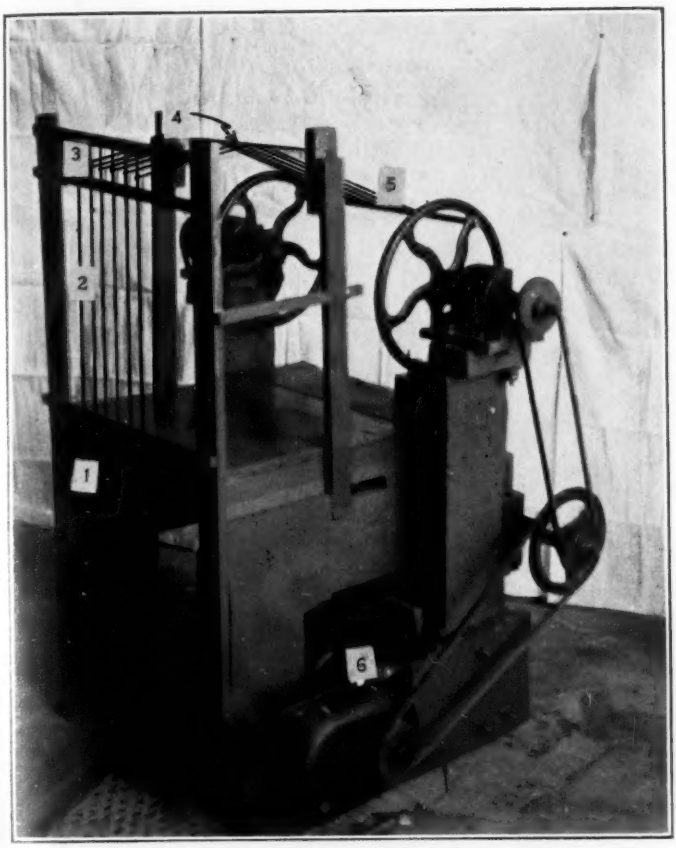

FIGURE 3.—*Machine for abrading yarns.*

1. Weights on lower ends of specimens, 20 grams each; 2, yarn specimens; 3, heddle eyes; 4, guide bar to maintain constant angle at heddle eye; 5, driving bar; and 6, driving mechanism.
[NOTE.—This machine may be provided with a handle for hand operation.]

UNIV. OF MICH.

III. EFFECT OF SIZING ON THE PERFORMANCE OF YARNS

The data in table 3 show that sizing tends to increase the strength of the yarn and also to increase its ability to resist permanent elongation when stretched. The action of the loom tends to stretch all yarns an equal amount. If some yarns in a warp sheet are poorly sized, they would fail to recover from this stretching as fully as other yarns, would become slack, and might even become entangled. Moreover, a difference in length of yarns in the same warp would cause an uneven distribution of the load, which might cause an excessive number of breaks. For these reasons it is important that the sized yarns be uniform.

IV. SUGGESTED MILL CONTROL

This suggests the possibility of establishing certain simple tests which can be applied in the mill to determine whether or not a warp is properly sized. At present this can be ascertained only after the warp has been threaded into the loom, and some fabric woven—a very expensive procedure. A test which could be applied to the yarn as it leaves the slasher would enable the mill man to duplicate satisfactory yarn without question, and would also permit him to experiment with possible changes in his sizing procedure.

In the present work, it was necessary to develop such tests. The equipment is simple but sufficiently accurate for the purpose. It is described here with the thought that some mills may find it worthwhile to install similar devices.

Cut from the warp sheet a number of yarns. Since uniformity is one of the criteria, a sufficient number of samples (50 are recommended) should be taken to be representative of the whole. Measure either the set under a 35-g load, using the apparatus shown in figure 1, or the length with the apparatus shown in figure 2. Transfer the specimens to the abrading machine shown in figure 3 and run for a predetermined number of strokes. Transfer back to the original apparatus and repeat the original measurements.

Certain standards must be established for each individual case, by testing yarns of known satisfactory quality, and fixing the number of strokes of the abrading machine to produce a sufficient change in the properties of the yarn so that it can be readily measured.

The authors express their appreciation to Professors E. W. Camp, C. B. Ordway, and W. E. Tarrant, of the Alabama Polytechnic Institute Textile School, for assistance and suggestions.

WASHINGTON, March 22, 1937.

U. S. Department of Commerce National Bureau of Standards

RESEARCH PAPER RP994

Part of Journal of Research of the National Bureau of Standards, Volume 18, May 1937

MAGNETIC METHOD FOR MEASURING THE THICKNESS OF NICKEL COATINGS ON NONMAGNETIC BASE METALS

By Abner Brenner

ABSTRACT

The local thickness of an electroplated nickel coating on a nonmagnetic base metal may be measured by the force of attraction of a small permanent magnet, the attractive force being determined with a simple spring balance. It was found that the attractive force between the magnet and coating is proportional to the thickness of the coating. The instrument is calibrated with nickel coatings of known thickness which have been deposited under about the same conditions as the coatings to be tested. Nickel coatings deposited under different conditions have somewhat different magnetic properties, which become uniform by heating the samples to 400° C (750° F). Specimens of unknown history should be annealed before testing. Measurements on coatings as deposited are correct within ±15 percent and on annealed coatings within ±10 percent.

The effect on magnetic measurements of factors such as curvature of the surface, type of base metal, and superposed chromium coatings is discussed.

The magnetic method was shown to be applicable to the testing of nickel-plated brass plumbing fixtures.

	Page
I. Introduction	566
II. Principle	566
III. Method of measurement	567
1. Types of balances	567
(a) Lever balance	567
(b) Torsion balance	567
(c) Spring balance	568
2. Position of magnet and direction of applied force	569
3. Size and composition of the magnet	569
4. Standardization of apparatus	570
(a) Preparation of thickness standards	570
(b) Calibration	571
IV. Magnetic properties of nickel deposits	572
1. Relation between magnetic attraction and thickness	572
2. Effects of conditions of deposition	574
(a) Nickel as deposited	574
(b) Annealed coatings	574
(c) "Bright nickel" deposits	575
(d) Effects of codeposited iron or cobalt	575
3. Relation of composition, hardness, and magnetic properties	576
4. Effect of base metal	577
V. Dimensional factors in magnetic thickness measurements	577
1. Area of coating	577
2. Curvature of surface	578
3. Parallel nickel coatings	579
4. Superposed chromium coatings	581
VI. Applicability to commercial testing	581
VII. Conclusions	582

I. INTRODUCTION

Until recently, the thickness of electroplated coatings was usually specified in terms of the average thickness, which may be computed from the weight of coating found, for example, by chemical analysis, on a measured area. However, many specifications now refer to the minimum thickness on significant surfaces, for the determination of which it is necessary to measure the local thickness at one or more points.

For the latter purpose the most generally applicable procedure is the metallographic method, in which the thickness of a suitably prepared cross section is measured by means of a microscope and scale. This method requires experience and expensive equipment and results in destruction of the specimen tested.

The "dropping" method [1] for zinc and cadmium deposits, and the very similar jet method [2] for nickel coatings, depend on the time required for a specified reagent to dissolve the coating. The "chord" method [3] involves the width of the cut made when the coating on a flat surface is just penetrated by a grinding wheel of known radius, or on a curved surface by a flat grinding tool. These methods destroy the coatings but have little effect on the base metal, which can usually be refinished.

Especially for factory inspection, there is a great need for a nondestructive test for thickness, which, if conditions warrant, may be applied to the entire product of a plant. The present paper describes a nondestructive method for measuring the thickness of nickel coatings on nonmagnetic base metals.

II. PRINCIPLE

The proposed method depends on the force of attraction between a permanent magnet and the nickel coating. It is entirely distinct from those methods [4] in which the thickness of a nonmagnetic coating (which may be nonmetallic) upon steel or iron is measured in terms of the reluctance of a magnetic circuit which passes through a coil and through the steel under the coating. In effect, this latter method measures the gap between the magnet and the base metal, and its use is confined to nonmagnetic coatings on steel having uniform thickness and magnetic properties.

The same principle is involved in a method [5] in which the thickness of a nonmagnetic coating on steel is measured in terms of the force required to detach a magnetic needle from the surface.

It is well known that nickel is ferromagnetic and has a permeability about one-fourth that of iron. In the present work it was found that the attractive forces between a permanent magnet and thin layers of nickel, having the same magnetic permeability, are proportional within about 10 percent to the thickness of the layers, for nickel coatings from 0.0005 mm (0.00002 in.) to 0.025 mm (0.001 in.), which is the

[1] S. G. Clarke, J. Electrodepositors' Tech. Soc. 8, Paper no. 11 (May 1933); and R. O. Hull and P. W. C. Strausser, Monthly Rev. Am. Electroplaters' Soc. 22 (March 1935).
[2] S. G. Clarke, J. Electrodepositors' Tech. Soc. 12, preprint (1936).
[3] W. Blum and A. Brenner. *Mesle's chord method for measuring the thickness of metal coatings.* J. Research NBS 16, 171 (1936) RP 866.
[4] Electric Thickness Gage, General Electric Co. Instruments 8, 341 (1935).
A similar device was demonstrated by Octavius Knight at a conference on electroplating in New York on September 26, 1934.
[5] I. V. Radtchenko and F. K. Shestakovsky, J. Tech. Phys. (USSR), 5, 1372 (1935).

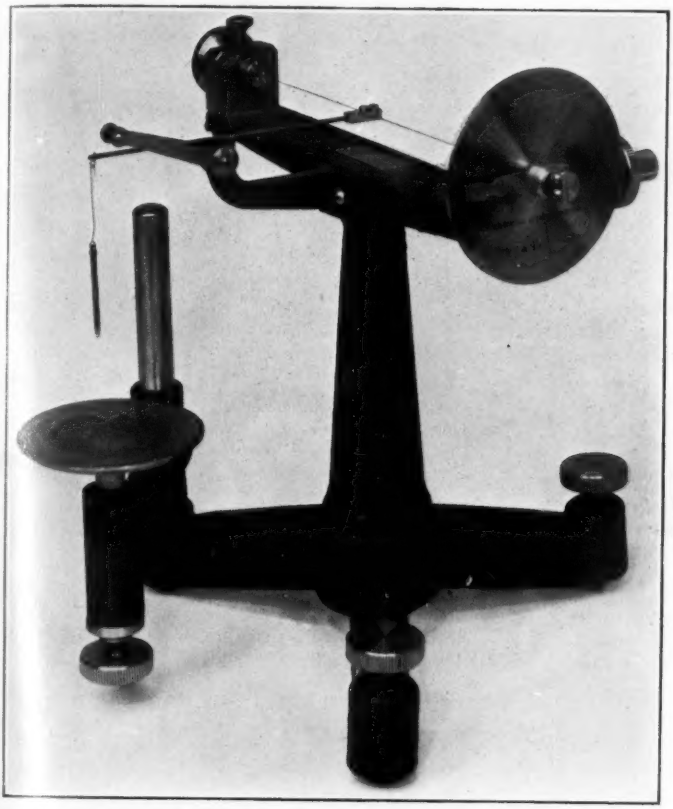

FIGURE 1.—*de Noüy tensiometer used as a magnetic balance.*

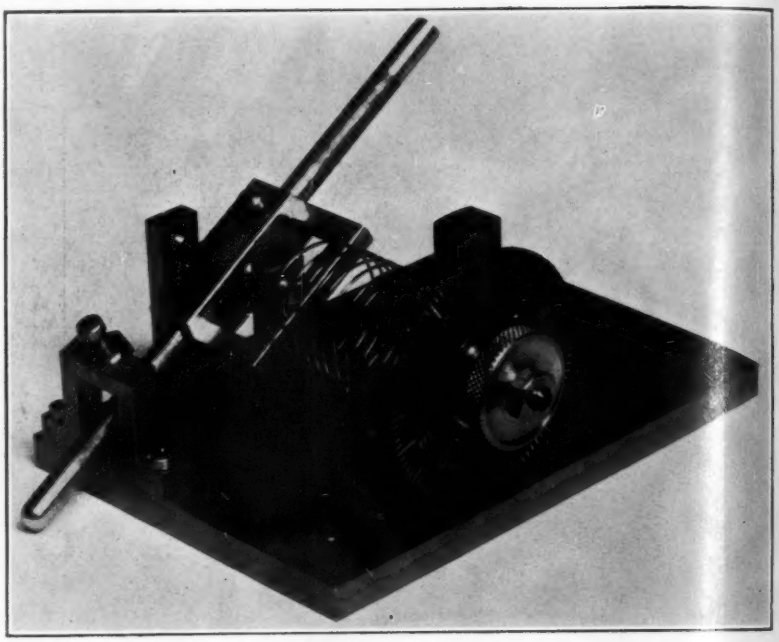

FIGURE 2.—*Sanford magnetic balance with cover removed.*

range of thickness of practically all commercial nickel coatings upon nonferrous metals. For thicker coatings an empirical curve may be constructed.

In principle, the proposed method involves merely the measurement of the force required to detach one pole of a permanent magnet from the nickel coating, and the comparison of this force with that required to detach the same magnet from a similar nickel coating of known thickness.

Nickel coatings deposited under different conditions have somewhat different magnetic permeabilities. It was found that if such coatings are annealed at 400° C (750° F) they acquire about the same permeability. The magnetic method is therefore more reliable for annealed coatings than for coatings as deposited.

III. METHOD OF MEASUREMENT

1. TYPES OF BALANCES

In order to determine the force of attraction between the magnet and the coating, any convenient device may be used that will measure forces of 1 to 5 g with a precision of about 1 percent. As the instrument must be calibrated empirically, it is necessary to know only the relative (and not the actual) loads, for example, in terms of proportional scale divisions. Three types of balances were employed in this investigation, namely, lever, torsion, and spring balances. In their design and operation, an effort was made to define conditions that will yield a precision of at least 5 percent, which is adequate for commercial testing of nickel coatings. Unless otherwise stated, all conclusions regarding favorable conditions or limitations will be based upon that criterion.

(a) LEVER BALANCE

An analytical balance was used in preliminary measurements to determine the validity and sensitivity of the method. The magnet was suspended and balanced from one arm so that it could be brought into contact with the nickel surface. Weights were then added to the other arm until the magnet was just detached. In one test a cylindrical bar magnet made of 36-percent cobalt steel, and 15 cm (6 in.) long and 5 mm (0.2 in.) in diameter, with a hemispherical end, was attracted to a nickel coating 0.025 mm (0.001 in.) thick with a force of about 2.5 g. This load could be measured readily to within 1 percent.

Thickness tests with such a balance are not convenient, especially for coatings on articles of irregular shape. This method is therefore not recommended except for orienting experiments.

(b) TORSION BALANCE

A du Noüy tensiometer for measuring surface tension can be readily adapted to the desired purpose. As shown in figure 1, a small bar magnet 2 mm (0.08 in.) in diameter and 3.0 cm (1.2 in.) long is suspended from the lever arm in place of the platinum loop that is used in surface-tension measurements. The torsion in the wire is adjusted so that with the freely suspended magnet a zero reading is obtained. The nickel surface to be tested is then raised until it is just in contact

with the magnet, and the force necessary to detach the magnet is measured on the scale.

When equipped with a freely suspended magnet, this instrument yields slightly more reproducible results than does either of the spring balances to be described. It is, however, not so compact or convenient as the latter, and the zero point requires more frequent adjustment.

(c) SPRING BALANCE

The simplest form of spring balance consists merely of a vertical helical spring, from the lower end of which a small magnet is suspended. The force necessary to detach the magnet from a nickel coating is measured by the extension of the spring. A few tests with such a device showed that it is usable but inconvenient and requires frequent adjustments.

A compact, portable spring balance, shown in figure 2, was designed a few years ago by R. L. Sanford [6] for measuring the magnetic permeability of austenitic steel. One of these instruments, which will be referred to as the "Sanford balance", was used in making most of the thickness measurements referred to in this paper. In this device two small bar magnets, each 5 mm (0.2 in.) in diameter and 5 cm (2 in.) long, are arranged astatically (to eliminate the effect of the earth's magnetic field) and are pivoted upon a sensitive jeweled bearing. The force required to detach the end of one magnet from a magnetic surface is measured by means of a spring and dial.

The sensitivity of this instrument can be varied by proper selection of the spring. With a suitable spring it was found that each division on the dial corresponded to approximately 0.00025 mm (0.00001 in.) of nickel, so that the 100 divisions covered the range of thickness usually applied to nonferrous metals. The reproducibility was about ±3 percent on coatings down to about 0.005 mm (0.0002 in.).

The Sanford balance was found to be satisfactory upon plane and most convex surfaces but not upon concave surfaces, because the magnet does not extend below the base of the instrument. The "modified Sanford" balance shown in figures 3 and 4 was designed to overcome this limitation. By removing the false bottom, the end of the magnet can be applied to a concave surface. The two small magnets, arranged astatically, are vertical, that is, normal to the surface tested, as then a more nearly uniform flux is produced about the end of the magnet than exists with an inclined magnet. The two magnets are carried on a duralumin lever arm, which reduces the weight of the moving parts and increases the sensitivity. The rack and pinion facilitate the application of the magnet to large or irregularly shaped articles. Both forms of Sanford balance are applicable in any position, which is an advantage in testing large articles or those in fixed positions.

When testing with a magnetic balance, it is expedient to make a rapid preliminary measurement in order to get an approximate reading, which is then approached more slowly in the subsequent test. The plated surface should be clean. Lack of duplication of readings is usually caused by grease or other foreign material on the surface.

---

[6] R. L. Sanford, *A magnetic balance for the inspection of austenitic steel.* BS J. Research 10, 321 (1933) RP532.

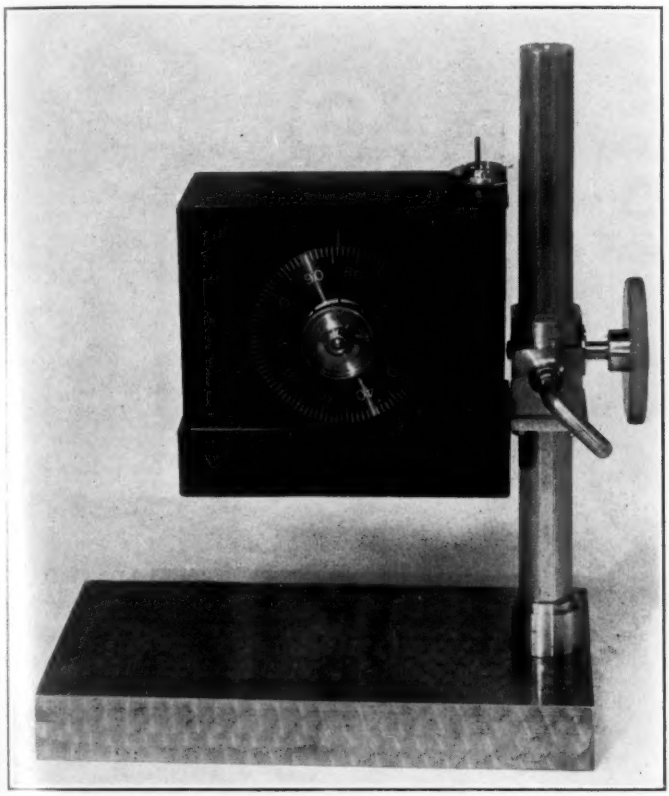

FIGURE 3.—*Modified Sanford magnetic balance.*

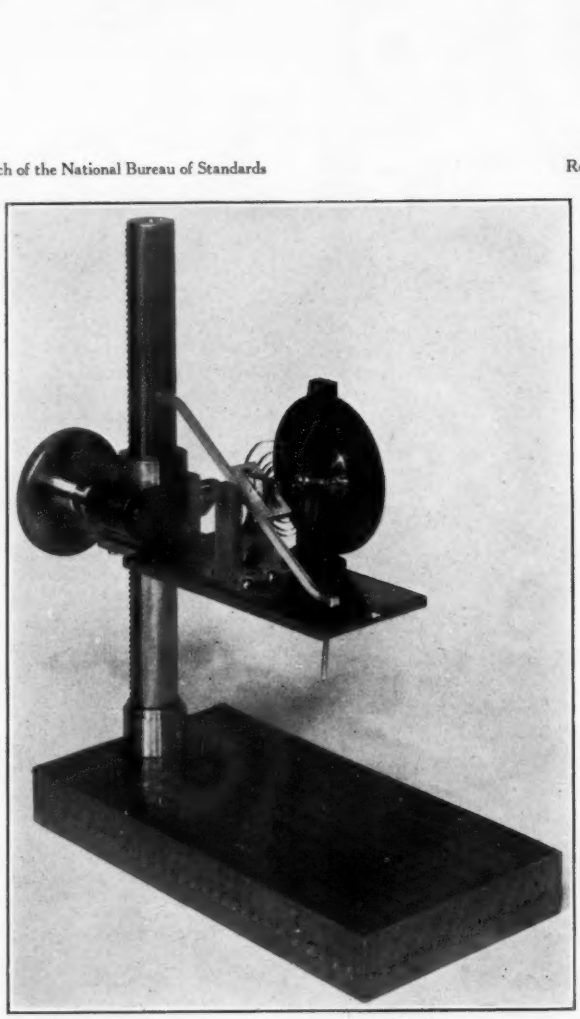

FIGURE 4.—*Modified balance with cover and false-bottom removed.*

2. POSITION OF MAGNET AND DIRECTION OF APPLIED FORCE

The maximum force of attraction between a magnet and a nickel coating is exerted in a direction normal to the surfaces at the point of contact. If a magnet is pulled from a surface in a normal direction, the detaching force is equal to the attractive force. However, if the detaching force is not applied along the normal, it measures only a component of the attractive force, and the detaching force is proportional to the cosine of the angle between its direction and the normal to the surface. This relation was confirmed experimentally. The angle of inclination of the bar magnet to the normal is not important; only the direction of the detaching force enters into consideration.

When using a freely suspended magnet on a lever balance or tensiometer, the surface to be measured should be set normal to the magnet. In this case, the detaching force is equal to the attractive force. A departure of 10° from the normal reduces the detaching force by only 2 percent.

With a balance having a magnet rigidly attached to a lever arm, the direction of the detaching force is along the tangent to the circle described by the end of the magnet and having the pivot as the center. With both the Sanford balance and the modified instrument, the detaching force is about 75 percent of the attractive force. When making measurements, the angle between the normal to the surface and the direction of the detaching force should always be the same. This condition is met by having the plated surface normal to the magnet of the modified balance, or parallel to the base of the original Sanford balance. For a precision of 5 percent, the angle between the magnet and the normal to the surface should vary by not more than 5°. Less variation can be permitted in this angle than with a freely suspended magnet, as the cosine changes more rapidly in the neighborhood of 40° than near 0°. When either type of Sanford balance is set on a plane surface, the magnets will contact the surface at the proper angle. On curved surfaces, the magnet of the modified balance can be set normal to the surface, by eye, within about 5°. When testing a cylindrical surface it is easier to secure the proper position if the axis of the lever which carries the magnets is placed parallel to the axis of the cylinder, rather than perpendicular to it.

3. SIZE AND COMPOSITION OF THE MAGNET

The magnet may be of any composition that is suitable for permanent magnets. Most of the experiments here reported were made with magnets of 36-percent cobalt steel suitably heat treated. A few tests with Alnico magnets showed that they have somewhat more attractive force for a given weight, and depart less from linearity between attractive force and thickness of nickel coating than do the cobalt-steel magnets. Their principal disadvantage is that they cannot be machined, but must be ground to the desired size and shape. The strength of new magnets of either type tends to decrease during the first few weeks, after which, however, they require calibration only at long intervals. They should not be brought into contact with other magnets or with strongly magnetic metals.

In general, small magnets are preferable to large ones because a more sensitive balance may be used, they are more suitable for measuring small or curved surfaces, and they are less affected by a nickel coating on the opposite side of a plated sheet. On the other hand, the attractive force of magnets 2 mm (0.08 in.) or less in diameter shows larger departures from linearity with respect to thickness, especially of thin coatings, and hence must be calibrated for a greater number of thicknesses. Taking all of these factors into account, an Alnico magnet 2 mm (0.08 in.) in diameter and 3 cm (1.2 in.) long was selected for the instrument shown in figure 4. The contact end of the magnet is hemispherical.

4. STANDARDIZATION OF APPARATUS

(a) PREPARATION OF THICKNESS STANDARDS

It is necessary to calibrate the apparatus with nickel deposits of known thickness and of the same magnetic permeability as those to be tested subsequently. The preparation of deposits of uniform, accurately known thickness upon flat plates involves many difficulties.

For most of the tests, the nickel coating was deposited on one side of a flat plate, 10 by 15 cm (4 by 6 in.), the other side of which was insulated with a suitable stop-off lacquer. The specimens were mounted in a metal rack so that there was less than 6 mm (0.25 in.) either between adjacent specimens or between specimens and the rack, and the plating was done in a rectangular tank of which the rack and specimens completely filled the cross section.

The average thickness, computed from the total weight of nickel deposited on a plate, was the basis of most of the magnetic measurements. On such specimens, the thickness of coating near the edges was from 10 to 20 percent above the average, but on 70 percent of the area the thickness was uniform and not more than 4 percent below the average thickness computed from the total weight of deposit. The average thickness over the 70 percent that constituted the central portion was computed more accurately by cutting off strips about 1 cm (0.4 in.) wide from each edge, determining the weight of nickel on them, and deducting this amount from the total weight of the original deposit. The magnitude of this correction was from 3 to 5 percent. Magnetic and metallographic measurements at numerous points on this central portion showed that the mean deviation from the average thickness was about ± 4 percent, and the maximum deviation was about ± 8 percent.

On many specimens, the thickness of deposit was confirmed by microscopic measurements of metallographic sections at the same points that were measured magnetically.

For measuring the effects of curvature upon magnetic tests, cylinders and spheres were plated uniformly by rotating them during the plating process.

The solutions and conditions used in plating are summarized in table 1.

TABLE 1.—*Conditions used in nickel plating*

Bath	Type	Composition	Concentration			Usual conditions				
			N	g/liter	oz/gal	pH	Temperature		Current density	
							°C	°F	amp/dm²	amp/ft²
E	Standard	$NiSO_4.7H_2O$	1.4	200	27	5.3	35	95	2	19
		$NiCl_2.6H_2O$	0.4	45	6					
		H_3BO_3	.5 *M*	30	4					
F	Low pH	$NiSO_4.7H_2O$	1.4	200	27	2.9	35	95	2	19
		$NiCl_2.6H_2O$	0.4	45	6					
		H_3BO_3	.5 *M*	30	4					
G	High sulphate	$NiSO_4.7H_2O$	.55	77	10	5.7	27	81	1	9
		NH_4Cl	.3	15	2					
		Na_2SO_4	1.6	120	16					
		H_3BO_3	0.25 *M*	15	2					
H	KCl[a]	$NiSO_4.7H_2O$	1.7	240	32	3.0	35	95	1.5	14
		KCl	0.25	19	2.5					
		H_3BO_3	.5 *M*	30	4					
I	Double salt	$NiSO_4(NH_4)_2SO_4.6H_2O$	4	75	10	5.3	30	86	0.3	28
		NH_4Cl	.3	15	2					
		H_3BO_3	.25 *M*	15	2					

[a] Bath used by G. E. Gardam and D. J. Macnaughtan, Trans. Faraday Soc. **29**, 756 (1933), and designated as "NSB.KC".

(B) CALIBRATION

If a linear relation exists, the calibration of a given magnet and instrument may be conveniently expressed in terms of the equation

$$C = T/F \qquad (1)$$

where

C = a constant.
T = the thickness of the nickel deposit, expressed in fractions of a millimeter or an inch.
F = the attractive force (or more strictly, the detaching force), expressed in grams or in scale divisions.

In effect, C is the thickness of nickel corresponding to 1 g or one scale division. As most commercial specifications for thickness are expressed in fractions of an inch, usually less than 0.001 inch, C may be conveniently expressed as hundred thousandths of an inch per scale division. If, for example,

$T/F = 0.00030/20 = 0.000015$, then
$C = 1.5 \times 10^{-5}$ inch, or conventionally, $C = 1.5$.

In calibrating a magnet or instrument it is preferable to employ several similar standards of known thicknesses, in order to obtain average values of C that apply to that type of coating. The constancy of C for similar nickel deposits of different thicknesses indicates that a linear relation exists between thickness and magnetic attraction. Similarly, the constancy of C for dissimilar nickel coatings of the same thickness is a measure of the constancy of magnetic properties of different nickel deposits. In general, an increase in the value of C represents a decrease in the magnetic permeability of the nickel, and vice versa.

IV. MAGNETIC PROPERTIES OF NICKEL DEPOSITS

1. RELATION BETWEEN MAGNETIC ATTRACTION AND THICKNESS

Table 2 summarizes the relation of thickness to magnetic attraction, expressed in terms of C for coatings as deposited and of C' for coatings that were annealed, for the reason above mentioned. The data in tables 2 and 3 were obtained with the Sanford balance. The actual values of the constants C and C' apply only to this particular instrument and are useful only for comparison. Other magnets would give parallel results, although the values of C and C' might differ from those of the above instrument. Each value of C or C' in the tables is the average of 10 to 20 measurements on one or more specimens.

For any given type of nickel deposit, it is evident that the value of C is constant to within about 10 percent for thicknesses from 0.0001 to 0.001 in. (0.0025 to 0.025 mm). A few results not included in table 2 show that for much thinner coatings, such as 0.00002 to 0.00005 in. (0.0005 to 0.0013 mm), the value of C is about 20 percent below the average in the table.

The average value of C varies, however, by about 20 percent for different types of nickel deposits, which must, therefore, have different magnetic permeabilities.

TABLE 2.—*Ratio between thickness of nickel (T) and magnetic attraction (F)*

$C = T/F$ for coatings as deposited; $C' = T/F$ after annealing [1]
(Flat plates. Sanford balance)
In this table the values of C and C' are to be multiplied by 10^{-6}

Bath	Base metal	Average thickness of nickel (inch)										Avg.	Avg. dev.	Avg.	Avg. dev.
		10×10^{-6}		20×10^{-6}		30×10^{-6}		50×10^{-6}		100×10^{-6}					
		C	C'	C	C'	C	C'	C	C'	C	C'	C	%	C'	%
E	Low brass	1.66	1.06	1.91	1.13	1.88	1.14	1.74	1.12	1.49	1.09	1.74	±8	1.11	±3
F	Low brass	1.75	1.12	1.84	1.14	1.84	1.11	1.70	1.09	1.82	1.07	1.79	±3	1.11	±2
G	Low brass	2.00	1.22	2.21	1.26	-----	-----	2.27	1.22	2.21	1.20	2.17	±4	1.23	±2
G	Zinc	1.63	-----	1.78	-----	1.71	-----	1.93	-----	1.68	-----	1.75	±5	-----	-----
G	Zinc die-cast XXI	2.16	1.29	-----	-----	2.26	1.27	2.11	1.25	2.08	1.20	2.15	±3	1.25	±3
G	Zinc die-cast XXIII	2.02	-----	2.24	1.26	2.13	-----	2.13	1.22	2.14	1.14	2.13	±3	1.21	±3
H	Low brass	-----	-----	2.18	1.28	-----	-----	2.08	1.19	-----	-----	2.13	±3	1.24	±4
I	Low brass	-----	-----	2.03	1.24	-----	-----	2.24	1.17	-----	-----	2.14	±5	1.20	±3
Average		1.87	1.17	2.03	1.22	1.96	1.17	2.03	1.18	1.90	1.14	1.98	-----	1.19	-----
Average deviation for different baths (%)												±10	-----	±5	-----

[1] Coatings on brass were heated to 400° C (750° F) for 30 minutes; on zinc and zinc-base die-castings to 280° C (535° F) for 60 minutes.

TABLE 3.—*Effect of operating conditions on the magnetic constants of nickel*

[Values of C and C′ derived from coatings 0.013 mm (0.0005 in.) thick on flat-rolled brass. Sanford balance]

Experiment	pH	Current density		Temperature		C	Deviation from avg C	C′	Deviation from avg C′	Variable
		amp/dm²	amp/ft²	°C	°F		%		%	
STANDARD BATH *E*										
1	5.0	1	9	35	95	1.76×10^{-3}	−7	1.12×10^{-3}	−5	Current density.
2	5.0	2	19	35	95	1.74	−8	1.12	−5	
3	5.0	4	37	35	95	1.77	−6	1.16	−2	
4	5.4	2	19	21	70	2.20	+16	1.19	+1	Temperature.
5	5.4	2	19	35	95	1.91	+1	1.23	+4	
6	5.4	2	19	45	113	2.01	+6	1.24	+5	
7	5.4	2	19	60	140	(2.54)	(+34)	1.22	+3	
8	2.7	2	19	35	95	1.70	−10	1.09	−8	pH.
9	2.9	2	19	35	95	1.80	−5	1.11	−6	
10	4.4	2	19	35	95	2.03	+7	1.23	+4	
11	4.8	2	19	35	95	1.76	−7	1.10	−7	
12	5.2	2	19	35	95	1.80	−5	1.11	−6	
13	5.6	2	19	35	95	2.00	+6	1.18	0	
14	5.8	2	19	35	95	(2.7)	(+40)	1.18	0	
15	5.8	2	19	35	95	(3.3)	(+70)	1.19	+1	
16	5.9	2	19	35	95	(5.6)	(+190)	1.25	+6	
17	5.8	1	9	35	95	(3.2)	(+70)	1.17	−1	Current density at high pH.
18	5.8	2	19	35	95	(3.3)	(+70)	1.19	+1	
19	5.8	4	37	35	95	(4.4)	(+130)	1.22	+3	
20	5.2	2	19	35	95	2.06	+9	1.21	+3	2 ml/liter of 3% H_2O_2.
21	5.2	2	19	35	95	(5.4)	(+180)	(1.33)	(+13)	5 ml/liter of 3% H_2O_2.
22	5.2	2	19	35	95	(7.6)	(+300)	(1.84)	(+57)	10 ml/liter of 3% H_2O_2
Average, excluding values in parentheses						1.89	±7	1.18	±4	
HIGH-SULPHATE BATH *G*										
23	6.1	1	9	35	95	2.08	−2	1.18	−1	Current density.
24	6.1	2	19	35	95	2.14	0	1.29	+8	
25	6.1	1	9	27	81	2.31	+8	1.17	−2	Temperature.
26	6.1	1	9	33	91	2.08	−2	1.18	−1	
27	6.1	1	9	48	118	1.78	−16	1.19	0	
28	4.5	1	9	27	81	2.28	+7	1.21	+2	pH.
29	5.7	1	9	27	81	2.21	+4	1.23	+3	
30	6.1	1	9	27	81	2.31	+8	1.17	−2	
31	6.4	1	9	27	81	1.93	−9	1.17	−2	
32	6.6	1	9	27	81	2.20	+3	1.13	−5	
Average						2.13	±6	1.19	±3	
33						1.38		1.24		Bright nickel.[1]
34						1.17		1.11		Bright nickel.[1]

[1] Deposits in experiments 33 and 34 are from different commercial baths.

As shown in table 2, suitable annealing of the various nickel coatings causes them to acquire about the same magnetic properties, that is, the average values of C' (for annealed coatings) are more nearly uniform than the values of C (for unannealed coatings). Moreover, the linear relation was more closely followed by the annealed coatings, for which C' is constant within 5 percent, for the entire range of thickness from 0.0005 to 0.025 mm (0.00002 to 0.001 in.). This linear relationship was found to hold also for nickel coatings on curved surfaces.

These results were obtained with the Sanford balance, which has magnets 5 cm (2 in.) in length and 5 mm (0.2 in.) in diameter. For smaller magnets the linear relation does not hold quite so well for coatings thinner than about 0.0075 mm (0.0003 in.). For example, the modified Sanford balance with magnets 3 cm (1.2 in.) in length and 2 mm (0.08 in.) in diameter showed a departure of about 10 percent from linearity for thin annealed coatings. Therefore, small magnets should be calibrated against at least three thicknesses of nickel coatings, for example, 0.013 mm (0.0005 in.), 0.0075 mm (0.0003 in.), and 0.0025 mm (0.0001 in.).

2. EFFECTS OF CONDITIONS OF DEPOSITION

(A) NICKEL AS DEPOSITED

Table 3 summarizes more extensive experiments in which the plating conditions were systematically varied. The results show that for deposits plated out of the standard bath, the value of C is fairly constant over a range of conditions that includes most commercial plating. The value of C is increased, that is, the nickel is made less magnetically permeable, by an increase in temperature above 45° C (113° F), or by an increase in pH above 5.5 (experiments 7 and 14). At a high pH, an increase in current density (experiment 19) still further increases C, but not at a low pH (experiment 3). The amount of hydrogen peroxide usually added to reduce pitting (experiment 20) has no marked effect on C, but additions of more than 2 ml/liter (0.26 fl oz/gal) of 3-percent peroxide (experiments 21 and 22) have a marked effect on C.

For deposits plated out of the high-sulphate bath, the average value of C is somewhat higher than in the standard bath, but an increase in pH (experiments 28 to 32) has much less effect in the high-sulphate than in the standard bath.

The conclusion from these tests on coatings as deposited is that the magnetic method may be applied to unannealed coatings only if the conditions of operation are maintained fairly uniform. Under such conditions, it is merely necessary to calibrate the instrument at intervals against deposits of known or measured thickness that were produced in the same bath and under the prescribed conditions. With these precautions, the method may be conveniently applied in factory production without introducing errors greater than about 15 percent.

The direct method is not, however, satisfactory for inspecting coatings of unknown origin that may have been plated under varied conditions. For such testing, prior annealing of the deposits is necessary.

(B) ANNEALED COATINGS

The lower and more constant values of C' in tables 2 and 3 for annealed coatings show that heating nickel deposits to 400° C (750° F) for 15 to 30 minutes makes them more magnetic and at the same time more nearly alike in magnetic permeability. The use of a single average constant for the principal types of nickel deposits yields results that are correct within about 10 percent. The only exceptions are experiments 21 and 22, in which an excess of hydrogen peroxide was used.

Annealing of nickel coatings in air at 400° C (750° F) produces a yellowish discoloration of oxide which, however, does not interfere

with magnetic measurements. It can be removed with a warm cyanide solution. Annealing can be done more quickly at still higher temperatures, but then there is increased oxidation of the nickel surface. When the usual thin layer of chromium is present over the nickel, no appreciable change in color or luster is produced on annealing at 400° C, and the chromium has no effect on the magnetic readings.

The values of C' in table 2 for zinc-base die-castings were determined after annealing at 280° C (535° F) for 1 hour. This is about the highest temperature that can be used on such alloys without damaging the coatings, and even at that temperature there is softening and distortion of the castings. The magnetic method is not nondestructive for such articles if annealing is required.

No consistent results could be obtained on nickel-plated zinc annealed at 280° C. Apparently the coating and base metal had alloyed. It is surprising that the die-castings that contained over 90 percent of zinc showed no such alloying at that temperature.

(C) "BRIGHT NICKEL" DEPOSITS

No attempt was made to study exhaustively the behavior of bright nickel deposits, such as are now being produced from numerous patented or proprietary baths. Results on deposits made commercially from two different baths that contained organic addition agents are reported in experiments 33 and 34 of table 3. These data show that, as deposited, these coatings yielded lower values of C, that is, were much more magnetic than ordinary nickel. On annealing they changed but little, and the values of C' approached closely to the average value of C' for other nickel deposits. These few tests indicate that it may be possible to test bright nickel directly if the instrument has been calibrated against similar deposits; but that it would be safer to anneal the coatings and use the average value of C'

(D) EFFECTS OF CODEPOSITED IRON OR COBALT

As both iron and cobalt are more magnetic than nickel, their presence in a nickel deposit would be expected to yield low values of both C and C'. The results in table 4 confirm this prediction. The deposits containing iron were prepared from regular nickel baths to which ferrous sulphate was added. The ratio of iron to nickel in the deposits was about twice that in the baths. The single nickel-cobalt alloy that was tested was prepared commercially from a bright nickel bath containing cobalt and an organic addition agent.

TABLE 4.—*Effect of iron and cobalt on magnetic thickness measurements*

Thickness	Fe	Co	C	Percentage of error in thickness caused by 1% of		Annealed		
						C'	Percentage of error in thickness caused by 1% of	
				Fe	Co		Fe	Co
Inch	%	%		%	%		%	%
50×10^{-6}	0		1.85×10^{-6}			1.17×10^{-6}		
25	3.5		1.77	1.3		1.03	3.9	
66	3.5		1.50	6.6		1.02	4.2	
25	11		1.24	4.5		0.80	4.3	
55	11		1.24	4.5		.78	4.5	
30		20	1.09		3.5	.83		2.0
Average				4.2	3.5		4.2	2.0

These few results indicate that in either annealed or unannealed coatings the presence of each percent of iron causes an error of about +4 percent, and in annealed coatings each percent of cobalt an error of about +2 percent in the magnetic readings. With the present general use of anodes containing more than 99 percent of nickel, coatings will not contain over 1 percent of iron or cobalt and hence introduce significant errors. If cobalt is intentionally introduced, as in the bright deposit tested, the magnetic method is applicable only if the cobalt content is kept fairly constant, and if the instrument is standardized against similar coatings.

3. RELATION OF COMPOSITION, HARDNESS, AND MAGNETIC PROPERTIES

In order to throw light on the variations in magnetic properties, a few corresponding, but thicker, nickel deposits were analyzed [7] for oxygen and hydrogen by vacuum fusion. The results in table 5 show that in the standard bath an increase in pH raised the oxygen

TABLE 5.—*Relation between gas content and properties of electrodeposited nickel*

Experiment	Bath	pH	Oxygen (% by wt)	Hydrogen (% by wt)	Brinell hardness no.	Magnetic constant		Variable
						C	C'	
1	*E*	5.2	0.004	0.0017	120	1.7×10^{-5}	1.10×10^{-5}	Standard.
2	*E*	5.8	.021	.0060	269	2.7	1.18	Standard, high pH.
3	*G*	6.6	.014	.0053	470	2.2	1.13	High sulphate, high pH.

content of the deposit more than fivefold. In the high-sulphate bath (experiment 3) at a high pH, there was almost as much oxygen as in experiment 2. These amounts of oxygen correspond to about 3 times as much nickel hydroxide, $Ni(OH)_2$, in which form the oxygen is most likely present. The contents of hydrogen were roughly proportional to those of oxygen, but in all cases far exceeded the amounts of hydrogen needed to combine with the oxygen in $Ni(OH)_2$ or H_2O. The contents of hydrogen and oxygen are in the same order as the values of C for the unannealed deposits, that is, a high value of C (low magnetic permeability) corresponds to a high content of oxygen and hydrogen. The fact that in experiment 2 the deposit is harder than in experiment 1 is consistent with the hypothesis of Macnaughtan and his associates [8] that hardness is caused by, or associated with, included basic material. However, as deposit 3, with less oxygen, is harder than no. 2, it is evident that other factors, such as grain size, may also influence the hardness.

If the basic material is concentrated on the grain boundaries, it may reduce the magnetic permeability either by hindering magnetic coupling of the grains, or by producing internal strains, which are known to reduce the permeability. The increase in permeability by heating to as low a temperature as 400° C is more consistent with the removal of strains than with a reaction with, or absorption of, the oxide. Analysis of an annealed specimen of nickel showed that the annealing considerably reduced the content of hydrogen but did not change that of oxygen. It is evident that the subject warrants more exhaustive study.

[7] Analyses were made by V. Holm.
[8] D. J. Macnaughtan, G. E. Gardam, and R. A. J. Hammond, Trans. Faraday Soc. 29, 720 (1933).

4. EFFECT OF BASE METAL

The method is necessarily limited to nonmagnetic base metals. None of the common nonferrous metals tested was magnetic enough to interfere with the application of this method. Even nickel-brass, which contains about 20 percent of nickel, is nonmagnetic, and hence nickel coatings over nickel-brass can be measured magnetically. However, when testing coatings on unknown alloys, it is desirable to apply the magnet to a portion of the unplated or stripped surface. If only a small magnetic attraction is observed, this may be deducted from the readings made on the coatings. Any large magnetic effect makes the method inapplicable to such base metals.

Nickel coatings were plated on a number of different base metals for the purpose of determining the effect of the base metal on the magnetic properties of the coating. For nickel coatings plated on copper, various kinds of rolled, extruded, and cast brass, rolled nickel-brass, and zinc-base die castings, the values of C and C' showed no effect of the base metal greater than 5 percent. For unannealed coatings on sheet zinc the value of C was 15 percent lower than on the other base metals.

V. DIMENSIONAL FACTORS IN MAGNETIC THICKNESS MEASUREMENTS

1. AREA OF COATING

Only a limited portion of the nickel surface exerts an appreciable effect upon the magnetic attraction. To determine the magnitudes of the effective areas, the attraction of a given sized magnet was measured, first to a relatively large plane surface of nickel, which for present purposes may be considered as an "infinite plane", and then to successively smaller disks of the same plated sheet.

TABLE 6.—*Effect of area of nickel coating on attractive force of typical magnets.*

Expressed as percentage of the attraction to an infinite plane. Deposits about 0.013 mm (0.0005 in.) thick.

Experiment	Magnet							Balance	Percentage of attraction of disks of the following diameters:				
	Diameter		Length		Material	F	F/W[a]		4 cm (1.6 in.)	2 cm (0.8 in.)	1 cm (0.4 in.)	0.75 cm (0.3 in.)	0.5 cm (0.2 in.)
	cm	in.	cm	in.		g			*Percent*	*Percent*	*Percent*	*Percent*	*Percent*
1	1.4	0.56	12	5	36% of Co	4.8	0.03	Lever	84	56	17	10	7
2	.5	.2	15	6	36% of Co	2.4	.1	do	100	93	73	64	48
3[b]	.2	.08	15	6	36% of Co	2.8	.1	do	100	94	79	73	66
4	.5	.20	5	2	36% of Co	1.7	.2	Sanford	100	97	77	66	52
5	.2	.08	3	1.2	36% of Co	1.1	1.5	Lever	100	100	90	87	78
6	.2	.08	3	1.2	Tool steel	0.5	.6	du Noüy	100	100	89	87	77
7	.2	.08	2.4	1.0	Alnico	1.2	2.1	do	100	100	90	88	78
8	.2	.08	.7	0.3	do	.9	6.0	do	100	100	97	94	87
9	.1	.04	6.0	2.4	36% of Co	.7	1.8	do	100	100	94	94	90
10	.1	.04	3.0	1.2	36% of Co	.6	3.8	do	100	100	96	95	90

[a] F=Force of attraction (in grams) between the magnet and a nickel coating 0.025 mm (0.001 in.) thick. W=Weight of magnet (in grams).

[b] The magnet diameter was 0.5 cm (0.2 in.), except on 1 end, where a length of 0.5 cm was reduced to a diameter of 0.2 cm (0.08 in.)

The results in table 6 show that the smaller the diameter of the magnet the smaller is the area over which the magnet exerts 90 percent of its attraction to an infinite plane.

As a first approximation, the diameter of the disk that is effective is about 5 times the diameter of the magnet. Reliable measurements upon small areas therefore require the use of small magnets, preferably not more than about 2 mm (0.08 in.) in diameter.

The area influenced by the magnet is even more significant in making thickness measurements near an edge or corner. These measurements should be made with the magnet placed at such a distance from the edge or corner as to include in its field a disk of the diameter that was found by tests such as those in table 6 to yield 90 percent or more of the attractive force. For most small magnets this distance is about twice the diameter of the magnet.

With either form of the Sanford balance, consistent measurements can be made nearer to an edge than indicated above if the lever arm of the balance extends over the surface of the coating and not over the edge. Reliable measurements can then be obtained at a distance from the edge equal to about one-half the diameter of the magnet.

2. CURVATURE OF SURFACE

The tests thus far described were made on flat surfaces. To test the effects of curvature, brass cylinders and spheres were plated uniformly with nickel. The magnetic attractions of the coatings were measured and were expressed in terms of the attraction to an infinite plane having the same thickness of nickel.

TABLE 7.—*Effect of curvature expressed as percentage of the attraction to an infinite plane*

Deposits about 0.013 mm (0.0005 in.) thick

Experiment	Shape	Radius		Percentage attraction of magnets of following diameters—			
				0.5 cm 0.2 in.	* 0.2 cm 0.08 in.	0.2 cm 0.08 in.	0.1 cm 0.04 in.
		cm	in.	%	%	%	%
1	Sphere	1	0.4	93	94	93	93
2	do	0.6	.25	84	89	88	91
3	do	.3	.13	65	78	88	97
4	do	.16	.06	37	51	65	78
5	Cylinder	1.4	.6	100	102	100	100
6	do	0.6	.25	101	100	100	100
7	do	.3	.13	93	94	94	98
8	do	.16	.06	75	83	86	88

* See table 6, magnet 3.

The results in table 7 show that, in order to yield about 95 percent of the maximum attractive force, a sphere should have a radius at least 5 times the diameter of the magnet, and a cylinder should have a radius at least twice the diameter of the magnet. Smaller spheres or cylinders can be measured if an empirical correction is made.

No quantitative tests were made upon concave surfaces, but their geometry indicates that a decrease in the radius of curvature would increase the magnetic attraction above that on a plane surface. As a first approximation it may be assumed that the limitations on the radius of curvature will be the same as on convex surfaces.

3. PARALLEL NICKEL COATINGS

The above measurements were all made on specimens plated with nickel on only one side. Any nickel coating that is present on the back of a sheet will exert an effect upon the measurement on the front, that depends largely upon the thickness of the intervening base metal. This effect is illustrated in figure 5, in which are plotted the proportions of the usual attractive forces of these particular magnets that were exerted by coatings separated from the magnet by various distances.

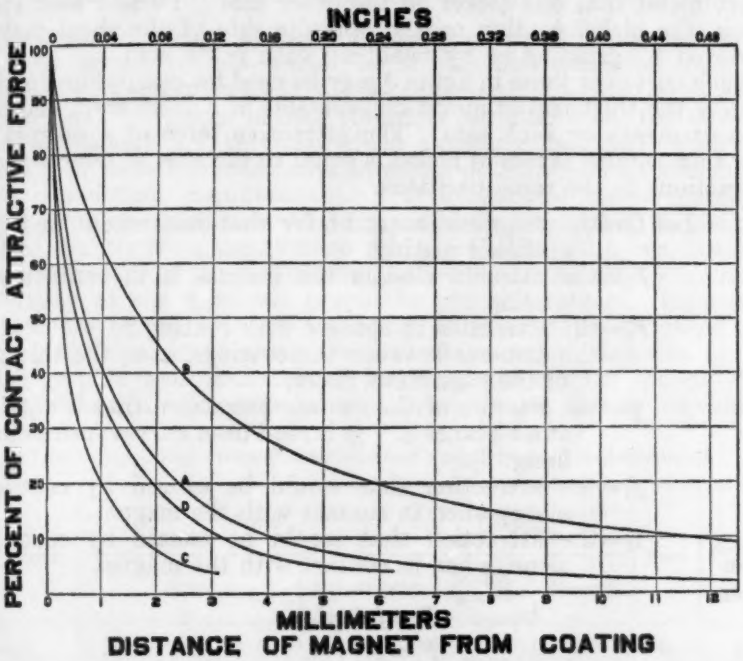
INCHES
0 0.04 0.08 0.12 0.16 0.20 0.24 0.28 0.32 0.36 0.40 0.44 0.48
PERCENT OF CONTACT ATTRACTIVE FORCE
100 90 80 70 60 50 40 30 20 10
B
A
D
C
0 1 2 3 4 5 6 7 8 9 10 11 12
MILLIMETERS
DISTANCE OF MAGNET FROM COATING

FIGURE 5.—*Decrease in magnetic attraction with distance of magnet from coating*

(Expressed as percentage of attractive force when magnet and coating are in contact)

Curve	Magnet				Deposit
	Diameter		Length		
	mm	in.	mm	in.	
A	5	0.2	150	6	As deposited.
B	5	.2	150	6	Annealed.
C	2	.08	30	1.2	As deposited.
D	2	.08	30	1.2	Annealed.

These separations were obtained by placing a brass sheet of the designated thickness between the magnet and the coating. The attractive force varies inversely as the square of the distance from the effective pole of the magnet. As, however, this pole does not coincide with the end of the magnet, from which point the distances were measured, the inverse square law is not followed by these curves.

The curves show that the attractive force falls off more rapidly with increase in distance of the less permeable, unannealed coatings (A and C) than of the annealed coatings (B and D). Figure 5 and additional data show that with unannealed coatings the thickness of sheet must be at least 1.5 times the diameter of the magnet in order to reduce the effect of a coating on the far side to 5 percent or less, and with annealed coatings at least 3 times the diameter of the magnet. It is evident, therefore, that the magnetic method cannot generally be used directly to measure the thickness of nickel on one side of sheet metal that has nickel on the other side. To test such specimens, the nickel coating on the opposite side of the sheet may be removed by grinding or by swabbing with nitric acid.

Such curves as those in figure 5 may be used for computing approximately the thickness of nickel on each side of a sheet from magnetic measurements on each side. The attractive force of a magnet for two thin parallel layers of nickel is equal to the sum of their separate attractions in the same positions.

Let C=the magnetic constant for that instrument and type of nickel coating.

F_1=the attraction when the magnet is in contact with coating 1.

F_2=the attraction in contact with coating 2.

d=the distance between the coatings, i. e., the thickness of the base metal sheet.

p=the fraction of the contact attraction that is obtained at a distance d. (p is read from curves such as those in fig. 5).

f_1=the attraction that would be caused by coating 1 alone, when in contact with the magnet.

f_2=the attraction that would be caused by coating 2 alone, when in contact with the magnet.

Then,

$$F_1=f_1+pf_2, \tag{2}$$

$$F_2=pf_1+f_2, \tag{3}$$

hence,

$$f_1=\frac{F_1-pF_2}{1-p^2} \tag{4}$$

$$f_2=\frac{F_2-pF_1}{1-p^2} \tag{5}$$

$$f(\text{avg.})=\frac{f_1+f_2}{2}=\frac{F_1+F_2}{2(1+p)}. \tag{6}$$

The corresponding thicknesses are obtained by

$$T_1=Cf_1, \tag{7}$$

$$T_2=Cf_2, \tag{8}$$

$$T(\text{avg.})=Cf(\text{avg.}). \tag{9}$$

A few measurements of coatings of known thickness on both sides of a sheet yielded correct results within about 5 percent for each side and for the average, provided the two thicknesses were about the same. If, however, one coating is several times as thick as the other, large proportional errors are made in computing the thickness of the thin coating. The above method is therefore only an approximation, but it may be useful in testing a given fairly uniform product.

4. SUPERPOSED CHROMIUM COATINGS

As previously noted, the presence of chromium over the nickel is an advantage if the coatings are to be annealed, as it prevents oxidation. The curves of figure 5 and other data show that decorative chromium coatings, which are usually less than 0.0013 mm (0.00005 in.) thick, have very little effect on the attractive force of the underlying nickel. Tests may therefore be made directly on the chromium-plated surfaces.

VI. APPLICABILITY TO COMMERCIAL TESTING

The accuracy of the method was finally checked by comparing the magnetic measurements with the thicknesses measured metallographically at approximately the same points. The results in table 8 show that on pieces plated uniformly or otherwise, the average error was about ±5 percent, which compares favorably with the accuracy of metallographic measurements of thin coatings and meets most commercial requirements. The systematic errors obtained with a given specimen show that the magnetic constant of the coating differed slightly from the average value of C obtained by calibration.

The accuracy of routine measurements will depend largely upon the uniformity of the magnetic properties of the coatings. Especially if these are tested without annealing, it is desirable to check the magnet calibration at intervals against annealed deposits or by metallographic measurements of specimens of similar shape. The latter precaution will minimize any errors due to size or curvature.

TABLE 8.—*Comparison of magnetic and metallographic measurements*

Experiment	Article			Local thickness of nickel		Error	Average error
	Shape	Size, diameter		Metallographic	Magnetic		
		cm	in.	in.	in.	%	%
1	Cylinder (annealed)	2.8	1.1	39×10⁻⁶	40×10⁻⁶	+3	+1
				38	39	+3	
				42	41	−3	
				42	42	0	
2	Cylinder (not annealed)	5	2	56	60	+7	+5
				58	59	+2	
				59	61	+3	
				56	60	+7	
3	Cylinder (annealed)	5.8	2.3	91	99	+9	+6
				90	101	+12	
				80	85	+6	
				70	74	+6	
				67	68	+1	
				65	68	+5	
				70	71	+1	
				74	81	+9	
4	Flat (annealed)	10×15	4×6	63	63	0	−6
				44	42	−5	
				36	34	−6	
				37	31	−16	
				37	33	−11	
				44	46	+5	
	Average error						±5

The approximate accuracy of the method for miscellaneous plated pieces was confirmed by making exploratory magnetic measurements upon about 50 plated brass plumbing fixtures that were subsequently stripped to determine their compliance with Federal specifications for average thickness. The coatings were annealed at 400° C prior to the magnetic testing, and a single magnetic constant was applied.

The average of the magnetic measurements on each piece agreed within 15 percent with the average thickness found by stripping, on almost all of the pieces that approached the specified minimum average of 0.00018 in. (0.0045 mm). This agreement is good, in view of the fact that there is no practical way to "weight" the magnetic readings with respect to corresponding areas, as is done effectively by stripping. The magnetic method is not therefore a convenient or very accurate method for measuring average thickness. It is designed chiefly for measuring the local thickness and distribution.

The results with the above fixtures throw light on the actual distribution of nickel on typical articles, such as plumbing fixtures. The average ratio of the maximum to the minimum thickness was about 2.5:1, but on some pieces this ratio was as high as 5:1. If a minimum thickness, e. g., of 0.0001 inch (0.0025 mm) of nickel were specified on such articles, it is apparent that on some pieces an average thickness of at least 0.0003 inch would have to be applied.

VII. CONCLUSIONS

1. The attractions of a small permanent magnet for nickel coatings on nonmagnetic base metals are proportional to their thicknesses, up to about 0.025 mm (0.001 inch); and can, therefore, be used to measure the thickness at any point.

2. This magnetic attraction can be measured by any fairly sensitive balance, for example, (a) a lever balance, such as is used for chemical analysis, (b) a torsion balance, such as a du Noüy tensiometer, or (c) a spring balance, such as that devised by R. L. Sanford for magnetic measurements.

3. The magnetic permeabilities of nickel deposits depend to some extent on the conditions of deposition. In general, deposits produced at a high pH, or from baths that yield hard or fine-grained deposits, are less permeable magnetically than soft deposits. The so-called "bright nickel" coatings, from baths with organic addition agents, are, however, more permeable than normal deposits.

4. Nickel deposited at a high pH is harder and contains more oxygen and hydrogen than that at a low pH.

5. Heating at 400° C (750° F) for 15 to 30 minutes causes nearly all nickel deposits to acquire about the same magnetic permeability.

6. The magnetic method can be quickly applied to nickel coatings deposited on nonferrous metals under fairly uniform conditions, provided that the instrument has been calibrated against similar nickel coatings of known thickness.

7. If nickel coatings of unknown history have been annealed at 400° C (750° F), their thickness may be measured magnetcially, provided the constant for annealed coatings is used.

8. Each percent of iron in a nickel deposit introduces an error of about +4 percent in the thickness measurements, and each percent of cobalt an error of about +2 percent.

9. On plane surfaces the magnetic measurement yields correct results if the diameter of the area tested is at least 5 times the diameter of the magnet.

10. Measurements closer to an edge or corner than about twice the diameter of the magnet are inaccurate unless the magnet has been especially calibrated for such positions.

11. On curved surfaces the results are practically the same as on planes, provided the radius of curvature of a sphere is at least 5 times the diameter of the magnet and the radius of a cylinder twice the diameter of the magnet.

12. The measurements on sheet metal are affected by the presence of a nickel coating on the other side unless the thickness of the base metal is at least 3 times the diameter of the magnet. It is possible to compute the approximate thickness on each side of a thin sheet from magnetic measurements made on both sides.

13. The presence of the usual thin decorative chromium coatings over the nickel has no appreciable effect on the thickness measurements, and is advantageous because it prevents oxidation of the nickel during annealing.

14. The magnetic method is rapid and nondestructive, and for thin coatings its accuracy approaches that of metallographic measurements.

The author acknowledges the advice and assistance received from R. L. Sanford and W. Blum in this investigation.

WASHINGTON, March 3, 1937.

136221—37——6

U. S. DEPARTMENT OF COMMERCE NATIONAL BUREAU OF STANDARDS

RESEARCH PAPER RP995

Part of Journal of Research of the National Bureau of Standards, Volume 18, May 1937

THE SYSTEM PbO–B_2O_3

By R. F. Geller and E. N. Bunting

ABSTRACT

The system PbO-B_2O_3, of interest to investigators and manufacturers of ceramic glazes and glasses, was studied by well-known methods involving quenching and petrographic examination. In addition, limits of liquid immiscibility were obtained by direct observation. Seven crystalline forms of binary compounds were found and the chemical compositions of six of these established. A number of compositions were studied also as glasses to obtain data on thermal expansion, softening behavior, and relative solubility.

CONTENTS

	Page
I. Introduction	585
II. Preparatory work	586
1. Preparation of mixtures	586
2. Chemical analyses	586
III. Experimental procedure	586
IV. Results	587
1. Phase relations	587
2. Two-liquid area	591
3. Compositions as glasses	591
V. Discussion	592
VI. Summary	593

I. INTRODUCTION

The study of this system is part of a general investigation of phase relations involving PbO with other oxide constituents of ceramic glazes and glasses. The first study [1] covered the system PbO-SiO_2 and the second [2] covered the system K_2O-PbO-SiO_2.

Although there are other oxides of lead, only the monoxide is stable above approximately 450° C.[3]

For mixtures containing over 30 percent of B_2O_3 the present study was limited to data at the liquidus only, partly because of their very high viscosity at temperatures below the liquidus and partly because of the hygroscopic nature of melts containing over approximately 40 percent of B_2O_3. The melting point of PbO is taken from the study referred to in footnote 1, and the melting point of B_2O_3 (294 ± 1° C) is taken from a report by Cole and Taylor.[4] This value has been questioned by Morey and Merwin.[5]

[1] R. F. Geller, A. S. Creamer, and E. N. Bunting, J. Research NBS 13, 237 (1934) RP705.
[2] R. F. Geller and E. N. Bunting, J. Research NBS 17, 277 (1936) RP911.
[3] J. W. Mellor, A Comprehensive Treatise on Inorganic and Theoretical Chemistry, 7, 672. (Longmans, Green and Co., New York, N. Y.)
[4] S. S. Cole and N. W. Taylor, J. Am. Ceram. Soc. 18, 55 (1935).
[5] G. W. Morey and H. E. Merwin, J. Am. Chem. Soc. 58, 2248 (1936).

II. PREPARATORY WORK

1. PREPARATION OF MIXTURES

"End members" were sublimed litharge (PbO) containing 0.02 percent of total detected impurities, and boric acid of reagent quality containing less than 0.01 percent of total detected impurities.

All fusions were made in platinum, using electrically heated furnaces. The well mixed ingredients were allowed to react overnight at about 800° C and were then taken to 1,000° C to drive off all water from the boric acid. As shown by the values in table 1, losses by volatilization during preparation of the melts were in direct relation to the percentage of each oxide in the batch mixture. Thirty melts were analyzed chemically and portions used in various combinations to obtain additional preparations.

Although melts containing less than 40 percent of B_2O_3 appeared stable in air many of higher B_2O_3 content were very hygroscopic and therefore, for convenience, all preparations were stored over P_2O_5. The variation in time required for crystal growth to attain equilibrium was also extreme. Because of quench growths clear glass could not be obtained with those melts in which the content of PbO was higher than 94 percent, while melts containing over 28 percent of B_2O_3 did not attain equlibrium when held as long as 1 month at temperatures below the solidus.

TABLE 1.—*Relative volatilization of* PbO *and of* B_2O_3 *from lead-borate melts*

PbO put in batch [a]	PbO found in melt	PbO put in batch [a]	PbO found in melt	PbO put in batch [a]	PbO found in melt
%	%	%	%	%	%
96.9	96.6	82.1	82.5	56.8	58.5
94.6	94.2	80.8	81.3	50.6	52.0
93.5	93.7	79.8	80.4	46.8	48.6
92.6	92.7	79.0	79.5	43.4	44.9
92.3	92.2	77.7	78.5	35.2	36.7
91.2	91.2	76.5	77.1	29.0	30.1
90.2	90.1	75.5	76.0	25.2	25.9
87.8	88.0	71.6	72.5	14.0	14.1
86.1	86.4	67.2	68.3	4.9	5.1
86.0	86.2	60.6	61.8	1.9	2.1

[a] Calculated on the anhydrous basis, the difference between the PbO content given and 100 percent being B_2O_3.

A higher "found" value for PbO shows that B_2O_3 volatilized more rapidly than did PbO. Equal values for "batch" and "found" content show that the PbO and B_2O_3 volatilized in equal proportionate amounts.

2. CHEMICAL ANALYSES

The PbO content was determined as sulfate by double or, when necessary to obtain constant values, by triple evaporation with HF and H_2SO_4. The B_2O_3 was determined by difference. All analyses were made by A. S. Creamer.

III. EXPERIMENTAL PROCEDURE

Thermal studies were made by the quenching, and by the differential thermocouple, method. The latter method was not productive of significant results. Both methods are well established.[6] Pt to Pt-Rh thermocouples were used for temperature measurements and were cal-

[6] F. C. Kracek, N. L. Bowen, G. W. Morey, J. Phys. Chem. 33, 1857 (1929).

ibrated by observing the melting temperature of KCl (770.3° C). When air quenching did not suffice, the samples were dropped into CCl_4.

The petrographic microscope was used to determine the phases present in quenched samples. Identification of the crystalline phases was limited practically to the establishment of optical character and indices of refraction. Samples in solid media (ranging in index of refraction from 1.74 to 2.58), were examined by means of white light passed through a no. 25 Wratten filter, which type of illumination had been used in determining the indices of the media.

Maximum temperatures in the area of liquid immiscibility were determined by direct observation of melts heated and cooled slowly through the critical range. Change from clear to opaque glass (or vice versa) usually occurred in a range of 4° C or less. The sample (approximately 1 g in a 25-ml crucible) was observed through fused-quartz windows. A spotlight was directed on the melt when the furnace was too cool to provide sufficient illumination. Accuracy of the method was determined by observing the melting and freezing of KCl.

Determinations of linear thermal expansion and observations of the temperature of initial softening (T_s values) of compositions as glasses were made by the interferometer method, using electrically heated furnaces, a temperature rise of from 2.0 to 2.5° C per minute, and chromel-alumel thermocouples for temperature measurements.

Values for relative solubility were obtained on approximately 0.5-g samples which passed a no. 200, and were retained on a no. 325, U. S. Standard sieve. Each sample was boiled for ½ hour, under reflux, in 100 ml of 4-percent acetic acid and the PbO dissolved was estimated by titration with ammonium molybdate solution, using tannic acid solution as the external indicator.

IV. RESULTS

1. PHASE RELATIONS

Results of the quenching tests are summarized in table 2, and the phase relations indicated by them are shown in figures 1 and 2.

PbO melts at 886 ± 2° C and is the primary phase in melts containing from 93.7 to 100 percent of PbO.

$4PbO.B_2O_3$ is the primary phase, in the β form, from 88 percent to 91.7 percent of PbO and, in the α form, from 91.7 percent to 93.7 percent of PbO.

$\alpha 4PbO.B_2O_3$ melts congruently at 565° C[7] and reverts to the β form either very sluggishly or not at all. The eutectic composition between α4:1 and PbO melts at 560° C. Optical properties of the α form are: indices of refraction, maximum, 2.15, minimum, 2.20;[8] character was not established.

$\beta 4PbO.B_2O_3$ apparently melts congruently at about 555° C, and the eutectic temperature between the β form and PbO is about 549° C. Determination of the melting temperature is not shown clearly by the quenched samples because of the simultaneous process of transformation of the β to the α form, which transformation under equilibrium conditions is estimated to proceed at a maximum rate at about 552° C. Optical properties of the β form are: indices of refraction α2.15, β2.20, γ2.24; character biaxial negative; optic axial angle ($2V$) about 80°.

[7] For accuracy of temperatures given in the text see footnote (a) to table 2.
[8] All index of refraction values are accurate within ±0.01.

TABLE 2.—*Data from quenching and petrographic examination*

PbO	B_2O_3	t[a]	Primary phase	Reaction
%	%	°C		
96.6	3.4	[b]	PbO	
94.5	5.5	655 ±5	PbO	Liquidus.
93.7	6.3	560	PbO and α4:1	Eutectic.
93.7	6.3	549	PbO and β4:1	Do.
93.7	6.3	553	----------	β4:1→α4:1 transformation.
93.2	6.8	564	α4:1	Liquidus.
92.7	7.3	565	α4:1	Melting of compound.
92.7	7.3	552	----------	β4:1→α4:1 transformation.
92.2	7.8	561	α4:1	Liquidus.
92.2	7.8	554	----------	β4:1→α4:1 transformation.
91.2	8.8	548	β4:1	Liquidus.
90.1	9.9	537	β4:1	Do.
88.0	12.0	493	α2:1 and β4:1	Eutectic.
88.0	12.0	473	----------	β2:1→α2:1 transformation.
87.3	12.7	497	α2:1	Liquidus.
87.3	12.7	475	----------	β2:1→α2:1 transformation.
86.6	13.4	517	5:4	Liquidus.
86.6	13.4	496	----------	α2:1 melts incongruently.
86.4	13.6	517	5:4	Liquidus.
86.4	13.6	498	----------	α2:1 melts incongruently.
86.4	13.6	472	----------	β2:1→α2:1 transformation.
86.2	13.8	518	5:4	Liquidus.
86.0	14.0	525	5:4	Do.
84.9	15.1	535	5:4	Do.
83.7	16.3	542	5:4	Do.
82.5	17.5	583	1:2	Do.
82.5	17.5	545 ±5	----------	5:4+liquid⇌1:2+liquid.
81.3	18.7	623	1:2	Liquidus.
81.3	18.7	545 to 580	----------	[c]
80.3	19.7	642	1:2	Liquidus.
80.3	19.7	550 to 560	----------	[c]
79.5	20.5	669	1:2	Liquidus.
79.5	20.5	545 to 580	----------	[c]
78.5	21.5	675	1:2	Liquidus.
78.5	21.5	530 to 590	----------	[d]
77.1	22.9	698	1:2	Liquidus.
77.1	22.9	530 to 595	----------	[d]
76.1	23.9	705	1:2	Liquidus.
76.1	23.9	548	----------	5:4+1:2⇌1:2+liquid.
72.5	27.5	738	1:2	Liquidus.
68.3	31.7	757	1:2	Do.
61.8	38.2	767	1:2	Do.
61.4	38.6	[e]	1:2	Melting of compound.
58.5	41.5	763	1:2	Liquidus.[f]
52.0	48.0	758	1:2	Do.
48.6	51.4	754	1:2	Do.
44.9	55.1	746	1:2	Do.
42.8	57.2	750 ±5	----------	1 liquid⇌2 liquids.
36.7	63.3	744	1:2	Liquidus.[f]
36.7	63.3	777 ±5	----------	1 liquid⇌2 liquids.
30.1	69.9	785 ±5	----------	1 liquid⇌2 liquids.
25.9	74.1	742	1:2	1:2+liquid⇌2 liquids.[f]
25.9	74.1	780 ±5	----------	1 liquid⇌2 liquids.
14.1	85.9	742	1:2	Liquidus.[f]
14.1	85.9	777 ±5	----------	1 liquid⇌2 liquids.
5.1	94.9	700 ±5	----------	1 liquid⇌2 liquids.
2.1	97.9	610 ±5	----------	1 liquid⇌2 liquids.

[a] Accurate within ±3° C, unless otherwise stated.

[b] Quench growths only from temperatures above 830° C.

[c] Crystals of index of refraction 1.89 and 1.91 and glass. Above the temperature range indicated these crystals were replaced by $PbO.2B_2O_3$. (See A, fig. 2.)

[d] Between 530 and 545 to 550° C quenched samples contained the crystals of index 1.89 and 1.91 and $5PbO.4B_2O_3$. Above 550° C, and below the maximum temperature indicated, the samples contained the crystals of index 1.89 and 1.91 and glass, while at higher temperatures they contained $PbO.2B_2O_3$ and glass. This change to the 1:2 compound and glass is apparently not reversible.

[e] This mixture was not prepared. The melting point is estimated to be 768±3° C.

[f] After holding from 4 to 6 weeks at crystallizing temperatures this composition contained $PbO.2B_2O_3$, clear glass, and an emulsion-like isotropic phase resembling the 2-liquid specimens of melts higher in B_2O_3 content.

$2PbO.B_2O_3$ exists in two allotropic forms, the α form being the primary phase in compositions containing from 87.3 to 88.0 percent of PbO, while the β form does not appear at the liquidus.

$\alpha 2PbO.B_2O_3$ melts incongruently at 497° C to form $5PbO.4B_2O_3$ and liquid. The eutectic composition between α2:1 and β4:1 melts

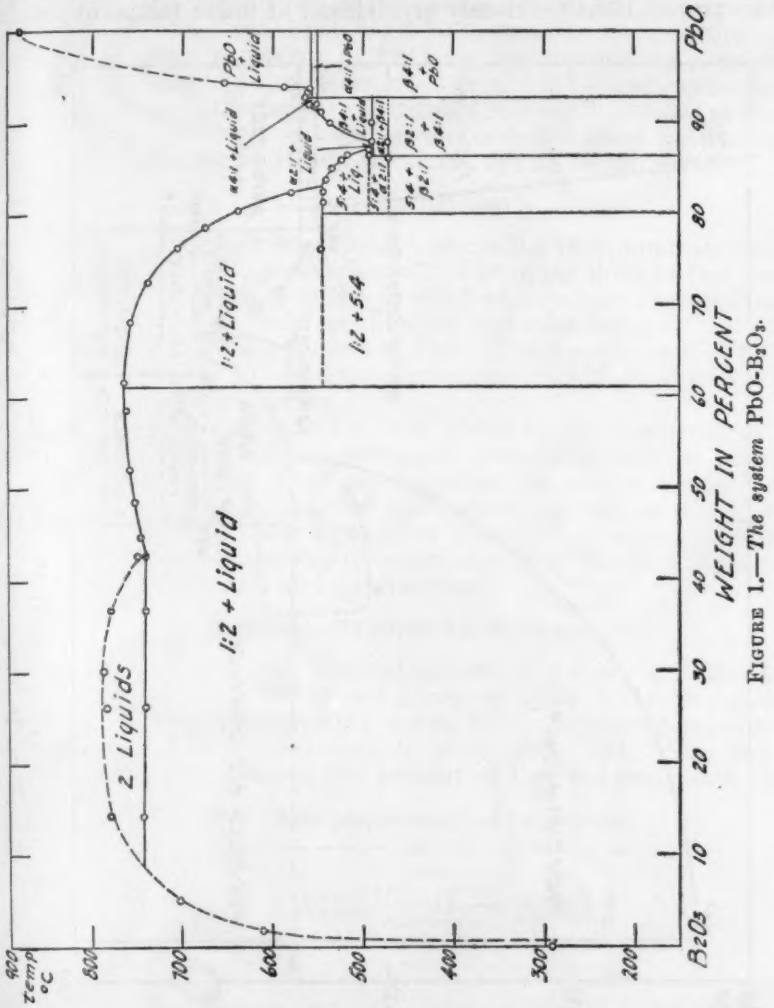

FIGURE 1.—The system PbO-B_2O_3.

at 493° C. Optical properties of the α form are: indices of refraction α1.965, γ2.025; biaxial negative character, $2V$ about 60°.

$\beta 2PbO.B_2O_3$ inverts to the α form at about 473° C, and the reaction is apparently irreversible. The inversion is too rapid to permit determination of either the melting point of the compound or the temperature of melting of the β2:1-β4:1 eutectic composition, although the latter is indicated to be between 470 and 475° C. Indices of refraction are: α2.08, β2.10, γ2.11. The optic axial angle is very large and positive character is indicated.

$5PbO.4B_2O_3$ melts incongruently at 548° C to form liquid and crystals. The chemical composition of the crystals resulting from this decomposition has not been established. The crystals are doubly refracting, with a minimum index of 1.89 and a maximum of 1.91. They were found only in the area *A* (fig. 2) and apparently formed from preparations previously crystallized at lower temperatures. At

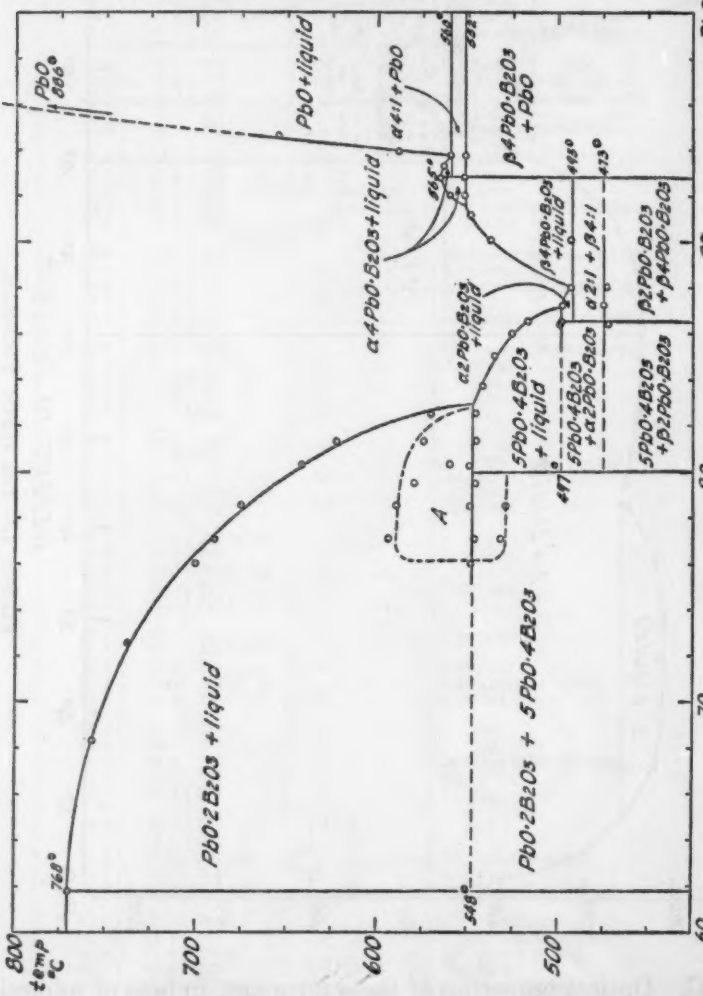

FIGURE 2.—$PbO.2B_2O_3$–PbO portion of the PbO–B_2O_3 system.

higher temperatures they were replaced by crystals of the 1:2 compound, but there was no consistent relation between composition and the temperature at which the unidentified phase disappeared. Their indices were constant over the composition range in which they formed, indicating that they are not the result of solid solution. The possibility that they might be the metaborate, or a polymorphic form of the diborate, was investigated by holding melts of these compositions for periods of 1 day to 3 weeks at temperatures in the range 500° C to 560° C. The results were negative.

$5PbO.4B_2O_3$ is the primary phase in compositions containing from 83 to 87.3 percent of PbO. The particles frequently were polysynthetically twinned. Character is biaxial negative; $2V$ about 65°; and the indices of refraction α1.91, β1.93, γ1.96.

$PbO.2B_2O_2$ predominates in the system, being the primary phase from the hypothetical $PbO.2B_2O_3$-B_2O_3 eutectic composition (containing less than 2 percent of PbO) to the composition containing 83 percent of PbO. It melts congruently at 768° C and, under favorable conditions, forms large, well defined laths with pointed ends and with parallel extinction. Character was not established but the maximum and minimum indices of refraction are 1.935 and 1.915.

2. TWO-LIQUID AREA

A narrow two-liquid area (fig. 1), extending from approximately 9 to 43 percent of PbO, was indicated. The upper limit of this area is determined by the temperatures at which change from clear to opaque liquid (or vice versa) could be observed, the crest being at 785° C for the melt containing 30.1 percent of PbO. The lower limit is at 742° C and was established by the disappearance of $PbO.2B_2O_3$ crystals from previously crystallized melts.

Actually, some immiscibility was observed in nearly all of the various partially crystallized specimens containing B_2O_3 in excess of the $PbO–2B_2O_3$ ratio. Even after holding for several weeks below the liquidus it was obvious that equilibrium had not been reached—evidence of the high viscosity of these melts. That a two-liquid area may exist under nonequilibrium conditions over this high B_2O_3 composition range is shown also by Guertler.[9]

3. COMPOSITIONS AS GLASSES

Index-of-refraction and thermal-expansion values, and the temperature of initial softening are given in table 3 for five glasses. Expressed in approximate mole ratios, these glasses represent compositions from $1PbO$ and $15B_2O_3$ to $3PbO$ and $1B_2O_3$. The test for relative solubility extracted 100 percent of the lead from each glass.

TABLE 3.—*Some properties of lead borate glasses*

PbO (by weight)	Index of refraction	Coefficient of linear thermal expansion from room temperature to 250° C	Beginning of softening, T_s
%			°C
36.8[a]	1.46 1.60	10.3×10^{-6}	476
52.0	1.66	6.8	487
61.8	1.75	6.9	491
79.5	1.92	9.8	394
90.1	2.11	13.2	286

[a] 2 immiscible glasses.

Glasses containing B_2O_3 in less than the 1:2 ratio (approximately 38 percent) appear stable in air. Those containing B_2O_3 in excess of this ratio are increasingly unstable as the content of B_2O_3 increases. 2 g

[9] W. Guertler, Z. anorg. Chem. **40**, 225 (1904). The region of immiscibility, as reported by Guertler, extends from 41 percent to practically zero percent of PbO, and the maximum temperature is approximately 625° C.

each of glasses containing 38.2, 41.5, 55.1, 74.1, and 85.5 percent of B_2O_3 were digested in 100 ml of warm water, which treatment dissolved 4.5, 6.5, 13.0, 47.0, and 67.0 percent, respectively. When the composition containing 74.1 percent of B_2O_3 was exposed to room atmosphere for 30 minutes, crystals had developed sufficiently in the glass of lower index (1.46) to be identified as boric acid.

An extensive investigation of lead borate glasses has been reported by Drs. Klemm and Berger [10] who studied, in particular, the thermal expansion as influenced by previous thermal history, by load, and by heating rate. Their values for initial softening (T_s), when using a load of 60 g/cm², show a maximum variation of only 15° C from the values given in table 3. With a load of 15 g/cm² the maximum variation was 45° C, their values being invariably higher. They give also a curve for specific gravity versus composition of lead borate glasses, which curve may be expressed by the equation:

$$S=\frac{(PbO)^2}{1600}+2$$

where

S = true specific gravity.
PbO = weight percentage of PbO in the glass.

V. DISCUSSION

Determination of phase equilibria in the lead borate system had been attempted previously by Mazzetti and De Carli [11], whose data were obtained from heating curves and microscopic examination without, apparently, holding compositions at crystallizing temperatures for prolonged periods of time. Their results were interpreted as indicating compounds of PbO and B_2O_3 in the molecular ratios of 1:1, 1:2, 2:5, and 1:3 having melting points of 500°, 570°, 520°, and 560° C, respectively. They state that the smallness of the crystals in the devitrified glass prevented identification.

In the present investigation the following results were accepted as proof that the crystals of index 1.91 and 1.96 were the compound 5:4 rather than the metaborate: (*a*) melts approximating this composition, when held several weeks at 500 ± 10° C, apparently crystallized to one phase; (*b*) previously crystallized mixtures containing slightly less than 80 percent of PbO (composition of $5PbO.4B_2O_3$ is 80.02% of PbO; 19.98% of B_2O_3) when held at temperatures between 500° and 540° C for 16 to 18 hours gave practically no liquid; (*c*) previously crystallized mixtures containing slightly more than 80 percent of PbO heated to the same temperatures gave liquid and the crystals designated as $5PbO.4B_2O_3$. However, certain heat treatments were productive of results which at first threw doubt on the conclusion that the crystals in question were the 5:4 compound. For example, compositions containing from 78 to 80 percent of PbO would contain crystals of $PbO.2B_2O_3$ and of $2PbO.B_2O_3$ if they were first held for several weeks at 600° to 650° C and then held at about 400° C. Evidently the melt was too viscous at the lower temperature to permit resorption of the 1:2 compound, thereby forcing crystallization of the 2:1 compound. The formation of the unidentified phase in area *A* (fig. 2) also might be

[10] A. Klemm and E. Berger, Glastech. Ber. **5**, 405 (1927-28).
[11] C. Mazzetti and F. De Carli, Gazz. chim. ital. **40**, 19 (1926).

misleading, but it is believed to be a metastable phase. $PbO.2B_2O_3$ and glass can be obtained by holding either glass or previously crystallized samples at temperatures between area *A* and the liquidus, while the unidentified phase was obtained only from melts previously crystallized at lower temperatures.

The melting temperature for $PbO.2B_2O_3$ given by Mazzetti and De Carli (570° C) is between the T_g value given in this report for the glass of similar composition (491° C) and the melting temperature given for the compound (768° C). It is probable that all of their determinations of liquidus temperatures were influenced by lack of complete crystallization. The high viscosity of this composition as a liquid, and the consequent slow growth of crystals, may be illustrated by the following data: the sample held 15 days at 475° C remained all liquid; the sample held 13 days at 650° C was partly crystallized, but the crystals were very small; the sample held 25 days at 560° C and then 25 days at 740° C was completely crystallized.

No evidence was obtained in this study of compounds higher in B_2O_3 than the lead diborate.

TABLE 4.—*Some optical properties of lead borate compounds*

Compound	Indices of refraction (values to ±0.01)			Optical character
	α	β	γ	
α4PbO.B_2O_3	(min 2.15; max 2.20)			Not established.
β4PbO.B_2O_3	2.15	2.20	2.24	Biaxial negative; 2V 80°.
α2PbO.B_2O_3	1.965	--------	2.025	Biaxial negative; 2V 60°.
β2PbO.B_2O_3	2.08	2.10	2.11	Biaxial positive; 2V 90°.
5PbO.4B_2O_3	1.91	1.93	1.96	Biaxial negative; 2V 65°.
PbO.2B_2O_3	(min 1.915; max 1.935)			Not established.

VI. SUMMARY

The system $PbO-B_2O_3$ was found to contain four compounds, the optical properties of which are summarized in table 4: $4PbO.B_2O_3$ occurring in two forms and melting congruently at 565° C; $2PbO.B_2O_3$ occurring in two forms and melting incongruently at 497° C; $5PbO.4B_2O_3$ melting incongruently at 548° C; and $PbO.2B_2O_3$ melting congruently at 768° C. The identity of an additional crystal phase was not established. The lowest melting eutectic has the composition 88 percent of PbO and 12 percent of B_2O_3, by weight, and melts at 493° C. Some properties of several of the compositions as glasses are given also.

WASHINGTON, March 13, 1937.

U. S. Department of Commerce National Bureau of Standards

RESEARCH PAPER RP996

Part of Journal of Research of the National Bureau of Standards, Volume 18, May 1937

PREPARATION OF IRON OXIDE AS A SOURCE OF HIGH-PURITY IRON

By Harold E. Cleaves and John G. Thompson

ABSTRACT

Selected ferric nitrate has been purified by recrystallization, yielding several lots of iron oxide of high purity. Examination of the products by spectrochemical and chemical methods, for the presence of 51 possible impurities, shows that silicon is the principal impurity in each of the oxides; in the best materials the silicon content is 0.005 or 0.006 percent. Four additional elements, aluminum, calcium, magnesium, and copper are present, but the sum of these four is less than 0.001 percent of each sample.

These oxides have been prepared as a preliminary step in the preparation of metallic iron of high purity.

CONTENTS

	Page
I. Introduction	595
II. Review of methods for the preparation of high-purity iron	596
III. Investigation of methods for the preparation of purified compounds of iron	597
1. Ferrous-oxalate method	597
2. Ferrous-formate method	598
3. Ferrous-chloride method	598
4. Ferrous-sulphate method	598
5. Ferric-nitrate method	599
6. Combined ferrous-chloride and ferric-nitrate method	601
7. Cupferron method	602
8. Summary of available methods	602
IV. Production of high-purity ferric oxide	602
V. Selected references	607

I. INTRODUCTION

One of the functions of the Metallurgical Division of the National Bureau of Standards is to compile available information on the preparation and properties of metals and alloys, particularly those of unusual purity. Previous activity in this field has resulted in the publication of several circulars, each dealing with one of the following metals and its alloys: copper, nickel, aluminum and magnesium, bismuth, zinc, and silver. The current study is concerned with the metal iron and consists in two phases (1) a review of available information from the technical literature, and (2) the preparation in the laboratory of iron of high purity and of definitely known composition. The first phase of the work has been completed, the results being published in the form of a monograph[15] [1] and summarized in another publication [16]. The present report describes the preparation of purified iron oxide, the first stage in the laboratory preparation of metallic iron of high purity.

[1] The numbers in brackets here and throughout the text refer to the list of selected references at the end of the paper.

II. REVIEW OF METHODS FOR THE PREPARATION OF HIGH-PURITY IRON

Available information indicates that the best product obtainable by the smelting of an iron ore with subsequent refining in the molten state is iron of about 99.8-percent purity.[2] Methods employed in the past for the preparation of iron of higher purity than this have been of two general types, electrolytic and chemical. Recently iron of high purity has been prepared by the cyclic formation and decomposition of iron carbonyl, but available information regarding this process is limited. Since the claim of extraordinary purity in the product has not yet been substantiated, and as elaborate apparatus is required for operating under high pressures and at elevated temperatures, the carbonyl process was eliminated from consideration in the present work. Sublimation processes likewise were eliminated from consideration because of manipulative difficulties and also because the recent work of Kroll [11] indicates that sublimation does not produce a satisfactory separation of iron from its associated impurities.

Records of the numerous investigations of electrolytic processes indicate that the best electrolytic irons were of somewhat higher purity than is obtainable by smelting and refining operations but, nevertheless, were not pure irons. Certain impurities, particularly nickel, were always present. None of the electrolytic processes yielded iron of as high purity as has been obtained for other electrolytic metals, zinc, aluminum, and lead, for example. The conclusion that the possibilities of electrolytic methods for the production of very pure iron were limited, was based upon the records of the many investigations of electrolytic iron during the period from 1910 to 1920, when interest in this product was highest. However, this conclusion has been confirmed by the results of a recent investigation of electrolytic iron at the National Physical Laboratory in England, according to the report of Adcock and Bristow [14].

Chemical methods involving the preparation of a purified compound of iron with subsequent reduction to the metal were used for the laboratory production of two irons, by Lambert and Thomson [7] and by Baxter and Hoover [8], that were probably the purest ever prepared. For this reason, and because of the difficulties and apparent limitations of the carbonyl and electrolytic processes, attention in the present investigation was concentrated on chemical methods.

Two distinct stages are involved in chemical methods for the preparation of high-purity iron (1) preparation of a purified compound of iron, and (2) conversion of the purified compound to metallic iron, by reduction and sintering (or melting). The greatest possible purity in the purified compound is essential as experience has shown that the subsequent conversion to metallic iron introduces contamination more often than it removes impurities. The present paper is concerned only with the preparation of a purified salt of iron. The conversion of this compound to metallic iron will be discussed in a subsequent paper.

[2] For detailed discussion of the various methods of producing iron of high purity, see references [15] and [16].

III. INVESTIGATION OF METHODS FOR THE PREPARATION OF PURIFIED COMPOUNDS OF IRON

Most of the attempts to prepare a very pure salt of iron have involved precipitation and recrystallization of compounds such as the oxalate, formate, chloride, sulphate, and nitrate. The usual practice has been to convert the purified compound to the oxide as the last step prior to reduction, and the ultimate goal in the preparation of a pure compound of iron is therefore the production of pure iron oxide. The latter compound, however, cannot be prepared directly from an impure source; the conversion to iron oxide is not in itself an efficient purification process. Consequently, the preparation of some other pure compound of iron is necessary as an intermediate step in the preparation of pure iron oxide.

Previous attempts to purify various compounds, and some results obtained in the present investigation, are briefly reviewed in the ensuing paragraphs.

1. FERROUS-OXALATE METHOD

Precipitation of crystalline ferrous oxalate from aqueous solutions was one of the first recorded methods for freeing iron from its associated impurities. Matthiessen and Szczepanowski [1] studied this compound prior to 1870; subsequently Dragendorff [2], McGillivray [3], Kreusler [6], and workers at the Physikalisch-Technische Reichsanstalt [5] investigated its preparation. The usual practice was to ignite the purified oxalate to form the oxide, which was subsequently reduced with hydrogen. Kreusler estimated that some iron which he prepared from ferrous oxalate was of very high purity; the metal was malleable and resistant to hydrochloric acid but dissolved readily in nitric acid. However, no analysis was given and some of the reported properties do not indicate exceptional purity. In the 1908 report of the extended work at the Physikalisch-Technische Reichsanstalt it was concluded that ferrous oxalate invariably contained manganese and other metallic constituents. McGillivray called attention to the fact that iron oxide prepared by ignition of ferrous oxalate was usually contaminated by carbon, and this was confirmed by the recent work of Sykes [10].

In the present investigation the starting material was reagent-grade ferrous sulphate in which the ratio of Mn to Fe was 0.134 to 100. Ferrous-oxalate crystals precipitated from a solution of this material by additions of oxalic acid or ammonium oxalate always contained manganese, usually about as much as the original sulphate. Fractional precipitation of ferrous oxalate did not result in concentration of the manganese in any one fraction, instead, it was distributed fairly uniformly in all fractions. Spectrochemical examination of oxide obtained by ignition of some of the oxalate crystals showed that small amounts of Al, Si, and Ni and somewhat larger amounts of Mg, Ca, and Cr were present in addition to the manganese.

The presence of appreciable amounts of so many metallic elements, the probable presence of carbon, and the evidence of previous workers indicate that the oxalate method is not promising for the preparation of very pure iron oxide.

2. FERROUS-FORMATE METHOD

The precipitation of ferrous formate is mentioned in the reports of the Physikalisch-Technische Reichsanstalt [5] as having the same disadvantages as the ferrous-oxalate method, particularly in the failure to eliminate manganese and other impurities. To confirm this conclusion, ferrous formate was precipitated by additions of formic acid to a solution of ferrous sulphate, with additions of ammonia to maintain approximate neutrality in the solution. The yield was small and spectrochemical examination showed the presence of comparable amounts of the same impurities that were found in the oxalate crystals. The ferrous-formate method did not appear to be promising.

3. FERROUS-CHLORIDE METHOD

The precipitation of ferrous-chloride crystals from aqueous solutions by additions of concentrated hydrochloric acid was considered by McGillivray [3] to be an improvement over the oxalate method. Richards and Baxter [4] used ferrous chloride as the starting material in their determination of the atomic weight of iron but converted the chloride to other salts of iron for further purification. Aqueous solutions of ferrous chloride were frequently used as electrolytes in the preparation of iron, but the purity of the electrolyte was seldom a matter of particular concern; the process of electrolysis was assumed to eliminate minor impurities either present in the original electrolyte or introduced by solution of the iron anode. In recent work at the National Physical Laboratory [12, 13, 14] in England, it was concluded that contamination of electrolytic iron by nickel, cobalt, and copper could not be avoided, and that iron of higher purity could be prepared by decomposing purified ferrous chloride with steam and reducing the resulting ferric oxide with hydrogen. A complete description of the preparation of this purified ferrous chloride is not yet available.

In the present investigation crystals were precipitated from aqueous solutions of ferrous chloride of reagent grade, either by chilling the solution or by pouring it into concentrated hydrochloric acid. In either case the crystals were redissolved and reprecipitated several times, but spectrochemical examination of the final products showed that appreciable amounts of manganese were present in addition to several other metallic impurities. These results, together with the low yields of crystals obtained, indicated that recrystallization of of ferrous chloride was not suitable for our purposes.

4. FERROUS-SULPHATE METHOD

Decomposition of reagent-grade ferrous sulphate by fusion with sodium sulphate and reduction of the resulting oxide with hydrogen was reported to be the best of four methods studied by Matthiessen and Szczepanowski [1]. Aqueous solutions of ferrous or ferrous-ammonium sulphate were frequently used in the electrodeposition of iron, but as in the case of the ferrous-chloride electrolytes, the purity of the ferrous-sulphate solution was seldom a matter of concern. The solutions usually were prepared from commercial irons and retained the impurities thereof. When purified salts were used to prepare the original electrolyte, the solution was soon contaminated in use by impurities from the soluble anodes. However, Richards and Baxter [4] employed electrolysis of a ferrous-sulphate–ammonium-oxalate

solution as one of the intermediate steps in their preparation of a pure compound for the determination of the atomic weight of iron.

In the present investigation little attention was devoted to recrystallization of sulphates, primarily because of the known difficulty of obtaining a sulphur-free product from such a source and the objectionable nature of this element as an impurity in iron. Furthermore, examination of reagent-grade materials showed that both ferrous sulphate and ferrous-ammonium sulphate contained appreciable amounts of manganese and other metallic impurities.

5. FERRIC-NITRATE METHOD

Recrystallization of ferric nitrate ($Fe(NO_3)_3.9H_2O$) was used by Richards and Baxter [4] as the final stage in the purification of iron compounds prior to conversion to the oxide for atomic-weight determinations. In an extended investigation at the Physikalisch-Technische Reichsanstalt [5] it was concluded that recrystallization of ferric nitrate constituted the best available method for the preparation of a very pure salt of iron. Lambert and Thomson [7] and Baxter and Hoover [8] used this method to prepare purified salts of iron, and the metallic iron eventually obtained in these two investigations was probably the best ever made. From these results, obtained by previous workers, crystallization of ferric nitrate seemed worthy of careful study in the present investigation.

Ferric nitrate, because of its large content of water and low melting point, is not a satisfactory compound for reduction and for spectrochemical examination. One of the first considerations, therefore, was the procedure to be used in converting ferric nitrate to a more suitable compound. Lambert and Thomson [7] and Baxter and his coworkers [4, 8] heated or ignited ferric nitrate and obtained products variously described as ferric oxide or a mixture of the oxide and basic nitrate. In the work at the Physikalisch-Technische Reichsanstalt [5], ferric nitrate was heated to 50° C, melting in its own water of crystallization. Anhydrous ammonia was passed into the melt, forming ferric oxide and ammonium nitrate. After cooling the latter compound was removed by washing with water. Attempts to duplicate this procedure in the present investigation were not successful. A large amount of heat was evolved by the reaction between ammonia and ferric nitrate, and the resulting evaporation of water thickened the mixture to a hard mass, which frequently plugged the ammonia delivery tube. Additions of water resulted in the formation of basic ferric nitrate without improving the operation. The conversion of nitrate to oxide was never complete in our experiments; the product invariably was a mixture of oxide and basic nitrate.

Precipitation of hydrated ferric oxide by additions of gaseous ammonia to a dilute solution of ferric nitrate in distilled water, washing the precipitate by decantation to free it from nitrate, and finally filtering and drying, appeared to be a decided improvement over earlier procedures for obtaining uncontaminated ferric oxide. Precipitation from dilute aqueous solution, therefore, was employed throughout the present investigation for the conversion of ferric nitrate to the oxide.

Ferric nitrate is so soluble in water that its recrystallization from this medium is difficult and inefficient. When only 125 ml of water

was added to 1,000 g of ferric nitrate ($FeNO_3)_3.9H_2O$) and the resulting solution was chilled to 15° C, only about 70 percent of the ferric nitrate crystallized from the solution. The crystals so obtained were redissolved and reprecipitated and the process was repeated through five successive crystallizations. Examination of the products showed that manganese, present in the original material to the extent of 0.0047 percent, was materially reduced by the first crystallization and could not be detected in the products of the fourth and fifth crystallizations. The number and amounts of the other metallic impurities, determined by spectrochemical examination, were less than in the methods previously investigated. Recrystallization of ferric nitrate, therefore, appeared to be promising as a purification process, particularly for the elimination of manganese, which is not removed by the other methods. However, the yield obtained in crystallization from aqueous solutions was low; only 29 percent of the original material was recovered after four crystallizations. Consequently, attention was turned to the possibility of crystallizing ferric nitrate from other media.

Crystallization from solution in concentrated nitric acid was found to be impracticable as the crystallization was difficult to induce and at best proceeded at a very slow rate. Much better results were obtained with a medium consisting of 10 volumes of concentrated nitric acid and 1 volume of distilled water. 1,000 g of ferric-nitrate crystals of reagent grade dissolved readily in 450 ml of this 10:1 nitric acid at 50 or 60° C. If this solution was cooled to 15° C about 90 percent of the ferric nitrate separated out as crystals. Somewhat higher recoveries were obtained when the solution was cooled to temperatures below 15° C; on the other hand, noticeably lower recoveries were obtained at temperatures above 15° C. Consequently, all crystallizations from 10:1 nitric acid were conducted at 15° C, or below.

A series of crystallizations from this medium was carried out. Each crop of crystals was separated from the mother liquor and, after drying in a Büchner funnel with suction, was then available for resolution and recrystallization. The proportions of 450 ml of 10:1 acid to 1,000 g of ferric-nitrate crystals were maintained in all of the solutions. Spectrochemical examination of samples of ferric oxide derived from this series of crystallizations showed that the higher yields obtained by crystallization from 10:1 nitric acid, as compared with aqueous solutions, did not involve a sacrifice of purity in the product. Chromium persisted through six crystallizations, but the elimination of manganese was complete in two crystallizations.

The other impurities in the recrystallized ferric nitrate consisted chiefly of small amounts of aluminum, calcium, magnesium, and silicon. The amounts of these constituents varied in an irregular manner from one crystallization to the next, which indicated that they were being replenished from time to time. Two possible sources of contamination were considered: (1) Nonvolatile matter in the nitric acid and (2) dust and particles of fly ash in the laboratory atmosphere. Concentrated nitric acid was found to contain nonvolatile matter to the extent of only 0.0004 percent by weight, which presumably indicated slight solvent action of the concentrated acid on the soft-glass bottles in which it was stored. However, a relatively large volume of acid is used in a series of crystallizations and the cumulative effect of even these amounts of impurities might be appreciable. When

the same acid was distilled in Pyrex it still contained a trace of volatile solids, presumably ammonium salts, but the nonvolatile residue from 50 ml of distillate was too small to be weighable, certainly less than 0.0001 percent by weight. The possibility of contamination from the nitric acid therefore is slight, particularly if the acid is freshly distilled.

Contamination by dust particles was avoided during most of the crystallization process by conducting the operations in covered containers. However, in the filtration and drying of the nitrate crystals, large volumes of air were drawn through the precipitate. To avoid the possibility of contamination in this operation the apparatus shown in figure 1 was constructed. With this arrangement the air supplied to the filter was previously cleaned by passage through filter paper.

Recrystallization of ferric nitrate from a strongly acid solution appears to be the most promising method so far investigated; except for its failure to eliminate chromium.

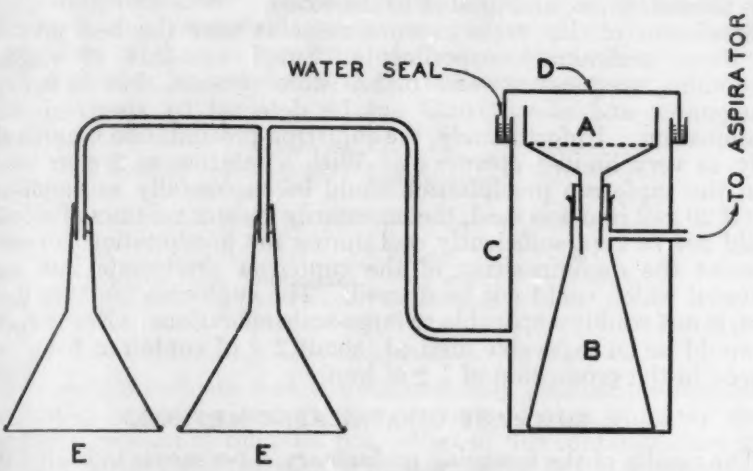

FIGURE 1.—*Dustproof filtering apparatus*

A, Büchner funnel (10 in.); *B*, filter flask; *C*, sheet-iron container; *D*, glass cover; *E*, filter paper (Whatman no. 2) cemented to lip of glass funnel (12 in.).

6. COMBINED FERROUS-CHLORIDE AND FERRIC-NITRATE METHOD

The products of the ferrous-chloride crystallizations contained manganese but were free from chromium; the products of nitrate crystallizations contained chromium but no manganese. Therefore, it appeared possible that a combination of the two methods would eliminate both impurities. Accordingly, ferrous chloride from several sources was crystallized twice and the product was converted to ferric nitrate which was crystallized twice. Spectrochemical examination of the final products showed that the combination method eliminated chromium but otherwise had no advantages over the straight nitrate method. Furthermore, the combination method was difficult and tedious in its manipulation and the yield was only about 30 percent. If chromium-free starting material were available the nitrate method would be decidedly preferable to the combined chloride-nitrate procedure.

7. CUPFERRON METHOD

In one of the procedures of analytical chemistry, the reagent cupferron is employed to separate iron from certain elements after interfering elements have been removed from the solution. To investigate the purity of this product an aqueous solution of ferrous sulphate (reagent grade) was slightly acidified with sulphuric acid and was treated with hydrogen sulphide to precipitate the heavy metals. The precipitate was removed by filtration, the filtrate was made ammoniacal, tartaric acid added, and the solution again treated with hydrogen sulphide, this time to precipitate the iron, nickel, cobalt, zinc, and a part of the manganese present. The precipitate was dissolved in hydrochloric acid, nitric acid added, and the solution oxidized by boiling. Perchloric acid was added and the solution evaporated to fumes to dehydrate silica. The residue was diluted and filtered. The acidity of the filtrate was adjusted and the iron precipitated from the chilled solution with cupferron. The precipitate was filtered, dried, and ignited to the oxide.

Specimens of this oxide in some respects were the best prepared in these preliminary experiments. Small amounts of calcium, chromium, magnesium, and nickel were present, but aluminum, manganese, and silicon could not be detected by spectrochemical examination. Unfortunately, the cupferron precipitation is applicable only to very limited operations. With a solution of 2 g or less of iron the cupferron precipitation could be successfully accomplished, but if 20 g of iron was used, the necessarily greater volumes of solution could not be kept sufficiently cool during the precipitation process to prevent the decomposition of the cupferron precipitate into tarry material which could not be filtered. The cupferron method, therefore, is not readily applicable to large-scale operations. Furthermore, it would be an expensive method, about 2 g of cupferron being consumed in the production of 1 g of iron.

8. SUMMARY OF AVAILABLE METHODS

The results of the foregoing preliminary experiments indicated that recrystallization of ferric nitrate from a nitric-acid solution was the most promising method for the preparation of an iron compound containing the least number and smallest amounts of impurities. The principal impurity in the nitrate crystals was chromium, and the elimination of this element apparently could be accomplished only by starting with ferric nitrate prepared from a chromium-free material such as electrolytic iron.

IV. PRODUCTION OF HIGH-PURITY FERRIC OXIDE

Raw material for the production of purified ferric oxide consisted of about 135 pounds of electrolytic iron, chiefly miscellaneous scrap from the work on electrolytic iron at this Bureau about 20 years ago [9]. The conversion of this material into one large, uniform lot of ferric nitrate, with one or two recrystallizations of the entire mass, followed by recrystallizations on a small scale in the laboratory, using freshly distilled acid and the dustproof filtering apparatus, should produce ferric oxide of uniform composition and high purity.

The aid of a producer of commercial chemicals was enlisted for the bulk conversion of the raw material and for the large-scale recrystal-

lizations. To determine the purification obtainable in commercial operations a pilot run was made at the commercial plant, converting a small lot of iron to nitrate with two subsequent crystallizations. The pilot run produced about 10 pounds of ferric-nitrate crystals. Spectrochemical examination of a representative sample, after conversion to the oxide, indicated that a very satisfactory degree of purity had been attained with two recrystallizations and that further recrystallizations on a large scale were unnecessary. The entire supply of electrolytic-iron scrap was therefore converted to ferric nitrate and recrystallized twice in the commercial plant, producing 306 pounds of purified crystals and 144 pounds of secondary crystals recovered from the mother liquor. The recovery of purified crystals from the large-scale operations was decidedly less than had been previously obtained in our operations on a laboratory scale.

A composite sample of the commercially purified crystals was recrystallized twice in the laboratory, using freshly distilled nitric acid and the dustproof filter. Portions of the original material and of the product of each recrystallization were converted to ferric oxide. Examination of the arc spectrum of these samples of oxide, using copper electrodes, indicated that impurities were present as follows:

Element	Commercially purified	First recrystallization	Second recrystallization
Si	Weak	Weak	Trace.
Ca	Very weak	Very weak	Very weak.
Al	Trace	Faint trace	None.
Mg	Trace	None	None.

These results indicate that the commercially purified product contained more impurities and greater amounts of each impurity than were in the product of the pilot run. Part of this contamination was believed to result from particles of foreign matter in the commercially refined crystals. When these crystals were dissolved in 10:1 nitric acid, there usually remained a small residue of particles of grit or of iron oxide, with an occasional particle resembling a small bit of porcelain. Filtration of the hot strongly acid solution was not practicable, but the residue could be largely eliminated by allowing the solution to stand for a few minutes and then siphoning off the clear solution. Spectrochemical examination of the products of recrystallization from such a solution showed that a single recrystallization improved the purity and that the purity of the product of a second recrystallization was approaching the limits of determination by that method of analysis. The presence of only two elements could be detected spectrochemically and these "traces" of calcium and silicon were estimated to be small.[3] Consequently, it was decided to subject an appreciable portion of the ferric nitrate to two recrystallizations, on the assumption that the product would be of satisfactory purity for our purposes. It was further decided to subject another portion to four recrystallizations, in the hope that additional purification might be attained thereby.

[3] It was not known until later, when more accurate quantitative calibration of the spectochemical data was available, that spectroscopic traces of silicon might represent as much as 0.01 percent by weight.

At this point it became necessary to suspend operations for approximately 1 year. When operations were resumed it was found that the nitrate crystals had become further contaminated by bits of enamel and iron rust from the enameled tank in which they were stored. The contamination was particularly evident in the material adjacent to the walls and bottom of the tank. This material was discarded, the rest was hand picked and washed and was then subjected to recrystallization according to the program previously adopted.

Details of the procedure for recrystallization of the nitrate and subsequent conversion to ferric oxide were as follows: a batch of 8 pounds of ferric-nitrate crystals in a covered 4-liter beaker [4] was dissolved in 1,650 ml of 10:1 [5] nitric acid [6] by warming on a steam bath. The beaker was allowed to stand for 15 minutes to permit the sediment to settle. The clear solution was then siphoned off and cooled to 15° C or less, in cold water. A seed crystal of ferric nitrate was added and the solution was stirred until crystallization was well under way, at which point stirring was discontinued. When the deposit of crystals on the walls of the beaker had become approximately ½ inch thick, the beaker was removed from the cold water. The heat liberated by the exothermic crystallization of ferric nitrate soon softened the crystalline cake so that it could be detached from the walls of the beaker and granulated by means of a large porcelain spatula. The beaker then was returned to the cold water and the process was repeated until crystallization was practically complete, as indicated by the contents of the beaker becoming a very thick slurry of uniform consistency and nearly white. This was transferred to a 25-cm Büchner funnel and filtered through no. 2 Whatman filter paper.[7] Suction was maintained overnight to remove as much as possible of the mother liquor.

The crystals were next returned to the 4-liter beaker, dissolved in fresh 10:1 acid by warming, and the solution was cooled and allowed to crystallize. The crystals were collected and dried with suction and the process repeated as often as desired. In redissolving each crop of crystals a constant proportion of acid to crystals was maintained by decreasing the amount of acid with each successive crystallization to compensate for the loss of ferric nitrate in the mother liquor of the preceding crystallization. Thus 1,650 ml of acid were used to dissolve the original 8 pounds of ferric nitrate; 1,540 ml to dissolve the first crop of crystals; 1,430 ml for the second crop; and 1,320 ml for the third crop.

The final crop of crystals was dissolved in 1,500 ml of distilled water at the boiling point. The solution was filtered through Whatman filter paper to eliminate traces of insoluble matter and was apportioned equally among four 10-gallon Pyrex carboys, which were then filled with distilled water. Anhydrous ammonia was passed into each carboy until a definite odor of ammonia was detectable and the precipitate of hydrated ferric oxide showed a definite tendency to flocculate. The suspension was allowed to stand overnight, after which the precipitate

[4] All of the glass apparatus and utensils were Pyrex.
[5] 10 volumes of concentrated acid plus 1 volume of distilled water.
[6] All of the nitric acid used throughout this procedure was freshly distilled in Pyrex.
[7] The cold mother liquor could be filtered through paper without difficulty but the hot concentrated ferric-nitrate solution could not.

occupied about 15 percent of the volume of the carboy. The clear supernatant liquid was siphoned off as completely as possible,[8] the carboys were refilled with distilled water, and the precipitate was dispersed throughout the solution by stirring with a stream of dust-free air. The washing by decantation was repeated until the supernatant liquid became slightly turbid instead of being perfectly clear. This condition, which indicated complete removal of ammonium nitrate from the hydrated ferric oxide, usually was attained after five washings.

After the final decantation the residual slurry of water and gelatinous precipitate was transferred to covered beakers and maintained for about 10 hours in a steam bath. This treatment not only reduced the apparent volume of the precipitate by about 75 percent, but also transformed it from a gelatinous condition to a relatively granular material.[9] The coagulated precipitate was filtered in a Büchner funnel with suction and was washed with boiling water. The filter medium consisted of bolting silk and a double thickness of filter paper. The hydrated ferric oxide, even after the coagulation treatment, adhered tightly to filter paper but could be readily separated from bolting silk. The filter cake was dried in an electric oven at about 150° C. After drying, the friable cake was placed in a glazed porcelain mortar and gently crushed with a porcelain pestle, without grinding. The product was combined with other lots of oxide of similar history.

The supply of purified ferric oxide thus obtained was separated into four lots, as follows:

Lot *A* represented two laboratory recrystallizations of the crystals from the large-scale crystallizations.

Lot *B* represented four laboratory recrystallizations of crystals.

Lot *C* represented two laboratory recrystallizations of the crystals that were recovered from the mother liquor in the large-scale crystallizations.

Lot *D* represented four laboratory recrystallizations of the crystals recovered from the mother liquor.

Each lot was thoroughly mixed and sampled for analysis. The arc spectra, using carbon electrodes for the region from 2470 to 3390 A and copper electrodes for the region from 2800 to 4800 A, were examined for the sensitive lines of 49 elements. Chemical analysis was employed to search for two additional elements, sulphur and phosphorus, that are not readily detectable by spectrochemical methods, and to confirm the spectrochemical evidence that only one element, silicon, was present in determinable amounts. The results obtained by the two analytical methods are shown in table 1.

[8] If the surface of the hydrated ferric oxide was disturbed during settling, by means of a small stream of distilled water, a depression remained in the surface of the fully settled precipitate. Inserting the tip of the siphon in this depression permitted practically complete removal of the supernatant liquid without loss of precipitate.

[9] This coagulation in the steam bath was not applicable to hydrated ferric oxide precipitated from more concentrated solutions. In one attempt to accelerate the process, four times the usual quantity of ferric-nitrate crystals was taken. No difficulty was encountered in the recrystallization process nor in the precipitation, settling and washing of the hydrated ferric oxide in the carboys. Each carboy contained four times the usual amount of hydrated ferric oxide, but there was apparently no difficulty in washing the precipitate free from ammonium nitrate, although more washings than usual were required. However, after the washings were completed, this lot of hydrated oxide could not be coagulated, but remained gelatinous and nonfilterable in spite of extended treatments in the steam bath and additions of small amounts of coagulants including ammonia, nitric acid, and ammonium nitrate. Apparently this hydrated ferric oxide differs appreciably from the products from identical sources but precipitated from a less concentrated solution. Subsequent work was limited to batches of 8 pounds of ferric nitrate, and no further difficulties in coagulation were encountered.

TABLE 1.—*Composition of purified iron oxide*

Element	Oxide *A*	Oxide *B*	Oxide *C*	Oxide *D*
Silicon	Trace (0.016) *	Trace (0.009) *	Faint trace (0.006) *	Faint trace (0.005).*
Aluminum	Trace	Faint trace	Faint trace	Faint trace.
Calcium	do	do	do	do.
Magnesium	do	do	do	do.
Copper	Faint trace	do	do	do.
Ag, As, Au, B, Ba, Be, Bi, Cb, Cd, Ce, Co, Cr, Ga, Ge, Hf, Hg, In, Ir, K, Li, Mn, Mo, Na, Ni, Os, Pb, Pd, Pt, Rh, Ru, Sb, Sc, Sn, Sr, Ta, Th, Ti, Tl, U, V, W, Y, Zn, Zr	Not detected	Not detected	Not detected	Not detected.
Sulphur	(Not detected) *		(Not detected) *	
Phosphorus	(Not detected) *		(Not detected) *	

* Data in parentheses are the results of chemical analysis; the limits of sensitivity of the methods employed were 0.001 percent of sulphur and 0.0005 percent of phosphorus. Spectrochemical terms are not comparable for different elements; a faint trace of silicon, for which the spectroscope is relatively insensitive, is 0.006 percent, but faint traces of aluminum, calcium, magnesium, and copper represent much less than 0.001 percent.

These data show that silicon alone is present in amounts that represent appreciable contamination; the sum of all impurities, except silicon, is estimated by the spectroscopist to be less than 0.002 percent for oxide *A* and less than 0.001 percent for oxides *B*, *C*, and *D*.

The high silicon contents of oxides *A* and *B* are the result of contamination introduced during the commercial purification of ferric nitrate. Iron oxide from a composite sample of the nitrate as received had a silicon content of 0.018 percent, whereas the silicon content of the electrolytic iron was about half that amount. It has been previously mentioned that the primary crystals, from which oxides *A* and *B* were prepared, on solution in 10:1 nitric acid showed a small amount of gritty, insoluble residue, including an occasional particle that resembled porcelain. On the other hand, the crystals that were recovered from the mother liquor in the large-scale operations did not show any insoluble residue when they were dissolved in 10:1 acid in preparing the low-silicon oxides *C* and *D*. The silicon contents of oxides *C* and *D* are about the same despite the additional recrystallizations employed in preparing oxide *D*, which indicates that the recrystallization process is not an efficient method for the elimination of silicon. If the silicon contents of oxides *C* and *D* represented contamination from dust particles or fly ash, or from impurities in the reagents used, the amounts of associated impurities should be roughly proportional to the silicon content. This is not the case; in each of the oxides the amount of silicon is much greater than the sum of all other impurities. The failure of the recrystallization process to eliminate silicon should have been investigated more thoroughly in the preliminary work, but at that time it was assumed that a spectrochemical trace of silicon was an unimportant and probably negligible amount.

The aim of this investigation was the production of iron oxide containing a minimum number of impurities with no impurity present in amounts in excess of 0.002 percent. This goal has been achieved except for the silicon contents. The latter, although disappointingly high for the purposes intended, are too small to offer much hope of their reduction or elimination from the oxide by mechanical means or

chemical treatment. Microscopic examination of the oxides revealed the presence of an occasional, minute particle with a refractive index approximately that of silica or a silicate, but these particles are too small and too few to permit their separation from the mass of ferric oxide. However, according to the evidence of Adcock and Bristow [14], there is at least a possibility that these silicon contents can be reduced by slagging in the reduction of the ferric oxide and subsequent melting of the sponge iron. The investigation of this possibility will be discussed in a future paper.

The authors express their indebtedness to many members of the Bureau staff for advice and assistance in this investigation, and particularly to Bourdon F. Scribner for the spectrochemical analyses, without which the work could not have been completed.

V. SELECTED REFERENCES

[1] Rep. Brit. Assn. Adv. Sci. **1868,** 342; **1869,** 82. Also Chem. News **20,** 101 (1869).
[2] Pharm. J. and Trans. **2,** 988 (1872).
[3] Ind. and Iron **21,** 69 (1896).
[4] Proc. Am. Acad. Arts. Sci. **35,** 253 (1900).
[5] Annual Reports of the Physikalisch-Technische Reichsanstalt. (1905 to 1909, Julius Springer, Berlin.)
[6] Verhand. deut. phys. Ges. **10,** 344 (1908).
[7] J. Chem. Soc. **97,** 2426 (1910).
[8] J. Am. Chem. Soc. **34,** 1657 (1912).
[9] Bul. BS **13,** 1 (1916–17). S266.
[10] Trans. Am. Soc. Steel Treating **10,** 839 (1926).
[11] Z. Elektrochem. **40,** 303 (1934).
[12] Engineering **138,** 150 (1934).
[13] Proc. Inst. Mech. Eng. **127,** 277 (1934).
[14] Proc. Roy. Soc. (London) [A] **153,** 172 (1935).
[15] The Metal—Iron. (McGraw-Hill Book Co., Inc., New York, N. Y., 1935).
[16] J. Research NBS **16,** 105 (1936). RP860.

Washington, February 2, 1937.

U. S. Department of Commerce National Bureau of Standards

RESEARCH PAPER RP997

Part of Journal of Research of the National Bureau of Standards, Volume 18, May 1937

METHOD FOR APPROXIMATING THE GLASS CONTENT OF PORTLAND CEMENT CLINKER [1]

By William Lerch and Lorrin T. Brownmiller*

ABSTRACT

This report describes a method for approximating the glass content of portland cement clinker. The method involves a determination of the heat of solution of the original clinker and of the same clinker which has subsequently been annealed under conditions designed to produce complete crystallization. The difference between the heat values so obtained is due principally to the latent heat of crystallization of the glass present in the original clinker. The ratio between that value and the latent heat of crystallization of the glass phase represents the glass content of the clinker. A curve is given showing the latent heat of crystallization of all possible glass compositions obtainable from melts at 1,400° C in the system CaO–Al_2O_3–SiO_2–Fe_2O_3 between the Al_2O_3/Fe_2O_3 ratios of 0.64 and 3.24.

CONTENTS

	Page
I. Introduction	609
II. Experimental procedure	612
1. Preparation of compositions corresponding to the liquid phase at 1,400° C	612
2. Microscopic and X-ray examination of the glass	614
3. Latent heat of crystallization of the liquid phase	615
4. Approximation of the glass content of portland cement clinker	617
III. Summary and conclusions	621
IV. References	622

I. INTRODUCTION

At the clinkering temperatures attained by present-day methods of portland cement manufacture, a considerable part of the charge is present as a liquid phase, the percentage of liquid produced being dependent on the chemical composition of the charge and on the maximum temperature attained. The disposition of this liquid phase in the clinker is dependent on the subsequent rate of cooling. If the cooling process is sufficiently rapid, a condition may be approached in which the liquid phase will be present as an "undercooled liquid" or glass. But if the cooling process is sufficiently slow to permit a continuous equilibrium, a completely crystalline product may be obtained. Intermediate rates of cooling may produce clinker of some degree of crystallization intermediate between these limits. Furthermore, the relative amounts and nature of the compounds formed on complete crystallization may be somewhat different if the liquid crystallizes independently than if equilibrium with the solid phases is maintained.

[1] The method should be applied to freshly burned, unhydrated portland cement clinker. It can not be applied to ground cements containing gypsum or to clinker which has been partially hydrated or carbonated.

*Research Associates at the National Bureau of Standards, representing the Portland Cement Association.

The methods of calculation of the compounds in portland cement proposed by Bogue [1][2] and Dahl [2] are based on the assumption that complete crystalline equilibrium has been attained. A number of reports have been published which indicate that this condition of equilibrium is not consistently attained in the commercial production of portland cement. The work of Rankin and Wright [3] has shown that the gamma form of $2CaO.SiO_2$ is the stable form at ordinary temperatures, whereas in present-day portland cement the $2CaO.SiO_2$ occurs in the beta form. Lea and Parker [4], Forsen [5], Spohn [6], Solacolu [7], and Kuhl [8] have found that the practical limit of lime saturation is lower than the theoretical limit on the basis of complete equilibrium. The presence of glass has also been confirmed by microscopic examination of commercial clinkers. Through microscopic examination by the immersion method and in polished section Insley [9] found certain clinkers to contain several percent of glass and the ratio of $3CaO.SiO_2$ to $2CaO.SiO_2$ in these clinkers to be greater than that obtained by calculation. Miller [10] also has reported the presence of glass in commercial clinker. He found the amount of glass to vary considerably but reported that "there are probably several percent of glass present in even a well-crystallized clinker." From studies of heats of solution of portland cements and portland cement compounds Swenson and Flint [11] found that experimentally obtained heats of solution of the cements are greater than those calculated on the basis of crystalline equilibrium.

Recent investigations reported by Lea and Parker [12, 4] on that portion of the quaternary system $CaO–Al_2O_3–SiO_2–Fe_2O_3$ which covers the region involved in portland cement, provide valuable data for a more complete understanding of the constitution of portland cement. From these data it becomes possible to calculate the quantity and composition of the liquid and crystalline phases which may be present under equilibrium conditions, at any temperature in *this quaternary system* under each of the following three assumptions:

1. That complete crystallization is attained with equilibrium maintained on cooling (calculations according to Bogue and Dahl).

2. That the equilibrium mixture of solid and liquid phases at any specified clinkering temperature is "frozen"; that is, that the liquid is solidified completely as glass.

3. That the crystalline phases at the clinkering temperatures are in equilibrium with their surroundings and remain unchanged while the liquid phase crystallizes independently on cooling.

Calculations based on these three alternatives permit wide variations in the computed constitutions as indicated from the results given in table 1, which is taken from the report of Lea and Parker [4].

It is recognized that the minor constituents of portland cement clinker (MgO) K_2O, Na_2O, MnO, TiO_2 etc.) will influence the equilibrium conditions at clinkering temperatures, and that they will influence the course of crystallization during cooling. The function of these constituents is not yet known and hence can not be definitely evaluated at the present time.

[2] Numbers in brackets refer to references at the end of this paper.

TABLE 1.—*Comparison of computed clinker compositions under different conditions of solidification*

(From Lea and Parker [4])

$C_3S = 3CaO.SiO_2$.
$C_2S = 2CaO.SiO_2$.
$C_3A = 3CaO.Al_2O_3$.
$C_4AF = 4CaO.Al_2O_3.Fe_2O_3$.
$C_5A_3 = 5CaO.3Al_2O_3$.

Constituents	Complete equilibrium crystallization	Crystallization at 1,400° C. Liquid gives glass	Crystallization at 1,400° C. Liquid crystallizes independently	Crystallization at 1,450° C. Liquid gives glass	Crystallization at 1,450° C. Liquid crystallizes independently
I. $CaO = 68.0\%$, $SiO_2 = 23.0\%$, $Al_2O_3 = 6.0\%$, $Fe_2O_3 = 3.0\%$. $Al_2O_3/Fe_2O_3 = 2.0$					
	%	%	%	%	%
C_3S	57.5	59.6	59.6	59.6	59.6
C_2S	22.5	16.2	21.2	15.6	21.0
C_3A	10.8	0	8.9	0	9.8
C_4AF	9.1	0	9.1	0	9.1
C_5A_3	0	0	1.0	0	0.5
Glass	0	24.3	0	24.8	0
II. $CaO = 68.0\%$, $SiO_2 = 23.0\%$, $Al_2O_3 = 7.0\%$, $Fe_2O_3 = 2.0\%$. $Al_2O_3/Fe_2O_3 = 3.5$					
C_3S	52.2	60.6	60.6	59.4	59.4
C_2S	26.5	15.4	20.9	15.3	21.4
C_3A	15.2	0	9.4	0	9.7
C_4AF	6.1	0	6.1	0	5.9
C_5A_3	0	0	3.8	0	3.8
Glass	0	25.1	0	25.5	0
III. $CaO = 66.0\%$, $SiO_2 = 24.0\%$, $Al_2O_3 = 7.5\%$, $Fe_2O_3 = 2.5\%$. $Al_2O_3/Fe_2O_3 = 3.0$					
C_3S	32.4	38.2	38.2	38.5	38.5
C_2S	44.5	34.3	40.2	33.3	39.9
C_3A	15.7	0	10.5	0	10.6
C_4AF	7.6	0	7.6	0	7.6
C_5A_3	0	0	3.6	0	3.5
Glass	0	27.6	0	28.1	0
IV. $CaO = 67.0\%$, $SiO_2 = 23.0\%$, $Al_2O_3 = 4.0\%$, $Fe_2O_3 = 6.0\%$. $Al_2O_3/Fe_2O_3 = .67$					
C_3S	62.7	54.6	60.9	55.1	61.5
C_2S	18.6	20.2	20.2	19.4	19.4
C_3A	0.5	0	0.4	0	0.5
C_4AF	18.2	0	18.2	0	18.2
CaO	0	0	0.3	0	0.7
C_5A_3	0	0	0	0	0
Glass	0	25.0	0	25.5	0

Under present commercial conditions of cement manufacture it seems improbable that the cooling conditions would be sufficiently rapid to completely "freeze" the liquid into glass, and it seems unlikely that the cooling conditions would be sufficiently slow to attain complete crystalline equilibrium. Thus it seems probable that most portland cement clinker would be in some intermediate state. The most rapidly cooled clinker may approach the composition computed on the assumption that the liquid freezes to glass; and the most slowly cooled clinker may approach the composition computed on the assumption of complete crystalline equilibrium.

Numerous attempts to correlate the properties of commercial portland cements with their oxide composition, or computed compound composition, have met with only partial success. The discrepancies suggest that the glass content of the clinker may have an important effect on some of the properties of the cement. A primary requirement for any investigation of the effect of the glass is the availability of a method of estimating the glass content of the clinker. The present report describes a heat of solution method for approximating the glass content of portland cement clinker.

II. EXPERIMENTAL PROCEDURE

1. PREPARATION OF COMPOSITIONS CORRESPONDING TO THE LIQUID PHASE AT 1,400° C

The method employed for the approximation of glass content of portland cement clinker is dependent on the latent heat of crystallization[3] of the liquid present at the clinkering temperature. From the

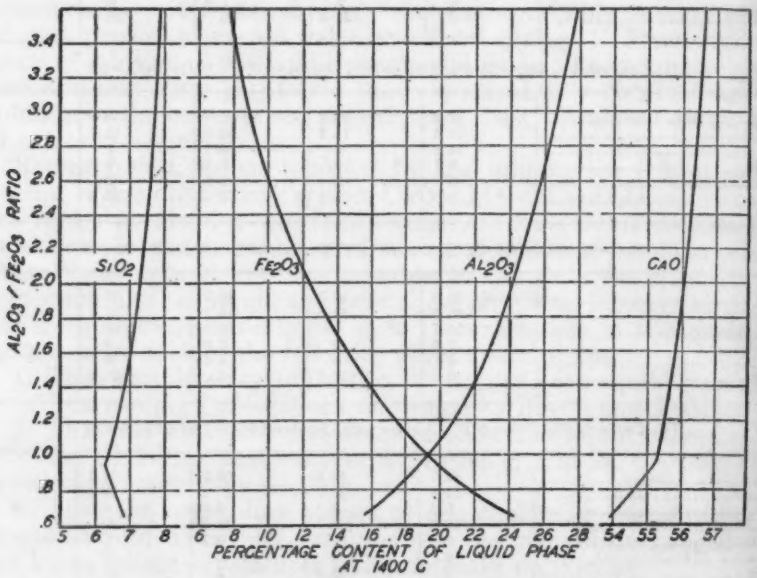

FIG. 1.—*Oxide composition of liquid at 1,400° C.*

(Lea and Parker).

work of Lea and Parker [4] it is possible to calculate the quantity of liquid and the composition of the liquid phase of any portland cement mixture in the system CaO–Al_2O_3–SiO_2–Fe_2O_3 when in equilibrium at any clinkering temperature. For most cements, the liquid composition at 1,400° or 1,450° C lies within the $3CaO.SiO_2$ primary phase volume, or on its boundary surfaces with $2CaO.SiO_2$ or CaO. At these temperatures the composition of the liquid phase of these cements will be largely dependent on the Al_2O_3/Fe_2O_3 ratio, and the

[3] The latent heat of crystallization is the difference in heat content between the crystalline and noncrystalline state of a system at the temperature at which crystallization occurs. In the method described this difference in heat content is determined by the heat of solution method at a temperature below that at which crystallization occurs. For convenience this difference is referred to as latent heat of crystallization.

quantity of liquid will be dependent on the quantities of Al_2O_3 and Fe_2O_3. The composition of the liquid at 1,400° C in the quaternary system CaO–Al_2O_3–SiO_2–Fe_2O_3, for any given Al_2O_3/Fe_2O_3 ratio between 0.64 and 3.6 may be obtained from figure 1.[4]

The clinkering temperature of most portland cements is probably between 1,400° and 1,450° C. Between these temperatures there are only slight changes in the composition of the liquid or in the quantity of liquid for any given cement composition. (See table 1.) Accordingly, a number of mixtures were prepared which were representative of the composition of the liquid phase at 1,400° C for various Al_2O_3/Fe_2O_3 ratios in the system CaO–$2CaO.SiO_2$–$5CaO.3Al_2O_3$–$4CaO.Al_2O_3.Fe_2O_3$. In some instances similar compositions were prepared with the addition of 8.0 percent of MgO. These compositions, listed in table 2, were used for the determination of the latent heat of crystallization.

TABLE 2.—*Latent heat of crystallization of liquid compositions of varying* Al_2O_3/Fe_2O_3 *ratio on the* C^3S-C^2S *surface at 1400°C.*

No.	Oxide composition						Potential compound composition at crystalline equilibrium							Calculated heat of solution of pure compounds	Crystalline material	Quenched compositions	Differences in obtained values	Correction for inversion of C_2S	Latent heat of crystallization
	CaO	MgO	Al_2O_3	Fe_2O_3	SiO_2	Al_2O_3/Fe_2O_3	C_3A	C_3A_3	C_4AF	C_2S	λC_2S	CaO	MgO						
	%	%	%	%	%	%	%	%	%	%	%	%	%	cal/g	cal/g	cal/g	cal/g	cal/g	cal/g
1R	53.9	----	15.3	24.0	6.8	0.64	----	----	73.0	25.8	----	1.3	----	602.1	601.0	637.0	36.0	0	36.0
2	55.2	----	18.7	19.9	6.3	0.94	15.8	----	60.5	23.8	----	----	----	629.2	629.0	672.0	43.0	0	43.0
3	55.7	----	23.5	13.9	6.9	1.7	35.8	2.1	42.3	----	19.8	----	----	654.4	653.5	702.0	48.5	1.2	47.3
4	56.2	----	24.6	12.3	7.0	2.0	38.0	4.5	37.4	----	20.1	----	----	662.0	663.7	714.7	51.0	1.2	49.8
5	56.3	----	26.2	10.0	7.6	2.62	35.6	12.2	30.4	----	21.8	----	----	667.2	672.5	720.3	47.8	1.3	46.5
11	56.5	----	27.2	8.4	7.7	3.24	37.1	15.0	25.5	----	22.2	----	----	673.1	673.5	725.1	51.6	1.3	50.3
6R	49.6	8.0	14.1	22.1	6.3	0.64	----	----	67.2	23.7	----	1.2	8.0	623.9	625.6	660.3	34.7	0	34.7
8	51.2	8.0	21.6	12.8	6.3	1.7	32.9	1.9	38.9	----	18.2	----	8.0	671.3	672.1	719.7	47.6	1.1	46.5
10	51.8	8.0	24.1	9.2	7.0	2.62	32.7	11.2	28.0	----	20.1	----	8.0	683.7	684.9	736.0	51.1	1.2	49.9

The compositions, prepared from intimate mixtures of chemically pure calcium carbonate, alumina, silica, ferric oxide, and magnesia, were heated in an electric furnace at 1,250° C for 1 hour and reground as a further precaution to obtain uniformity. Quenched and crystalline preparations were then made by the special heat treatments described below.

The quenched samples were prepared by quenching the liquid in mercury. A few grams of a given composition were wrapped in platinum foil and suspended in an electrically heated quenching furnace. The furnace was then heated to $1,450 \pm 10°$ C and held at that temperature for 15 minutes to permit complete melting of the charge. The charge was then dropped from the furnace and immersed in mercury to obtain rapid cooling. The preparations were considered to be a satisfactory glass when they were found by microscopic examination to be vitreous, nearly or quite homogeneous, and to contain very little or no birefracting material.

[4] The composition for the Al_2O_3/Fe_2O_3 ratio 0.64 as given in the text of the report by Lea and Parker is incorrect. The composition as used in figure 1 has been confirmed by personal correspondence with Lea.

The crystallized materials were prepared by carefully "annealing"[1] the charge in an electric furnace. The compositions were placed in the furnace and heated to 1,400° C. The temperature of the furnace was then caused to drop slowly over a period of 2 hours to 1,250° C, which is below the temperature of formation of liquid, and the charge was held at that temperature ±10° C for 15 hours.

The compositions which were computed to contain $2CaO.SiO_2$ at crystalline equilibrium all "dusted" after annealing because of the inversion of the beta $2CaO.SiO_2$ to the gamma form. The compositions which were computed not to contain $2CaO.SiO_2$ at crystalline equilibrium did not "dust."

Examinations for free lime were made on each of the quenched and crystallized compositions by White's [13] method and by the ammonium acetate method [14]. All quenched compositions gave negative results by both methods, which indicated the absence of free lime. The crystalline compositions no. 1R and no. 6R (table 2) contained 1.5 and 1.0 percent of free lime, respectively. The other crystalline compositions contained no free lime.

2. MICROSCOPIC AND X-RAY EXAMINATION OF THE GLASS

The quenched preparations were examined microscopically. They appeared vitreous with small amounts of birefracting material, particularly in the samples with low Al_2O_3/Fe_2O_3 ratios, which contained some glassy material showing evidences of strain. The index of refraction of all of the material in any one sample was not uniform but varied through the sample. Regrinding and requenching of the samples did not eliminate this variation of index of refraction. The extent of variation was dependent on the rate of cooling and on the composition. Compositions with high Al_2O_3/Fe_2O_3 ratios showed less variation than those with low Al_2O_3/Fe_2O_3 ratios. And those quenches which were immersed in mercury entirely on falling from the furnace showed less variation than those which floated on the surface of the mercury for a fraction of a second before submersion by pushing them into it by hand. Much smaller charges (0.1 g or less) were then quenched but in no case was it possible to eliminate the variation in index of refraction entirely, even under conditions of most rapid cooling of very small samples, although under these conditions the variation was at a minimum.

The following values were obtained for the index of refraction of a small quenched charge of composition 11 (table 2) with Al_2O_3/Fe_2O_3 ratio=3.24. Some of the material had an index of refraction as low as 1.724 ± 0.003 (red light). But the index of the greater portion of the sample was slightly higher, between 1.724 and 1.734. There was present also some material with an index which was as high as 1.755 ± 0.005. A quenched charge of composition 1R with Al_2O_3/Fe_2O_3 ratio=0.64 contained material with an index of 1.83 ± 0.01, and some material with an index as high as 1.92 ± 0.01.

Powder X-ray diffraction patterns were made of the quenched preparations used for the determination of the heat of solution. Diffraction lines were obtained from all preparations, which in general corresponded almost exactly with the cubic lines of crystalline $3CaO.Al_2O_3$. The strongest diffraction patterns were obtained from

[1] The term "annealing", as used in this report, involves a slow cooling process which might be expected to produce a maximum degree of crystallization.

the samples with the lower Al_2O_3/Fe_2O_3 ratios; samples 1R and 6R had the most intense patterns of the entire series of compositions given in table 2.

Figure 2 (A) is a reproduction of the X-ray pattern of composition 1R compared with that of $3CaO.Al_2O_3$. The lines of the two patterns are almost identical in position and relative intensity. This might be taken as evidence that $3CaO.Al_2O_3$ is present in composition 1R. However, the following facts are not in entire agreement with such an interpretation:

1. Sample 1R represents a composition in the ternary system CaO-$2CaO.SiO_2$-$4CaO.Al_2O_3.Fe_2O_3$. According to all experimental data published to date, $3CaO.Al_2O_3$ does not exist at equilibrium in any portion of that system.

2. The compounds of CaO and Fe_2O_3 usually crystallize much more rapidly than the compounds of CaO and Al_2O_3. Accordingly, the tendency would be for the crystallization of some compound of ferric oxide first of all under the cooling conditions outlined and not for the crystallization of $3CaO.Al_2O_3$.

3. The quenched compositions low in Al_2O_3 show very strong X-ray diffraction patterns, while those high in Al_2O_3, and consequently high in calculated $3CaO.Al_2O_3$, show much weaker patterns. If the diffraction lines were caused by $3CaO.Al_2O_3$, we should expect the compositions high in calculated $3CaO.Al_2O_3$ to show the more intense patterns.

4. The X-ray diffraction pattern of a mixture of $2CaO.SiO_2$ and $2CaO.Fe_2O_3$, when quenched from temperatures at which the mixture is liquid, is that of a cubic crystal with lines practically identical in position with the lines of composition 1*R* (fig. 2 (*B*)).[6] Accordingly, mixtures of CaO, SiO_2, and Fe_2O_3 also show a crystalline structure similar to that of $3CaO.Al_2O_3$, so that apparently we cannot rely on the X-ray alone for identification of that compound.

Considering these facts there is some doubt as to the existence of $3CaO.Al_2O_3$ in the quenched liquids. Further work is in progress to identify the phase in the quenched charges corresponding to the liquid phase of cement clinker, which shows the cubic structure. This material has been commonly called "glass" in the past, and the use of that term is continued here.

In rapidly cooled clinker the glass phase may be in a state comparable with that of the glasses quenched for these determinations of heat of solution and therefore cause diffraction lines in the X-ray pattern in positions corresponding to those of $3CaO.Al_2O_3$. If the lines obtained from the glasses are not due to the presence of $3CaO.Al_2O_3$, as now seems probable but with confirmation still missing, then $3CaO.Al_2O_3$ may have been erroneously identified in some of the cement clinker, as reported in a paper by Brownmiller and Bogue [15].

3. LATENT HEAT OF CRYSTALLIZATION OF THE LIQUID PHASE

The heats of solution of the quenched and crystalline materials were determined by the use of a vacuum-flask calorimeter [16]. The heats of solution were determined at room temperature, $23 \pm 3°$ C. The difference between the heat of solution of the quenched materials and the crystalline materials corrected for the heat evolved by the beta to gamma inversion of dicalcium silicate is recorded as the latent

[6] Diffraction lines of platinum are present in the pattern of the $2CaO.SiO_2$-$2CaO.Fe_2O_3$ mixture because of contamination by the platinum foil in which the charge was enclosed.

heat of crystallization. The results of the determinations of the heats of solution and the latent heats of crystallization are given in table 2. Each value for heat of solution is the mean of duplicate determinations, which agreed to within 3.0 cal/g in every case. With the quenched compositions the duplicate determinations of heat of solution were made on separate quenches of the same composition.

The heat of solution was also determined of the compounds which would be present at crystalline equilibrium for the compositions given in table 2. These compounds were prepared by heating the appropriate mixtures below the temperature of formation of liquid for sufficient time to attain complete combination. By this process the compounds were assumed to have been obtained in a completely crystalline condition. The solvent used for the heat of solution determinations was 420 g of 2 *N* HNO_3 containing 5 ml of 48-percent HF, which was found to be satisfactory for attaining complete solution of 3-g samples of all of the compounds used in this investigation. The same solvent was used for determining the heats of solution of the various compositions given in table 2. The heats of solution of the several compounds are given in table 3. The heats of solution, obtained in this manner, of some of these compounds are different from values given in a previous report [17], which is due to the use of different solvents.

TABLE 3.—*Heat of solution of cement compounds* [1]

Cement compounds	Heat of solution [2]
	cal/g
C_3A	783.3
C_5A_3	726.2
C_4AF	586.8
C_3S	632.0
γC_2S	556.8
βC_2S (with 0.4% of B_2O_3)	563.0
CaO	835.0
MgO	875.4

[1] 3 g dissolved in 420 g of 2 *N* HNO_3 containing 5 ml of 48-percent HF.
[2] The heats of solution were at room temperature, 23 ±3° C. The estimated uncertainty of these values was ±2.0 cal/g.

From the heats of solution of the several compounds it should be possible to calculate the heats of solution of the crystallized compositions listed in table 2. These values have been calculated and are given in the table. The close agreement between the calculated values and the determined values for the heats of solution of these crystalline compositions gives supporting evidence to indicate that nearly complete crystallization has been attained.

The latent heats of crystallization of the compositions containing 8.0 percent of MgO were found to be nearly the same as those of the corresponding compositions containing no MgO, (compare 1R and 6R, 3 and 8, 5 and 10). This indicates that the presence of MgO up to 8.0 percent does not materially change the latent heat of crystallization of these compositions. The 8.0 percent of MgO used in these compositions would correspond to 2.0 percent of MgO in a cement composition containing 25 percent of liquid at the clinkering temperature. By microscopic examination of the quenched samples prepared from the compositions containing 8.0 percent of MgO, it was found in each composition that some MgO was present as periclase. This

FIGURE 2.—*X-ray pattern of crystalline* $3CaO.Al_2O_3$ *and quenched-liquid compositions.*

(*A*). Upper—Pattern of crystalline $3CaO.Al_2O_3$. Lower—Pattern of composition *1R* (table 2) consisting of 53.9% of CaO, 15.3% of Al_2O_3, 6.8% of SiO_2, 24.0% of Fe_2O_3 quenched from 1,450° C.

(*B*). Upper—Pattern of composition *1R* (table 2) consisting of 53.9% of CaO, 15.3% of Al_2O_3, 6.8% of SiO_2, 24.0% of Fe_2O_3 quenched from 1,450° C. Lower—Pattern of composition consisting of 45.9% of CaO, 7.0% of SiO_2, 47.1% of Fe_2O_3 quenched from 1,540° C.

x—Indicate platinum lines.

UNIV. OF MICH.

seems to indicate that liquids of these compositions do not dissolve as much as 8.0 percent of MgO at 1,450° C.

In the study of the system $2CaO.SiO_2$–MgO–$5CaO.3Al_2O_3$ Hansen [18] found that melting occurs at 1,315° C, and that MgO dissolves readily and extensively, up to 7.0 percent, in the liquid formed at 1,315° C or at higher temperatures. When the charges were cooled rapidly the liquid was converted to a glass and the MgO remained in solution in this glass. The solubility of the MgO in the liquid of the system CaO–MgO–$2CaO.SiO_2$–$5CaO.Al_2O_3$ was found by McMurdie and Insley [19] to vary from 5 to 33 percent but, in the region of portland cement to fall between 6 and 18 percent. Brownmiller [20] has found that at 1,400° to 1,450° C about 4 to 6 percent of MgO dissolves in the liquid of the CaO–Al_2O_3–SiO_2–Fe_2O_3 system having

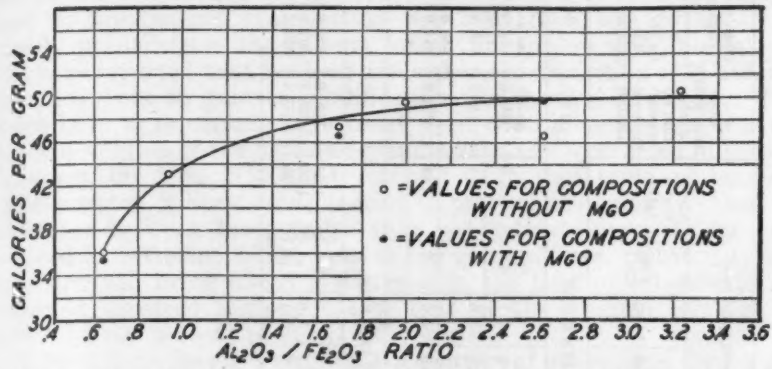

FIGURE 3.—*Latent heat of crystallization of liquid compositions of varying alumina: ferric oxide ratios on the tricalcium silicate-dicalcium silicate surface at 1,400° C.*

Al_2O_3/Fe_2O_3 ratios between 0.68 and 3.0. The solution of MgO in the liquid phase of portland cement clinkers is also indicated by Lea and Parker [4].

The latent heats of crystallization of the compositions given in table 2 are shown in figure 3 plotted against the Al_2O_3/Fe_2O_3 ratios. The latent heats of crystallization of compositions of other Al_2O_3/Fe_2O_3 ratios not given in table 2 may be obtained from figure 3.

4. APPROXIMATION OF THE GLASS CONTENT OF PORTLAND CEMENT CLINKER

Having determined the latent heat of crystallization of the liquid compositions of varying Al_2O_3/Fe_2O_3 ratio, it remained to apply these data in the development of a method for approximating the glass content of portland cement clinker. A group of laboratory compositions of various Al_2O_3/Fe_2O_3 ratios was selected for study. The clinker of these compositions was prepared from commercial raw materials and burned in an experimental rotary kiln. The clinker obtained from this kiln is usually small, about ¼ to ½ inch in diameter, and, in the usual process of operation, is cooled from the clinkering temperature to about 1,000° C in 2 or 3 minutes. These clinkers are referred to in table 4 as "rapidly cooled." In some cases clinkers of corresponding compositions were heated in an auxiliary furnace at 1,100° C for 3 to 4 hours. These clinkers are referred to as "specially treated."

TABLE 4.—*Approximate glass content of laboratory clinkers of varying* Al_2O_3/Fe_2O_3 *ratio*

No.	Method of cooling	Partial oxide composition					Potential crystalline compound composition						Al_2O_3/Fe_2O_3 ratio	Calculated heat of solution at crystalline equilibrium	Obtained heat of solution		Difference		Approximate glass content	Quaternary liquid content at 1,400° C
		CaO	MgO	Al_2O_3	Fe_2O_3	SiO_2	C_3A	C_4AF	C_3S	γC_2S	MgO	Free CaO			Original clinker	Annealed clinker	Obtained	Correction for inversion of C_3S		
K3 CLINKERS																				
		%	%	%	%	%	%	%	%	%	%	%		*cal/g*	*cal/g*	*cal/g*	*cal/g*	*cal/g*	%	%
5F	Rapid	64.7	3.7	7.0	2.0	22.1	15.1	6.1	45.5	29.0	3.7	0.0	3.5	635.5	644.6	632.8	11.8	10.1	20	25.0
5E	Specially treated [1]														647.7	637.8	9.9	8.2	16	25.0
8F	Rapid	66.6	3.0	6.8	2.0	21.0	14.7	6.1	61.0	14.3	3.0	.5	3.4	646.6	659.8	650.3	9.5	8.6	17	24.4
8E	Specially treated														656.0	650.3	5.7	4.8	10	24.4
25F	Rapid	63.3	5.0	5.9	3.2	22.2	10.3	9.7	45.0	30.0	5.0	.0	1.84	632.9	644.0	631.9	12.1	10.3	21	24.4
25E	Specially treated														641.8	631.3	10.5	8.7	18	24.4
K2 CLINKERS																				
233	Rapid	62.6	3.1	7.4	5.1	21.2	11.0	15.5	36.7	33.0	3.1	0.0	1.45	620.0	626.8	614.0	12.8	10.8	23	33.0
10a	do	65.0	3.0	4.6	4.5	22.6	4.6	13.6	53.5	24.5	3.0	.5	1.02	620.7	631.5	621.1	10.4	8.9	20	23.5
225	do	61.1	3.1	7.4	8.4	19.3	5.4	25.6	40.4	24.8	3.1	.5	.88	613.4	624.6	611.3	13.3	11.8	28	40.2

[1] Specially treated clinker was heated at 1,100° C for 3 to 4 hours.

The heats of solution were determined of samples of clinker as prepared by these two methods. A quantity of the clinker prepared by each method was annealed in an electric furnace by heating to 1,400° C and allowing the temperature to decrease slowly over a 2-hour period to 1,250° C, which is below the temperature of formation of liquid. The charge was then held at 1,250° ±10° C for 15 hours, following which the heats of solution were determined. The results are given in table 4, together with the partial oxide composition and the potential compound composition at crystalline equilibrium. Each value for the heat of solution is the mean of duplicate determinations which agreed to within 3.0 cal/g in every case.

The original clinker as prepared in the rotary kiln had not dusted and in this clinker the $2CaO.SiO_2$ was in the beta form. When the clinker was annealed in the electric furance dusting occurred on cooling and by microscopic examination the $2CaO.SiO_2$ was found to be mostly or entirely in the gamma form. Johannson and Thorvaldson [21] have reported that the heat evolved in the transition of $2CaO.SiO_2$ from the beta to gamma modification is 6.0 cal/g at 20° C. This value is in approximate agreement with the difference between the heats of solution of the beta and gamma $2CaO.SiO_2$ reported in table 3. However, the beta $2CaO.SiO_2$ referred to in that table contained a small amount of boric oxide (added to prevent inversion) so that the difference between these values may not indicate precisely the heat evolved on inversion of the beta to the gamma form. Obviously this inversion will bring about a decrease in the heat of solution of the annealed (dusted) samples below that of the original clinkers by 0.06 cal/g per percent of $2CaO.SiO_2$ present.

Table 4 gives the observed heats of solution of the original clinker and of the annealed clinker, the differences between these heats of solution, and these differences corrected for the heat evolved on the inversion of the $2CaO.SiO_2$. This corrected value for the difference between the heat of solution of the original clinker and the annealed clinker is assumed to represent the latent heat of crystallization of the glass present in the original clinker. The approximate glass content of the original clinker was then obtained by dividing this corrected difference in the heats of solution, by the latent heat of crystallization of a liquid composition of the Al_2O_3/Fe_2O_3 ratio of that clinker as obtained from figure 3. For conversion to percentage glass content this quotient was multiplied by 100. Table 4 also contains the quaternary liquid content at 1,400° C, for these clinkers, as calculated from Lea and Parker [4].

It is recognized that certain errors are involved in this method of approximating the glass content of portland cement clinker. The more important sources of error involved in the method are due to: (1) The thermal changes involved in the secondary reactions which occur during the process of crystallization; and (2) the variation in the latent heat of crystallization of an intermediate glass due to the change which may occur in the Al_2O_3/Fe_2O_3 ratio if the several constituents do not crystallize at a uniform rate. The relative magnitudes of these errors may be estimated, but they can not be determined precisely because of lack of definite information as to the extent to which these reactions occur.

The latent heats of crystallization of liquid compositions as given in table 2, and figure 3 represent the thermal changes involved when

these compositions crystallize independently. But with cements having Al_2O_3/Fe_2O_3 ratios above 1.6, the liquid may interact with the solid phases, provided the cooling is sufficiently slow, to produce different percentages of some compounds. The order of difference may be noted by comparing the data in columns 1 and 3 in table 1. When the liquid crystallizes independently (column 3 of table 1) $5CaO.3Al_2O_3$ is formed, but in crystallization to complete equilibrium (column 1 of table 1) the alumina has combined with lime derived from the $3CaO.SiO_2$ to form $3CaO.Al_2O_3$; consequently the $3CaO.Al_2O_3$ content of the product is increased, the $3CaO.SiO_2$ decreased, and the $2CaO.SiO_2$ increased. These secondary reactions involve thermal changes the order of which may be approximated from a consideration of the heat effects of the principal changes involved.

By use of the heats of solution given in table 3, it is possible to calculate the heat of formation of $3CaO.Al_2O_3$ from $5CaO.3Al_2O_3$ and CaO. This reaction involves the absorption of 27.0 cal/g of $3CaO.Al_2O_3$ formed. Johannson and Thorvaldson [21] have reported that the formation of $3CaO.SiO_2$ from beta $2CaO.SiO_2$ and CaO involves an absorption of 2.06 cal/g of $3CaO.SiO_2$ formed. It requires 0.277 g of CaO to combine with $5CaO.3Al_2O_3$ to form 1 g of $3CaO.Al_2O_3$; and it requires 1.13 g of $3CaO.SiO_2$, dissociating to $2CaO.SiO_2$ and CaO to supply 0.277 g of CaO. Hence the dissociation of the $3CaO.SiO_2$ involved in the formation of 1 g of $3CaO.Al_2O_3$ results in the liberation of $2.06 \times 1.13 = 2.3$ cal. The net thermal change caused by the formation of $3CaO.Al_2O_3$ is an absorption of $27.0 - 2.3 = 24.7$ cal/g of $3CaO.Al_2O_3$, or 0.247 cal/g of clinker for each percent of $3CaO.Al_2O_3$ produced from the $5CaO.3Al_2O_3$. Since these reactions involve an absorption of heat and the independent crystallization of the liquid phase involves an evolution of heat, the applications of corrections for these secondary reactions would give values somewhat lower than the uncorrected figures.

The liquid phase at clinkering temperatures forms several crystalline compounds when slowly cooled, but except at the eutectic composition these compounds do not crystallize at a uniform proportionate rate. Thus when partial crystallization occurs the remaining liquid may not retain the composition or Al_2O_3/Fe_2O_3 ratio of the original liquid. Since the latent heat of crystallization varies with the Al_2O_3/Fe_2O_3 ratio, and the former is used (fig. 3) in approximating the glass content, it follows that the approximate glass content may be in error in proportion to the change in the Al_2O_3/Fe_2O_3 ratio of the liquid brought about by the partial crystallization.

Lea and Parker [4] have found that when the Al_2O_3/Fe_2O_3 ratio is above 1.38, $3CaO.Al_2O_3$ crystallizes on cooling, until the Al_2O_3/Fe_2O_3 ratio of the remaining liquid is 1.38, at which point $3CaO.Al_2O_3$ and $4CaO.Al_2O_3.Fe_2O_3$ crystallize together. If the ratio is below 1.38, the $4CaO.Al_2O_3.Fe_2O_3$ crystallizes until the ratio of 1.38 is reached. Thus, the liquid of clinker at 1,400° C, having an Al_2O_3/Fe_2O_3 ratio of 2.6, has (by fig. 3) a latent heat of crystallization of 50.0 cal/g. If partial crystallization of the liquid occurs so that the ratio in the remaining liquid is reduced to 1.5, the latent heat of crystallization of the liquid is reduced to 47.0 cal/g. If the observed difference in heats of solution of the original and annealed clinker is 5.2 cal/g, the approximate glass content would be $(5.2 \times 100)/50.0 = 10.4$ percent,

whereas the correct glass content should be $(5.2\times100)/47.0=11.0$ percent.

Experimental errors which may occur include those which would result from incomplete inversion of the $2CaO.SiO_2$ to the gamma modification during annealing, and errors in the determination of the heats of solution. These errors can be reduced to low magnitude by careful experimental manipulations. Other sources of error may occur from: absence of information on the exact amount of beta $2CaO.SiO_2$ which may be in the original clinker; failure to attain complete equilibrium at clinkering temperatures in the kiln; thermal changes resulting from the formation of solid solutions; and thermal changes resulting from alkalies, titania, manganese, and other minor constituents of commercial clinker.

Consideration has been given to the possibility of approximating the glass content of a portland cement clinker from the difference between the calculated heat of solution at crystalline equilibrium (calculated from the additive values of the heats of solution of the several crystalline compounds), and the obtained heat of solution of the clinker. Thus, the necessity of the annealing process and the subsequent determination of the heat of solution of the annealed sample would be eliminated. The calculated heats of solution at crystalline equilibrium are given in table 4, for the clinkers used in this investigation. In some instances these calculated values are in good agreement with the obtained heats of solution of the corresponding annealed samples, but in some instances there are rather large discrepancies. There are several factors involved which may account for these discrepancies among which may be mentioned: (1) Portland cement clinker contains varying quantities of minor constituents, alkalies, manganese, titania, etc., which can not, at present, be accounted for in these calculations of the heats of solution at crystalline equilibrium; (2) small errors in chemical analysis result in relatively large variations in calculated compounds; and (3) lack of homogeneity of the clinker. From these considerations it seems probable that more accurate results will follow the use of the value of the heat of solution obtained on the annealed clinker than from the use of the calculated value.

III. SUMMARY AND CONCLUSIONS

This report describes a heat of solution method for approximating the glass content of portland cement clinker. The method involves a determination of the heat of solution of the original clinker and of the same clinker which has subsequently been annealed under conditions designed to produce complete crystallization. The difference between these heats of solution is dependent upon the latent heat of crystallization of the liquid phase which would be present at clinkering temperatures. The latent heat of crystallization has been determined for several liquid phase compositions of varying Al_2O_3/Fe_2O_3 ratios, and from a curve drawn through these points (fig. 3) the latent heat of crystallization of liquid phase compositions of other Al_2O_3/Fe_2O_3 ratios may be obtained.

The method should be applied to freshly burned, unhydrated portland cement clinker. It cannot be applied to ground cements containing gypsum or to clinker which has been partially hydrated or carbonated.

The method involves certain errors for which exact correction factors cannot at present be applied. From a consideration of the nature and magnitude of these errors it seems probable that for the compositions studied the approximate glass contents, as obtained by this method, were correct to within ± 5 percent of the total sample.

The results obtained by this method, when applied to a number of laboratory clinkers prepared in an experimental rotary kiln from commercial raw materials, indicate that rapidly cooled portland cement clinker may contain a considerable quantity of glass.

From a comparison of the glass content of the rapidly cooled clinker and of the corresponding specially treated clinker (heated 3 to 4 hours at 1,100° C) it was observed that the glass content of the specially treated clinker was only slightly lower than that of the rapidly cooled clinker. This seems to indicate that heating for 3 to 4 hours at temperatures appreciably below the temperature of formation of liquid does not promote rapid crystallization.

The quenched liquid compositions, which are referred to as glass, were examined microscopically and by X-rays. Under practical cooling conditions it was impossible to solidify the liquids so that they showed no X-ray diffraction pattern. The diffraction pattern obtained was similar to the pattern obtained from $3CaO.Al_2O_3$. A similar pattern has also been obtained from quenched compositions of CaO-Fe_2O_3-SiO_2 which contained no Al_2O_3. The exact nature of the structure which gives this pattern is still in doubt.

The data contained in this report were obtained with experimental clinker and it was not determined how representative they are with respect to commercial clinker.

IV. REFERENCES

[1] R. H. Bogue, Ind. Eng. Chem., Anal. Ed. **1,** 192 (1929).
[2] L. A. Dahl, Rock Products, **32** no. 23, 50 (1929).
[3] G. A. Rankin and F. E. Wright, Am. J. Sci. **39,** 1 (1915)
[4] F. M. Lea and T. W. Parker, Dept. Sci. Ind. Res., Bldg. Research, Tech. Pap. 16 (1935.)
[5] L. Forsen, Zement **24,** no. 2, 17 (1935).
[6] E. Spohn, Tonind. Ztg. **59,** 849 (1935)
[7] S. Solacolu, Rock Products **36,** no. 4, 90 (1933).
[8] H. Kuhl, Tonind. Ztg. **59,** 1221 (1935).
[9] Insley, J. Research NBS **17,** 353 (1936) RP917.
[10] L. Miller, Proc. Am. Soc. Testing Materials **34,** II 300 (1934).
[11] J. A. Swenson and E. P. Flint, J. Research NBS **17,** 261 (1936) RP910.
[12] F. M. Lea and T. W. Parker, Phil. Trans. Roy. Soc. [A] **234,** (731) 1 (1934).
[13] A. H. White, Ind. Eng. Chem. **1,** 5 (1909).
[14] Wm. Lerch and R. H. Bogue, Ind. Eng. Chem. Anal. Ed. **2,** 296 (1930).
[15] L. T. Brownmiller and R. H. Bogue, BS J. Research **5,** 813 (1930) RP233.
[16] Wm. Lerch, Eng. News Record **113,** 523 (1934).
[17] Wm. Lerch and R. H. Bogue, BS J. Research **12,** 645 (1934) RP684.
[18] W. C. Hansen, J. Am. Chem. Soc. **50,** 3081 (1928).
[19] H. F. McMurdie and H. Insley, J. Research NBS **16,** 467 (1936) RP884.
[20] L. T. Brownmiller, Unpublished data.
[21] O. K. Johannson and J. Thorvaldson, J. Am. Chem. Soc. **56,** 11, 2327 (1934).

WASHINGTON, August 13, 1936.

U. S. Department of Commerce National Bureau of Standards

RESEARCH PAPER RP998

Part of Journal of Research of the National Bureau of Standards, Volume 18, May 1937

STATE OF THE SULFUR IN OXIDIZED WOOL

By Milton Harris and Arthur L. Smith [1]

ABSTRACT

During treatment with oxidizing agents, the disulfide sulfur in wool appears to be changed to higher states of oxidation. The existence of oxidation derivatives of the disulfide compounds is indicated by the alkali-solubility determination, the lead acetate test, by reduction with hydrochloric acid-potassium iodide solutions, and by cystine analyses.

The intermediate oxidation derivatives of cystine are unstable under the conditions necessary for protein hydrolysis, and at least one of them, cystine disulfoxide, is partially converted to cystine. The results indicate that the values obtained for the cystine content of oxidized wool may be expected to be higher than the actual cystine content since they represent the amount of cystine formed from the partially oxidized cystine compounds as well as from unoxidized cystine groups.

CONTENTS

	Page
I. Introduction	623
II. State of the sulfur in oxidized wool	624
III. Determination of cystine in oxidized wool	625
IV. References	628

I. INTRODUCTION

Recent investigations relating to the oxidation of wool [1, 2, 3, 4] [2] indicate that the stability of the fiber is closely related to the state of the sulfur in the wool protein. The bulk of the sulfur in untreated wool is present as cystine sulfur [5, 6] and it appears that the maximum stability of the fiber is obtained when the sulfur is in this form. Changes in the state of this sulfur, such as are produced by oxidizing and reducing agents or by light, may result in the direct degradation of the fiber, or in incipient damage, which may be greatly aggravated in the subsequent processing of the fiber. It is apparent, therefore, that the proportion of the total sulfur in wool which exists in the disulfide form is very significant.

The present report is concerned with new methods which have been used in studying the state of the sulfur in oxidized wool and with the limitations of the methods for the determination of cystine when applied to wool in which the sulfur has been changed to a higher state of oxidation.

[1] Research Associates at the National Bureau of Standards representing the American Association of Textile Chemists and Colorists. This work is aided by grants from the Textile Foundation, Inc., the Chemical Foundation, Inc., and the Eavenson and Levering Co.

[2] The numbers in brackets throughout the text correspond to the literature references at the end of this paper.

II. STATE OF THE SULFUR IN OXIDIZED WOOL

When wool is treated with oxidizing agents, one of the main points of attack appears to be the disulfide linkage. Intermediate oxidation products, such as R–SO–S–R, R–SO_2–S–R, etc., may be formed.[3] Although methods for the identification of the individual intermediate oxidation derivatives of sulfur are not known, evidence given by four different methods indicates that the disulfide sulfur in wool is changed to higher states of oxidation during treatment with oxidizing agents. These tests are the alkali-solubility determination, the lead acetate test, the reduction method using mixtures of hydrochloric acid and potassium iodide, and the determination of the cystine content.

The alkali-solubility test [7] has been shown to be a measure of the extent to which wool is oxidized. Presumably as the number of oxygen atoms on the sulfur increases, the bond between the disulfide sulfur atoms becomes increasingly labile and more wool goes into solution. Analogous reactions are obtained with cystine and its intermediate oxidation derivatives. Cystine disulfoxide (RSO_2–SR or RSO–SOR) has been shown by Lavine [8] to be much less stable in alkaline solution than cystine, whereas Toennies [9] has recently found cystine disulfone (RSO_2–SO_2R) to be even less stable than the disulfoxide.

The lead acetate test [2], which distinguishes between unbleached wool and wool bleached with hydrogen peroxide, also appears to depend on the state of oxidation of the sulfur. When untreated wool is subjected to this test, hydrogen sulfide is liberated and reacts with lead acetate to form lead sulfide according to the following scheme:

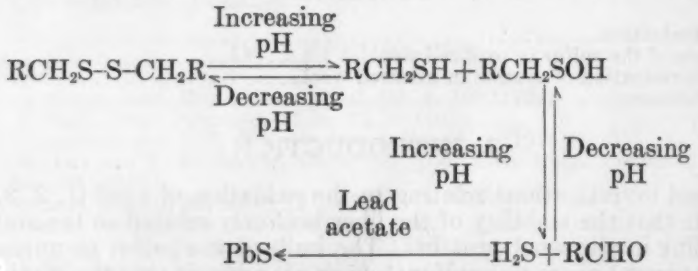

Cystine appears to react similarly but requires a higher pH for formation of the lead sulfide. Oxidized wool and cystine disulfoxide, on the other hand, do not form lead sulfide under the conditions in which it is formed in untreated wool and in cystine.

The following mechanism is suggested for those cases in which the disulfide sulfur has been partially oxidized. Since in each disulfide group one sulfur atom is positively and one negatively charged, the negative oxygen atoms or hydroxyl groups react with the positive sulfur, whereas the positive groups such as hydrogen react with the negative sulfur. The hydrolytic cleavage of a partially oxidized disulfide compound may then be represented as follows:

$$RSO\text{–}SR \xrightarrow{H_2O} RSO.OH + RSH$$

[3] One sulfur atom in a disulfide compound is positively and the other negatively charged. It would be expected that only the positive sulfur would take up oxygen until it formed a sulfonic acid, the bond between the sulfur atoms then being broken. The remaining sulfur could then be oxidized to a sulfonic acid. This mechanism appears to be more tenable than one in which there is simultaneous oxidation of both sulfur atoms, with the formation of such intermediates as R–SO–SO–R, R–SO_2–SO–R, etc.

The products of this reaction appear to be stable under the conditions of these experiments and further decomposition to form hydrogen sulfide does not occur.

The third method is based on the method used by Lavine [8] in his studies on cystine disulfoxide. Samples of oxidized wool were treated for 1 hour with mixtures of equal volumes of solutions of 4 *M* hydrochloric acid and 4 *M* potassium iodide, the ratio of wool to solution being 1 to 100. The reductions were conducted in the dark at 22 to 23° C. The oxidizing value of some of the intermediate oxidation products was determined by direct titration of the iodine liberated with sodium thiosulfate. The value obtained has no quantitative significance with respect to the extent of oxidation of the wool since, as has been shown by Lavine, only sulfur which has been oxidized below the sufonic acid state is reduced.

The cystine content of wool has been shown [1] to decrease with increased oxidation. That the values for the cystine content of oxidized wool have no quantitative significance will be shown later.

Of the four methods described, the alkali-solubility test is the most satisfactory. A comparison of the results obtained by the different methods is given in table 1.

TABLE 1.—*Effect of treatment for different lengths of time with hydrogen peroxide on the sulfur in wool*

[The alkali-solubility and cystine contents were determined on wool which had been treated at 50° C with 0.6 percent (2 vol.) hydrogen peroxide, while the remaining 2 tests were made on wool similarly treated, except that 3 percent (10 vol.) peroxide was used.]

Duration of treatment	Alkali-solubility	Cystine content	Lead-acetate test [1]	Hydrochloric-acid-potassium iodide test [2]
Hours	*Percent*	*Percent*		*Milliequivalent of iodine per gram of wool*
0	9.7	11.6	Positive	0
1	10.3	10.7	Negative	0.015
3	12.4	10.1	do	.024
5	15.2	10.0	do	
7	18.2	9.9	do	.038
9	20.1	9.6	do	.051
16	40.0	8.6	do	.072

[1] These results are obtained visually. The lead sufide formed in the reaction darkens the wool.
[2] Similar experiments with oxidized silk showed no significant changes in iodine liberated with increased oxidation.

III. DETERMINATION OF CYSTINE IN OXIDIZED WOOL

The available methods for the estimation of disulfide compounds have been classified and evaluated elsewhere [10] and need not be further discussed here. In the work reported in this paper, cystine was determined by the methods of Sullivan [11], Okuda [12], and Folin-Morenzi [13]. The latter two were used as described in the literature, while the Sullivan procedure was modified only with respect to the measurement of the color developed in the determination. A few interesting points regarding this procedure are here noted.

The amount of the colored substance developed by the reaction of cystine with sodium β-naphthoquinone-4-sulfonate was measured photometrically at the wave length 501 millimicrons. A calibration curve, shown in figure 1, was obtained by determining the transmit-

tancy of the red solutions formed when known amounts of cystine were treated according to the Sullivan procedure.

When this method was first used, erratic results were obtained, especially during the summer when the temperature rose above 30° C. It was found that the reaction is markedly affected by temperature, as shown in figure 2. The initial rate of development of color increases with increasing temperature, but at equilibrium, the amount of colored substance developed decreases with increasing temperature. Analyses of solutions containing 100 mg of cystine per liter were made, the color being allowed to develop at different temperatures for 30

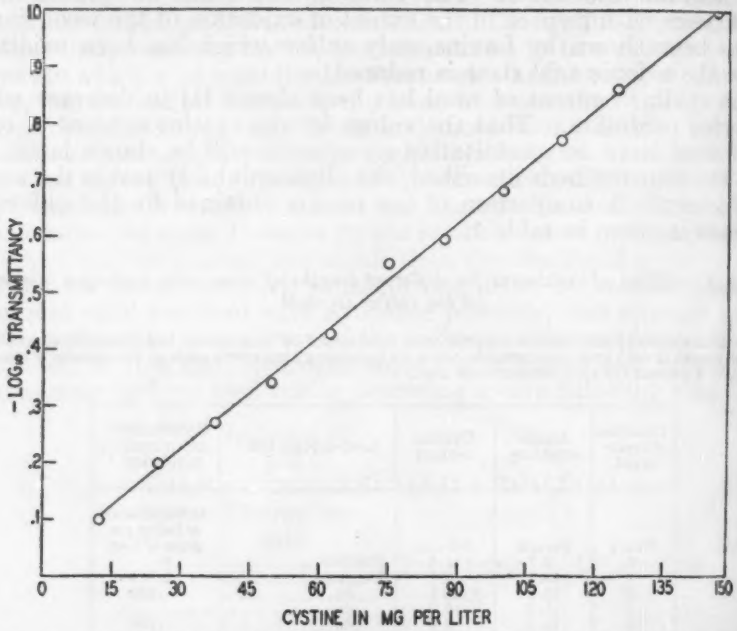

FIGURE 1.—*Transmittancy at wave length 501 millimicrons of the red solutions formed when known amounts of cystine were treated according to the Sullivan procedure.*

minutes. The results are shown in figure 3. There is practically no change between 24 and 30° C but above 30° C the apparent cystine content decreases rapidly with increasing temperature. The cystine determinations reported in this paper were made at 23 to 24° C.

Analyses of six samples of the untreated wool used in this work showed an average cystine content of 11.5 percent, with an average deviation from the mean of 0.2 percent.

The lability of the intermediate oxidation derivatives of cystine, shown by Toennies [9] and Lavine [8], suggested that similar derivatives formed in wool during oxidation might partially revert to cystine during the hydrolytic process, which is used in the analyses of proteins for cystine. In order to test this possibility, 10-mg samples of cystine disulfoxide[4] were treated with 5-ml portions of 6 *N* hydrochloric acid

[4] The cystine disulfoxide used in this work was furnished by Drs. Toennies and Lavine of the Lankenau Hospital Research Institute, Philadelphia, Pa.

in an oil bath at 120 to 125° C for different lengths of time, and the amount of cystine in the resulting solutions was determined by the Sullivan and the Okuda methods. A similar set of experiments, using 6 *N* sulfuric acid, was made and the cystine determined by the Folin-Morenzi method. The results recorded in table 2 show that 1 mole of cystine is formed from 2 moles of cystine disulfoxide.

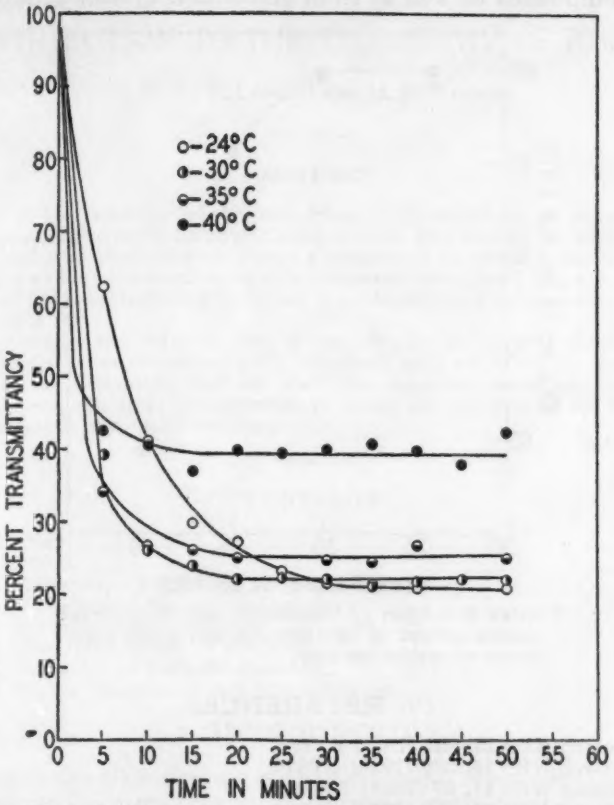

FIGURE 2.—*Effect of different temperatures on the rate of color development in the Sullivan method for the determination of cystine.*

TABLE 2.—*Decomposition of cystine disulfoxide during the hydrolysis used in cystine analyses*

The values represent the mole percentage of the cystine disulfoxide which has been converted to cystine.

Duration of hydrolysis	Cystine found		
	Sullivan	Okuda	Folin-Morenzi
Hours	*Percent*	*Percent*	*Percent*
1	46.5	53.8	45.7
3	48.3	54.6	50.0
5	46.1	52.0	47.5
7	48.6	54.3	47.0
10	47.5	45.8	45.8
20	52.0	56.4	46.7
50	45.3	52.4	49.1
75	52.3	51.4	48.2

The results of the above experiments indicate that under the conditions necessary for the hydrolysis of proteins, at least a portion of the oxidized disulfide groups revert to disulfide groups. Therefore, the values obtained for the cystine content of oxidized wool may be expected to be higher than the actual cystine content since they represent the amount of cystine formed from the partially oxidized cystine compounds as well as from unoxidized cystine groups.

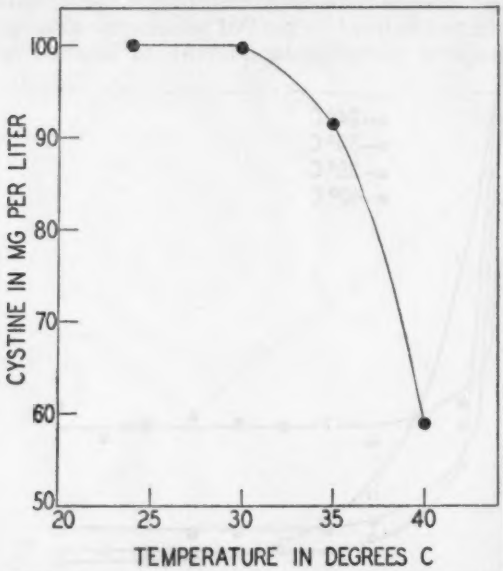

FIGURE 3.—*Effect of temperature on the apparent cystine content of solutions containing 100 milligrams of cystine per liter.*

IV. REFERENCES

[1] J. Research NBS **16,** 301 (1936) RP875.
[2] J. Research NBS **16,** 309 (1936) RP876.
[3] J. Research NBS **17,** 97 (1936) RP904.
[4] J. Research NBS **17,** 559 (1936) RP928.
[5] J. Research NBS **16,** 475 (1936) RP885.
[6] J. Research NBS **15,** 63 (1935) RP810.
[7] J. Research NBS **17,** 577 (1936) RP928.
[8] J. Biol. Chem. **113,** 583 (1936).
[9] Personal communication.
[10] J. Biol. Chem. **109,** 665 (1935).
[11] Public Health Reports **86,** (1930).
[12] J. Biochem. Japan **5,** 217 (1925).
[13] J. Biol. Chem. **83,** 109 (1929).

WASHINGTON, March 19, 1937.

U. S. Department of Commerce National Bureau of Standards

RESEARCH PAPER RP999

Part of Journal of Research of the National Bureau of Standards, Volume 18, May 1937

A CONTRIBUTION TO THE CHEMISTRY OF RHENIUM

By G. E. F. Lundell and H. B. Knowles

ABSTRACT

A study of the behavior of rhenium when dilute solutions of potassium perrhenate are acidified with sulphuric acid, cooled, and passed through the Jones reductor, indicates that rhenium forms a compound in which it has a valency of minus one, and that the rhenium in this compound is oxidized to a valency of plus one if the diluted sulphuric acid solution is protected from oxygen and warmed to approximately 50° C.

In the course of the investigation, it was also found (1) that rhenium can be electrodeposited from diluted (5+95) sulphuric acid solution; (2) that deposits are slightly contaminated; and (3) that the deposited metal can be oxidized directly to perrhenic acid by exposure to moist air, oxygen, or by making the deposit the anode in a water solution.

CONTENTS

	Page
I. Introduction	629
II. Experimental	630
1. Reagents, reductor, and reductor technique	630
2. Oxidation of the reduced compound	631
3. Potentiometric titrations	634
4. Electrodeposition of rhenium	635
5. Oxidation of metallic rhenium	636
6. Standardization of rhenium solutions	637

I. INTRODUCTION

In the periodic classification of the elements, rhenium is grouped with manganese and eka-manganese[1] in arrangements based on the atomic numbers of the elements, the number of shells in the atoms, and the type and number of electrons in the incompleted shells. In the ordinary periodic arrangements these elements are arranged in subgroup A of the seventh group, while fluorine, chlorine, bromine, iodine, and eka-iodine are placed in subgroup B.

The valencies of manganese range from two to seven in its ordinary compounds. The valencies of the members of the halogen subgroup range from minus one, which is common to all, to plus seven, which is exhibited by chlorine and iodine. If rhenium follows manganese in its valencies, one might expect the lowest valency to be two and the highest valency to be seven. If rhenium follows the halogen subgroup, the lowest valency should be minus one and the highest plus seven.

[1] Element of atomic number 43, named masurium by W. Noddack, I. Tacke, and O. Berg, (Die Naturwissenchaften 13, 567, 1925), who claim to have discovered evidence of its existence in certain platinum and columbium ores.

There is no question that rhenium exhibits a valency of seven in its oxidized compounds. On the other hand, its lower valencies have not been fixed, and, so far as we have been able to ascertain, no evidence as to a valency lower than plus one has been noted in any of its compounds.

The chief purpose of this article is to point out that rhenium apparently follows the halogens in their lower as well as in their higher valencies, and that a compound having a valency of minus one is formed when a *cold, dilute* solution of potassium perrhenate in diluted sulphuric acid (5+95)[2] is passed through a column of amalgamated zinc (Jones reductor).

Possibly, the reaction takes place as expressed by the equation,

$$ReO^-_4+8H^++8e=Re^-+4H_2O,$$

which is strictly analogous to the reactions,

$$IO^-_4+8H^++8e=I^-+4H_2O,$$
$$BrO^-_3+6H^++6e=Br^-+3H_2O,$$
$$ClO^-_3+6H^++6e=Cl^-+3H_2O,$$

which take place when solutions of periodates, iodates, bromates, chlorates (and even perchlorates to a slight extent) are similarly treated.

If the reaction proceeds as indicated, the product should, of course, be called hydrorhenic acid, corresponding to the halogen acids. As will be seen, we have not been able to isolate the compound, but we believe that the evidence shows quite conclusively that rhenium forms a compound in which it has a valency of minus one.

The sections that follow deal with the reactions that indicate the existence of this compound. In addition, there are included certain observations on the properties of rhenium and its compounds that were made in the course of the work.

II. EXPERIMENTAL

1. REAGENTS, REDUCTOR, AND TECHNIQUE

The source of the rhenium used in this investigation was a potassium perrhenate which had been examined by both chemical and spectrochemical methods. In the latter, only a trace of magnesium and faint traces of silicon, calcium, and iron were indicated as impurities, and their total amount was estimated to be of no significance in the present investigation. In the chemical tests, the percentage of Re_2O_7 in the salt was determined electrolytically by deposition from diluted sulphuric acid solution (5+95), followed by corrections for undeposited rhenium and for impurities in the deposit as described in section 6. The percentage of K_2O was determined by dissolving the salt in diluted sulphuric acid, filtering in turn after precipitations with hydrogen sulphide and ammonium hydroxide, evaporating, treating with sulphuric and hydrofluoric acids, igniting, and finally treating with water and igniting until constant weight was obtained. The percentage of Re_2O_7, 83.66, and of K_2O, 16.43, found, agreed with the calculated values 83.73 and 16.27 within the experimental errors of the

[2] Prepared by diluting 5 volumes of sulphuric acid (sp gr 1.84) with 95 volumes of water. When no dilution is specified the use of the concentrated reagent is intended.

methods of determination. No silicon, calcium, magnesium, or iron was found in 0.07-g samples.

The solution of the perrhenate used in the tests to be described was prepared by dissolving 16.6774 g of the salt and diluting to exactly 4 liters with diluted sulphuric acid (2.5+97.5). Its calculated rhenium content was 0.002684 g per ml as compared with 0.002681 found by actual test.

Reduction with zinc and sulphuric acid was done in every case in a Jones reductor 18 inches in length, 1 inch in diameter, and filled with 20-mesh granulated zinc which had been amalgamated with approximately 5 percent of mercury.

The diluted sulphuric acid (5+95), the water, and the sulphuric acid solution of the perrhenate used in the reduction were all thoroughly boiled to expel oxygen, allowed to cool under oxygen-free carbon dioxide, and chilled to approximately 5° C before passing them through the reductor.

Immediately before use, the reductor was washed with warm diluted sulphuric acid followed by cold water, and then freed from entrapped air by placing water in the receiver, tightly stoppering the top of the completely filled reductor, and then alternately applying and releasing suction until no more gas was set free. The receiver was then emptied and again attached. In most reductions all air was first washed out of the receiver, and the solution afterward caught in it was protected from air by the use of carbon dioxide, drawn from a cylinder of the liquefied gas and freed from any small oxygen content by passage over rolls of copper gauze heated at 500° C.

The procedure generally followed in reductions was first to draw through 50 ml of the cold diluted acid, next 500 ml of the cold diluted acid solution containing from 0.0134 to 0.0268 g of the perrhenate, then approximately 50 ml of the cold acid to wash out the rhenium, and finally approximately 100 ml of the cold water to wash out the acid. In some experiments the reduced rhenium solution was caught in the carbon-dioxide filled receiver, in others it was caught under an excess of an oxidant protected by carbon dioxide.

2. OXIDATION OF THE REDUCED COMPOUND

The reduced rhenium compound is a very powerful reducing agent, reacting with salts of copper and silver to yield the elements, with compounds such as titanic sulphate to form compounds of lower valency, and even with sulphuric acid if the concentration of the compound is appreciable or the solution is warm. The reaction of the reduced compound with sulphuric acid determines the conditions that must obtain in successful reductions in the Jones reductor, and necessitates the use of solutions that are rather dilute ($<$0.03 mg of Re per milliliter) and ice-cold. Under such conditions the reduced compound showed no detectable change in valency in 1½ hours when protected from the air by bubbling a brisk stream of carbon dioxide through the solution. The reduced compound can be quantitatively oxidized to the heptavalent state by passing a stream of air or oxygen through the solution.

In table 1 are shown the results obtained in experiments in which the reduced solution was caught (1) in a CO_2-filled receiver; (2) in an excess of acidified ferric sulphate solution; (3) in an excess of a solu-

tion of molybdic acid; and (4) in an excess of a standard solution of potassium permanganate. In (1), (2), and (3) the final solution was titrated immediately with a standard solution of potassium permanganate. In (4) the excess of permanganate was determined by adding 1 to 3 ml excess of an equivalent solution of ferrous sulphate and then titrating with permanganate. In all titrations care was taken to maintain an oxygen-free atmosphere.

The rhenium-oxygen ratios are based on the amounts of rhenium that were taken and the amounts of permanganate that were consumed. The average calculated valency, −1.04, is considered to be in substantial agreement with −1 in view of the difficulties of the determination.

TABLE 1.—*Valency of rhenium after reduction in a Jones reductor*

Re taken	0.1 *N* $KMnO_4$ required	Atomic ratio Re/O	Calculated valence change of Re	Calculated valence of Re
	1. SOLUTION CAUGHT UNDER CO_2			
g	*ml*			
0.002683	1.18	1:4.10	8.2	−1.2
.002683	1.21	1:4.20	8.4	−1.4
.005366	2.27	1:3.94	7.9	−0.9
.005366	2.27	1:3.94	7.9	−0.9
.008049	3.48	1:4.03	8.1	−1.1
.010732	4.69	1:4.07	8.1	−1.1
.013415	5.86	1:4.07	8.1	−1.1
.02683	11.45	1:3.98	8.0	−1.0
	2. SOLUTION CAUGHT UNDER EXCESS OF $Fe_2(SO_4)_3$			
0.002683	1.18	1:4.10	8.2	−1.2
.005366	2.26	1:3.92	7.8	−0.8
.008049	3.52	1:4.07	8.1	−1.1
.010732	4.68	1:4.06	8.1	−1.1
.0128	5.40	1:3.93	7.9	−0.9
.0129	5.55	1:4.01	8.0	−1.0
.013415	5.94	1:4.12	8.2	−1.2
.013415	5.75	1:3.99	8.0	−1.0
.013415	5.95	1:4.13	8.3	−1.3
	3. SOLUTION CAUGHT UNDER EXCESS OF H_2MoO_4			
0.013415	5.72	1:3.97	7.9	−0.9
	4. SOLUTION CAUGHT UNDER EXCESS OF $KMnO_4$			
0.0130	5.52	1:3.96	7.9	−0.9
.013415	5.70	1:3.96	7.9	−0.9
.013415	5.72	1:3.97	7.9	−0.9
.02683	11.51	1:4.00	8.0	−1.0
.040245 [a]	16.90	1:3.91	7.8	−0.8
.067075 [a]	27.66	1:3.84	7.7	−0.7
Average calculated valency				−1.04

[a] Not included in average because numerous experiments demonstrated that these concentrations are too great for complete reduction.

It might be argued that some of the permanganate was used up in reactions other than in the oxidation of rhenium. This seems unlikely, because results agreed within experimental error regardless of whether the reduced compound was titrated directly with dichromate, ceric sulphate, or permanganate, caught in an excess of permanganate, or titrated with permanganate after it had been caught under solu-

tions of ammonium vanadate, ammonium molybdate, potassium dichromate, ceric sulphate, titanic sulphate, or even potassium perrhenate—all of which are reduced to lower valencies by the rhenium compound. It seems hardly possible that substances of such differing oxidation-reduction potentials would enter into reactions (other than with rhenium) that all caused essentially the same consumption of oxidant.

It should be noted that a dilute solution of rhenium remains *colorless* during its passage through the Jones reductor, and that the cold solution of the reduced compound takes on a *yellow to amber yellow color* in the early stages of a titration in which permanganate is added very slowly. It is significant that the same *yellow color* slowly develops if the reduced solution is protected from oxygen and is allowed to become warm (approximately 50° C) as a current of oxygen-free carbon dioxide is passed through it. In either case, the solution again becomes colorless long before oxidation of the rhenium is complete.

As shown in table 2, the rhenium-oxygen ratio is 1:3, if the dilute sulphuric acid solution of the reduced rhenium compound is protected from oxygen, warmed moderately, and allowed to stand for 30 to 60 minutes. The rhenium-oxygen ratio indicates that the reduced compound has been oxidized to a valency of plus one in a solution containing no free oxygen and no compounds other than dilute sulphuric acid, zinc sulphate, and (at first) molecular hydrogen. It was suspected that under the changed conditions (digestion in warm solution) the reduced compound might have reduced sulphuric acid, possibly to form hyporhenous acid

$$HRe+H_2SO_4=HReO+H_2O+SO_2,$$

corresponding to the "hypo" acids of the halogens. No attempt was made to identify sulphur dioxide, but it was found that a volatile compound of sulphur is formed, because definite tests for the SO_4 ion were obtained when the stream of carbon dioxide was passed through an alkaline solution of hydrogen peroxide, which was afterwards acidified, boiled, and treated with barium chloride. The reduction of sulphuric acid is not surprising, since this also takes place with hydriodic acid but at somewhat higher concentrations and temperature.

TABLE 2.—*Valency of rhenium after reduction in a Jones reductor, followed by digestion in warm dilute sulphuric acid solution protected from oxygen*

Re taken	0.1 *N* $KMnO_4$ required	Atomic ratio Re/O	Calculated valence change of Re	Calculated valence of Re	Period of digestion	Final temperature
g	ml				min	°C
0.013415	4.31	1:2.99	5.98	+1.0	30	45
.013415	4.32	1:3.00	6.00	1.0	45	45
.013415	4.29	1:2.98	5.96	1.0	45	45
.013415	4.30	1:2.99	5.98	1.0	45	45
.02683	8.60	1:2.99	5.98	1.0	45	45
.013415 [a]	4.30	1:2.99	5.98	1.0	60	45
.013415 [a]	4.27	1:2.97	5.94	1.1	60	45
.013415 [b]	4.27	1:2.97	5.94	1.1	60	45
.013415 [b]	4.30	1:2.99	5.98	1.0	60	45
Average calculated valency				1.02		

[a] Titrated with $KReO_4$ at the start, and finished with $KMnO_4$. [b] H_2 used instead of CO_2.

The compound corresponding to the 1:3 ratio is not stable enough to withstand prolonged digestion in the warm sulphuric acid solution. It was noted that no detectable decomposition occurred when the compound was heated at 72° C and titrated in the course of 30 minutes. In other tests it was noted that there was a slight falling off in permanganate consumption in warm solutions that had been allowed to stand for some time, for example, 4.14 and 4.04 ml of 0.1 *N* at the end of 2 and 3 hours, as against 4.34 ml and 4.31 ml at the

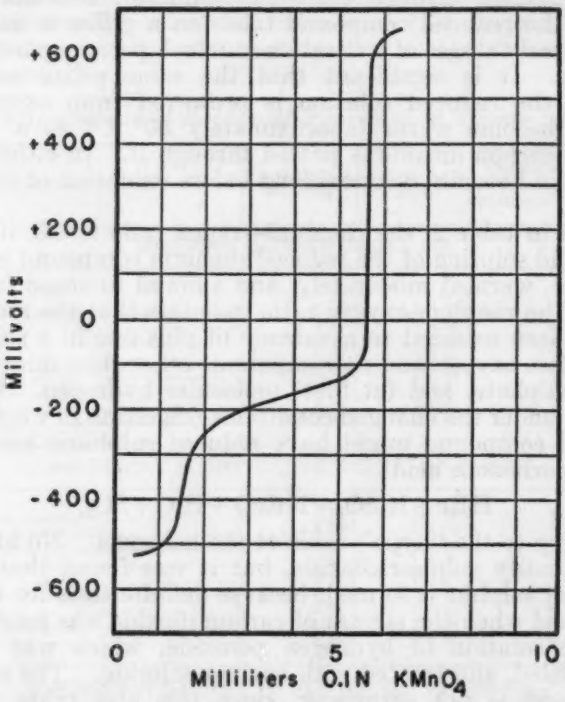

FIGURE 1.—*Typical curve obtained in potentiometric titrations of the reduced rhenium compound.*

end of 30 minutes and 1 hour, respectively. Incidentally, no evidence of the formation of a volatile compound of rhenium was discovered in this or any other stage of the work.

3. POTENTIOMETRIC TITRATION

In a number of experiments, attempts were made to titrate the solution of the reduced rhenium compound potentiometrically with 0.1 *N* $KMnO_4$ in the hope that potential changes might yield additional information on the course of the oxidation. In this work a 0.1 *N* calomel half-cell, a platinum indicator electrode, a Leeds & Northrup student type potentiometer, and the usual accessories were used. In a few tests a gold electrode was substituted for the platinum electrode, with no improvement in the results. When titrated immediately, solutions containing 0.0134 g of the reduced rhenium compound showed a marked increase in potential after the addition of from 1.40 to 1.50 ml of 0.1 *N* $KMnO_4$. During this titration the

solution gradually acquired the same yellowish color that had already been noted, and this color likewise disappeared on further addition of permanganate. A typical curve is shown in figure 1. It is interesting to note that the amount of rhenium taken should require 1.44 ml of 0.1 *N* $KMnO_4$ for oxidation from a minus one to a plus one valency. In a few cases a slight tendency for a break in potential at approximately 0.7 ml of 0.1 *N* $KMnO_4$ was noted, a point which would coincide with oxidation to a zero valency. No other sharp break occurred until the amount of permanganate required for complete oxidation had been added.

4. ELECTRODEPOSITION OF RHENIUM

In tests of methods which could be used to determine how much rhenium was present in the rhenium salt and in the portions of rhenium solution that were taken for test, it was found that rhenium could be deposited quite satisfactorily from solutions containing sulphuric acid, but not from solutions containing nitric acid.

The most satisfactory results were obtained by the use of (1) a stationary cathode of sand-blasted platinum gauze and a spiral platinum anode inclosed in an unglazed mullite thimble; (2) diluted sulphuric acid (5+95) as electrolyte; and (3) electrolysis overnight with a current density of 0.25 amp/dm² and 2.34 volts between electrodes. The deposits were quickly washed with water, alcohol, and ether, dried for 10 seconds at 105° C, cooled in a desiccator containing concentrated sulphuric acid, and weighed after 15 minutes.

TABLE 3.—*Electrodeposition of rhenium*

Weight of deposit	Weight of Re recovered in electrolyte	Total weight of Re indicated	Weight of Re calculated on assumption that $KReO_4$ was 100.0% pure	Weight of impurity indicated in deposit
g	g	g	g	g
0.0135	0.0001	0.0136	0.0134	0.0002
.0133	.0005	.0138	.0134	.0004
.0133	.0004	.0137	.0134	.0003
.0136	.0001	.0136	.0134	*.0002
.0136	.0001	.0136	.0134	*.0002
.0136	.0001	.0136	.0134	*.0002
.0268	.0011	.0279	.0268	.0011
.0269	.0011	.0280	.0268	.0012
.0275	.0007	.0282	.0268	.0014

* Determinations of the rhenium contents of these deposits indicated the presence of 0.00027, 0.00027, and 0.00019 g of impurities (see table 5).

Results obtained under these conditions are shown in table 3. In all of the tests the electrolytes were tested for rhenium by colorimetric comparison with standard solutions after adding potassium thiocyanate and stannous chloride, and extracting with ether.[3] The amounts recovered ranged from less than 0.1 mg to 1.1 mg. It will be noted that the total amount of rhenium found exceeded that expected in every case. The high results are believed to have been caused by slight oxidation, since most of the deposits appeared to be slightly stained either over the whole plate, or at some point such as the junction of the liquid and stem.

[3] L. C. Hurd and B. J. Babler. Ind. Eng. Chem. Anal. Ed. 8, 112 (1936).

In connection with the specification of a sulphuric acid solution in the electrolytic method, it should be remembered that more or less rhenium is lost by volatilization if sulphuric acid solutions are fumed strongly. No losses occur when hydrochloric or nitric acid solutions are evaporated to syrupy consistency under conditions that do not permit the formation of dry crusts. If evaporation with sulphuric acid is effected at as low a temperature as possible and stopped when fumes of the acid first appear, no loss of rhenium is believed to occur.

5. OXIDATION OF METALLIC RHENIUM

One of the most remarkable properties of rhenium that was observed in the course of the tests is the ease with which the metal can be oxidized to perrhenic acid. The phenomenon was first noticed with rhenium deposited on platinum gauze electrodes which had been left in a large covered glass vessel for 21 days. When the electrodes were removed, it was found that the rhenium deposits had almost entirely disappeared, and that the electrodes were covered with a liquid of marked acid character. Subsequent tests showed that no appreciable attack takes place if plated electrodes are stored in a *dry* atmosphere, but that attack is so rapid in moist oxygen that deposits weighing from 0.0134 to 0.0268 g were completely oxidized to perrhenic acid in 24 hours or less. In tests in which electrodes were weighed before and after oxidation of the deposits, it was found that the increase in weight was always in excess of that required by conversion of Re to $HReO_4$. Although no attempt was made to ascertain the nature of the contaminant, the excess in weight was undoubtedly caused by water of hydration.

In another series of tests a number of deposits were exposed in an atmosphere of moist oxygen, and the resulting oxidized deposits were combined, diluted to 500 ml with carbon-dioxide free water, and thoroughly mixed. One 50-ml portion was acidified with sulphuric acid and found to consume no permanganate, thus indicating complete oxidation of the rhenium. Another 50-ml portion, when carefully neutralized with potassium hydroxide, evaporated to dryness, and examined under the microscope, was found to yield crystals of exactly the same type as the potassium perrhenate used in the investigation. In table 4 are shown the results obtained in titrations of the remaining four 100-ml portions under the conditions set forth.

TABLE 4.—*Titration of perrhenic acid*

Indicator	Treatment of solution	Weight of 0.05 *N* NaOH solution	
		Required	Corrected to phenolphthalein end point
		g	g
Phenolphthalein	Not boiled	1.83	
Do	Boiled for 10 min and cooled	1.82	
Methyl red	Not boiled	1.78	1.83
Do	Boiled for 10 min and cooled	1.75	1.80

The results of the series of tests on the oxidized deposits indicate that (1) rhenium metal can be completely oxidized to perrhenic acid by exposing it to moist oxygen; (2) perrhenic acid is a reasonably strong acid; and (3) a dilute solution of perrhenic acid undergoes no change upon boiling for a short period.

6. STANDARDIZATION OF RHENIUM SOLUTIONS

The conditions that must be considered in establishing the rhenium content of a solution of a rhenium compound by electrodeposition are indicated in sections 4 and 5. These operations involve (1) electrodeposition of the rhenium; (2) determination of the amount of rhenium in the deposit by oxidizing the metal to perrhenic acid and then titrating with a standard alkaline solution; and (3) correction for any rhenium left in the electrolyte, as determined by colorimetric comparison with standard rhenium solutions.

TABLE 5.—*Standardization of a rhenium solution (5-ml portions of a solution containing 0.004169 (g) of $KReO_4$ per milliliter)*

Weight of deposit obtained by electrodeposition	Weight of rhenium			
	Calculated from titration of oxidized deposit	Left in electrolyte	Found in the 5-ml portion of solution	Calculated on assumption that $KReO_4$ was 100.0% pure
g	g	g	g	g
0.0136	0.01333	0.00007	0.01340	0.01342
.0136	.01333	.00005	.01338	.01342
.0136	.01341	.00002	.01343	.01342

The results that can be expected are illustrated in table 5. In these tests phenolphthalein was used as indicator, and titrations were made with a standard solution of sodium hydroxide under conditions that insured the absence of carbon dioxide. Calculations were made on the assumption that the oxidation of rhenium proceeds as indicated by the equation,

$$4Re+2H_2O+7O_2=4HReO_4,$$

and that the neutralization takes place according to the reaction,

$$HReO_4+NaOH=NaReO_4+H_2O.$$

It will be noted that the rhenium content of a deposit thus determined is less in every case than the weight of the deposit, as has already been stated.

While the method of standardization is not as simple and direct as might be desired, it has no difficult features, and is apparently capable of yielding quite accurate results, provided the amount of undeposited rhenium can be kept so low that the shortcomings of the colorimetric method can be ignored.

WASHINGTON, March 30, 1937.

○